THERMODYNAMIC AND KINETIC INVESTIGATIONS OF COMPLEXATION IN AQUEOUS SOLUTIONS OF THE LANTHANIDE SULFATES

By

DOUGLAS PAUL FAY

Bachelor of Science

Upper Iowa College

Fayette, Iowa

1965

Submitted to the Faculty of the Graduate College
of the Oklahoma State University
in partial fulfillment of the requirements
for the degree of
DOCTOR OF PHILOSOPHY
August, 1969

THERMODYNAMIC AND KINETIC INVESTIGATIONS OF COMPLEXATION IN AQUEOUS SOLUTIONS OF THE LANTHANIDE SULFATES

Thesis Approved:

Neil Purdie
Thesis Adviser

James Lange

Tom E. Moore

J. Paul Hawkins

D. D. Durham
Dean of the Graduate College

PREFACE

This study was done in an attempt to gain further insight into the detailed mechanism of complex formation in aqueous solutions of the lanthanide sulfates. Macroscopic thermodynamic parameters, although valuable, are not very useful in determining the exact nature of the species in solution and their detailed reactions. It was hoped that the combination of the macroscopic thermodynamic parameters, obtained from calorimetry, with detailed information on the energetics of the reaction mechanism, from a temperature dependent study of the rate constants, might be helpful in elucidating the structures and reactions of the species in solution. With this information it is often possible to sketch the actual path of the reaction being studied. It was also desirable to obtain further evidence for the assumptions that there is a change in coordination number within the series of trivalent lanthanide ions and that the rate-controlling step in complex formation of these species is that of cation desolvation.

I wish to take this opportunity to express my appreciation to my wife, Deanna, and son, Brian, whose patience, encouragement, and sacrifice were instrumental in the preparation of this dissertation. My sincere thanks are extended to my parents, John and Opal Fay, for their faith and guidance through the years.

Special appreciation is put forth to Mr. David Bohlen, my Freshman Chemistry Instructor at Upper Iowa, who instilled in me the desire to pursue my interests in Chemistry, and to Dr. Neil Purdie, who has been

not only a capable and dedicated research adviser but also a warm personal friend whom I shall always greatly admire.

My gratitude is also offered to the following persons: Dr. Tom E. Moore, Dr. James N. Lange, and Dr. J. Paul Devlin, members of my advisory committee, who gave freely of their time and knowledge in my behalf; Mr. Heinz Hall and his assistants in the instrument shop, whose suggestions and craftsmenship in construction of parts of the experimental apparatus have been most valuable; Mr. Wayne Adkins, of the glass shop, whose skill was necessary to the fabrication of a large part of the apparatus used in this study; and to those professors and students, necessarily nameless, whose association over the years I have greatly enjoyed.

My appreciation is also extended to the National Aeronautics and Space Administration for a fellowship and to the Oklahoma State University Department of Chemistry for various teaching assistantships.

TABLE OF CONTENTS

TABLE OF CONTENTS (Continued)

LIST OF TABLES

LIST OF TABLES (Continued)

LIST OF FIGURES

LIST OF FIGURES (Continued)

GLOSSARY OF SYMBOLS

$\overset{o}{a}$	distance of closest approach
A	constant of Debye-Hückel equation
A'	amplitude of chemical absorption
$\overset{o}{A}$	angstrom
A^{a-}	generalized ligand
B	constant of Debye-Hückel equation
B'	sound absorption due to solvent
c	velocity of sound
C_i	concentration of solute
d	incremental pen displacement
D	total pen displacement
e	electron charge
E_a	activation energy
f	frequency in cycles per second
f_c	frequency of maximum absorption
F	formality
G	Gibbs free energy
$G^{\ddagger}$	free energy of activation
h	Planck's constant
$\bar{h}_c$	average heat capacity
H	enthalpy
$H^{\ddagger}$	enthalpy of activation
Hz	hertz (equivalent to cycles per second)
i	current
I	sound intensity
k	Boltzmann's constant
k_{ij}	rate constant
K	equilibrium constant
$K^{\ddagger}$	equilibrium constant for activation
Ln^{3+}	generalized lanthanide ion
m	molality
M	molarity
M^{m+}	generalized metal ion
N	normality
N_L	Avogadro's number
p	pressure
q	Bjerrum distance

q_{cal}	incremental energy change in calories
Q	total energy change on reaction
R	molar gas constant
R_h	resistance of heater
S	entropy
$S^{\neq}$	entropy of activation
t	time
T	temperature
V	volume
z_i	charge on ion i
[]	concentration in moles per liter
α_T	total absorption coefficient of solution
α_{H_2O}	absorption coefficient of water
α_{chem}	absorption coefficient due to chemical relaxation.
β	degree of association
β_o	adiabatic compressibility of solvent as frequency goes to zero.
β_r'	relaxational compressibility (frequency dependent).
β_s	overall adiabatic compressibility
β_∞	instantaneous compressibility
γ_i	activity coefficient of ion i
Δ	generalized change in parameter
ε	macroscopic dielectric constant
$\theta(C)$	concentration factor [eqn. (38)]
λ	wavelength of sound
μ	ionic strength
μ_λ	absorption coefficient per wavelength
π^f	activity coefficient quotient
ρ	density
σ	degree of dissociation
τ	relaxation time
$\Phi(C)$	concentration factor [eqn. (37)]
ω	angular frequency in radians

CHAPTER I

INTRODUCTION

The formation of ion-pairs and complexes in solutions of electrolytes is a subject which has undergone considerable development during the past twenty years. More recently, the application of new physical methods and studies of the detailed thermodynamic properties and kinetic parameters of such reactions has provided much needed additional information for discussion of the important factors involved.

In a solution of an electrolyte it is desirable to have a detailed knowledge of the species present. New ions or uncharged molecules resulting from interactions in the solution may behave quite differently from the constituent ions of the electrolyte. Some properties of the solution will be profoundly affected, and the chemist, in order to understand these phenomena, will require to know the nature of the species present. There are a number of formidable difficulties in the analysis of such systems but recently a great deal of work has been done on the problem. Although the application of new physical-chemical methods has produced significant contributions to the field of equilibrium properties of electrolyte solutions and the way in which ion-pair and complex formation can be detected and quantitatively studied, the information obtained from measurements of an equilibrium system is to some extent limited, and it is desirable to know the relevant kinetic parameters. With this knowledge it is sometimes possible to sketch the

actual reaction mechanism by which the system approaches equilibrium. In general, the elucidation of the structure of an electrolyte solution may be regarded as a difficult problem which requires as many independent lines of attack as possible.

If we are to understand and control the chemistry of metal ions in solution we must understand the process by which their complexes are formed and interconverted. This is most often a matter of the replacement of one coordinated ligand by another. The substitution of a ligand in the inner sphere (leaving group) by an outside group (entering group) is the most fundamental of the reactions in metal ion chemistry. In fact, all discussions of reactions of metal complexes hinge on an understanding of the dynamics of their ligand substitution process, since it is an ever present possibility.

This study was undertaken in an attempt to gain more insight into the problem of complexation in aqueous solution, and in particular of the changes which occur upon the formation of complexes of the trivalent lanthanide cations with the sulfate anion. Experimentally the work has consisted of two major parts: (1) a calorimetric investigation of the thermodynamics of complexation of the 1:1 lanthanide sulfates and (2) a study of the temperature dependence of the rates of these same reactions. The significant developments and how they pertain to the aqueous properties of the lanthanide ions in particular is discussed in the following sections.

Thermodynamic Background

In recent years the complexing tendency of a variety of ligands towards the trivalent rare earth ions has been investigated and has led

to a rapid accumulation of information. Studies on the chelating tendencies of various multidentate ligands with the rare earths suggest that the lanthanide ions can expand their coordination number beyond six to eight, nine, or perhaps as high as twelve[1]. In aqueous solution the trivalent lanthanide ions undergo considerable hydrolysis with a concomitant lowering of the pH and formation of an aquo complex, $Ln^{3+}(H_2O)_x$. As a result of the lanthanide contraction the heavier lanthanides, with smaller radii, have a greater tendency to hydrolyze. The aquo complex has a definite structure and the "cloud" of water molecules has a geometry which differs from that of the bulk water.

According to the model of Frank and Wen[2], the ions at infinite separation are surrounded by three concentric regions: a primary or inner sphere of strongly bound water molecules, a second sphere with water molecules still ordered to some extent by electrostatic forces of polarization, and a third sphere having water influenced only slightly by the presence of the ion and essentially resembling the structure of the pure solvent. At short interionic distances the coulombic attraction of ions of opposite charge can bring about substitution of ions for solvent molecules in the first and second hydration spheres. The species produced are called ion-pairs; outer ion-pairs if solvent molecules exist between the ions and inner ion-pairs or complexes if the ions are in contact. Studies of the thermodynamics of ion-pair formation by classical methods such as conductivity measurements, spectrophotometry, polarography, potentiometry, and solubility measurements have been unable to distinguish between these species[3]. This is not unreasonable since the identity of the species existing in equilibrium could not be resolved due to the complexity of the system and from the

fact that the methods measure only the macroscopic properties of the system. Unless ligands having a strong structure-breaking influence are present, the "sheath" or "iceberg" of water molecules will remain intact and will "protect" the metal ion from the influence of other species.

When complexes are formed the approach of a ligand will perturb the hydration sphere and the ordered geometry will break down or be reorganized. Multidentate ligands will presumably have a stronger influence than unidentate ones based on a comparison of available free energy values. Duncan[4] has demonstrated that, provided no changes in the structure of the complex ion or the hydrated ion occur, the enthalpy of complexation for a series of cations with similar electronic configurations varies linearly with inverse cation radius. However, for the rare earths no such linear relationship is observed and probably is indicative of some structural change in the series.

In recent years an ever increasing number of investigations of the thermodynamic properties of various metal complexes have appeared in the literature[5,6]. In most of these investigations only the change in free energy for the various complexation reactions was determined. The purpose of these measurements was in most cases to decide, via the stability constants only, which species actually exist in solution. Free energy changes have frequently been correlated with properties of the metal ion and/or the ligand. However, the change in free energy is a net result of two parameters. A greater understanding of the important factors is obtained from a consideration of the contributory factors to the free energy change, namely the changes in enthalpy and entropy of complexation. The enthalpy change depends mainly on the dif-

ference in bond energy between the coordinated water and the ligand. Coordinated water should be taken in the widest sense to include the solvent layers beyond the first so that the enthalpy change associated with structural reorientation of more distant solvent molecules is also included. In other words, the reorganization of the hydrogen bonded structure surrounding the solute species may be important in determining the sign and magnitude of the enthalpy change. The entropy changes may be subdivided into a unitary and a cratic contribution[7]. Unitary entropy changes reflect losses in librational and vibrational degrees of freedom of the entering ligand. Cratic entropy changes are usually positive and reflect liberation of solvent molecules from a bound state and the concomitant reorganization of more distant solvent molecules. It is not a prerequisite for a spontaneous reaction that <u>both</u> enthalpy and entropy changes should be favorable. Usually chelation is motivated by a very favorable entropy change.

The stability constant, K, for a complex equilibrium of the type

$$M^{m+} + A^{a-} \rightleftarrows MA^{(m-a)+} \qquad (1)$$

is directly related to the free energy change, ΔG, by the relationship

$$\Delta G = -RT \ln K \qquad (2)$$

and is thus a reflection of the changes in enthalpy, ΔH, and entropy, ΔS, associated with the formation of the complex species according to

$$\Delta G = \Delta H - T\Delta S \qquad (3)$$

Since most of the systems studied are aqueous, the change in enthalpy upon complexation reflects the difference in bond energy of the metal

ion, M^{m+}, for the ligand and the "hydration sphere". Thus the measured enthalpy change also includes the energy involved in rearranging hydrogen bonds in the vicinity of the complex species[8]. Chelation is favored by entropy change in terms of release of originally bound water molecules. The majority of the trivalent lanthanide ion chelates are entropy stabilized. Few thermodynamic formation constants are available for the lanthanide complex series at a standard state of infinite dilution[9,10,11], but many concentration based values have been determined experimentally[5,6,12], often under conditions of constant ionic strength, i.e., constancy of activity coefficients. Enthalpy, and ultimately entropy changes, have been obtained for a number of systems in terms of the temperature dependence of the formation constant[5,6,12], but only in a few instances have the enthalpy changes been determined calorimetrically[3,11,13].

Free energy data indicate that for a given ligand a lanthanide ion gives, in general, a less stable complex than does a divalent transition metal ion. Predictions, in terms of the electrostatic concept of bonding, that the thermodynamic stability should increase with decreasing crystal radius or with increasing nuclear charge of the trivalent lanthanide ion, Ln^{3+}, for a given ligand, are in overall accord with the observations for the lighter ions (La^{3+} - Eu^{3+}), but not necessarily for the heavier ions (Gd^{3+} - Lu^{3+}). For the ions beyond Gd^{3+}, trends in stability are qualitatively of three types: (1) increase with increasing nuclear charge, (2) little or no change with increasing nuclear charge, and (3) maximum stability at some cation in the series[5].

Variations in enthalpy values for various ligands are seldom monotonic in the rare earth series but rather a maximum and/or minimum

often appears at various members in the series[14]. This general behavior appears to preclude explanations based upon ligand-field effects. The sinusoidal graphical representations of ΔH versus atomic number would require destabilization for the later members of the series if ligand-field effects were of major significance. However, by correcting for the complicating effect of a change in the effective hydration number of the uncomplexed lanthanide ion near the middle of the series, the enthalpy of the reaction of the diglycolate or dipicolinate ion with the crystalline ethylsulfates has been shown to vary almost linearly with atomic number[15]. However, in those cases where ligand-field effects are present, stabilization of the complex species with respect to those of La^{3+}, Gd^{3+}, and Lu^{3+} is of the order of only a few hundred calories per mole.

Concerning the variation in the entropy of formation of the various lanthanide complexes, it is observed that the change can be linear or non-linear with increase in the atomic number[16]. For this second group of complexes there usually exists a certain range in the middle of the series where the change is especially great. Within this range, where the entropy of complex formation changes abruptly, it is often possible to detect at least two forms of coordination compounds which differ from one another in the coordination number of the metal.

From conductance measurements at infinite dilution hydration spheres in three general size ranges have been proposed: La^{3+} - Nd^{3+}, Pm^{3+} - Tb^{3+}, and Dy^{3+} - Lu^{3+}, in order of increasing size[6]. In general, the larger the hydration sphere, the more exothermic is the complexation reaction. Correspondingly, the entropy change increases since more water molecules are released per cation.

It should now be possible to use the additional information of ΔH and ΔS to assist in distinguishing the structure of the metal complex. A number of ground rules have been proposed and in particular one suggested by Moeller[1]. Whether the coordination process is outer- or inner-sphere has been determined thermodynamically for 1:1 complexes involving thiocyanate[17]; nitrate, butyrate, and propionate[18]; glycolate, lactate, and α-hydroxybutyrate[19]; fluoride[20]; and sulfate ions[11,13,21]. Species (e.g. $LnNO_3^{2+}$, $LnSCN^{2+}$), for which the formation is favored by enthalpy change ($-\Delta H$) and opposed by entropy change ($-\Delta S$), largely retain the primary hydration sphere of the ion Ln^{3+} and are of the outer-sphere, ion-pair type. Those (e.g., LnF^{2+}, $LnOOCR^{2+}$, $LnSO_4^{+}$), for which the formation is opposed by enthalpy change ($+\Delta H$) but favored by entropy change ($+\Delta S$), suffer rupture of the primary hydration sphere and are of the inner-sphere type. In some cases the conclusions are supported by spectroscopic evidence[22] but the limitations to these criteria are immediately apparent upon a cursory review of the available literature.

Kinetic Background

It has been about sixty years since the earliest kinetic study of a complex ion reaction[23]. It is, however, only in the last fifteen years that anything approaching a concerted attack on the problem of the mechanism of these reactions has been made[24]. One of the challenges of investigating coordination compounds is understanding the variety of chemical intermediates and transition states possible during reaction. A knowledge of the reaction mechanism is an invaluable aid in the synthesis of new complexes and in the improvement of older methods.

Research on fast reactions in solution has developed enormously in the past few years[25]. Novel techniques have been developed[26], and numerous reactions which would once have been termed "instantaneous" have been investigated in detail. A wide range of reaction rates and a variety of reactions of metal complexes have been studied. The importance of the recently developed techniques for measuring very fast processes with half-lives of reaction in the micro- or millimicro second range cannot be overemphasized. Estimates of the lability of certain metal complexes (e.g., aquo, amine, and halide) have been resolved by electrochemical methods and from nuclear magnetic resonance (nmr) techniques[27]. In the latter case, the resonance line broadening of nuclei such as ^{17}O which is produced by paramagnetic ions can be interpreted in terms of the rate at which these nuclei, in labelled water molecules, are entering the coordination sphere of the paramagnetic ion, i.e., the exchange rate. In addition, the elegant relaxation methods pioneered by Eigen and his colleagues[25] can be used in which a chemical equilibrium is rapidly perturbed by some physical process. In the most restricted case, relaxation studies deal only with rate phenomena that are close to equilibrium and can be represented by linear relationships.

Another important property of a complex ion which has been used for kinetic measurements is its absorption spectrum, and the changes, often large, which occur in the visible, ultraviolet, or even infrared region can be extremely useful, not only in measuring rates of reaction but also in clarifying the detailed mechanism and the important role of the intermediates[28]. It has also been found that Raman line broadening can be used for the measurement of extremely fast rates[29].

Some insight into the mechanism of the replacement of coordinated

water in aquo complexes has been obtained from water and ligand exchange. The exchange of water between bulk solvent and the aquated metal ion is the simplest experiment in principle but, because of its general rapidity, is difficult to measure in practice.

Rates of reaction of the alkali metals[25,30], alkaline earths[25,31], and transition metal ions[25,32] with various ligands have been quite extensively studied. It is generally observed that the ions of these groups which have a noble gas electronic configuration show a linear rate dependence with inverse cation radius, but a similar relationship for the transition metal ions exists only after ligand-field stabilization corrections have been made. In practically every case the role of water exchange is paramount to ligand substitution. Chemically the lanthanides can be compared with both the transition metal ions and the alkaline earth ions, but of the two a closer resemblance with the latter is observed because of the relative unimportance of the ligand-field stabilization energy (LFSE). Therefore, one might expect to find a linear rate dependence with inverse cation radius across the rare earth series. Such is not the case and the small LFSE corrections alluded to in the thermodynamics section are inadequate in producing the expected linearity[15].

In the case where the entering group is murexide[33], sulfate[34,35,36], anthranilate[37,38], or oxalate[39], a sufficient number of the metal ions in the lanthanide series have been studied to permit an analysis of the dependence of the rate constants on inverse cation radius or atomic number. The dependence is similar for all four cases showing a maximum rate of complexation for the ions in the middle of the series. Because of the analogous non-linear trends with inverse cation radius

of such thermodynamic parameters as ΔG, ΔH, and ΔS of complexation, the same interpretation of a change in coordination of the cations near the middle of the series has been invoked to account for the non-linear trend in the rate constants.

The rates, however, differ in one respect. If the mechanism is dissociative (S_N1), so that the transition state is formed with a reduced coordination number, and the controlling step in the mechanism is the loss of a water molecule bound to the cation, the rate of complex formation should approximate to the rate of water exchange and be almost independent of the entering ligand. The ultrasonically measured rates of complexation for the lanthanide sulfates[34,34,36] compare favorably with the rate of water exchange obtained by ^{17}O nmr line broadening for Gd^{3+} in perchlorate medium[40]. These rates are, however, generally about one order of magnitude greater than those for the other systems studied by other techniques and under various conditions. Since these other ligands are considered to be bidentate ligands a direct comparison may not be justified and their slower rates may be indicative of a progressively slower rate of exchange of successive water molecules upon ring formation.

General Mechanism

The general mechanism used in this study is that proposed by Diebler and Eigen[41] and may be written as

$$M^{m+}_{(aq)} + A^{a-}_{(aq)} \underset{k_{21}}{\overset{k_{12}}{\rightleftharpoons}} \left[M^{m+} \quad O\begin{smallmatrix}H\\H\end{smallmatrix} \quad O\begin{smallmatrix}H\\H\end{smallmatrix} \quad A^{a-} \right](aq) \qquad k_{32} \uparrow \downarrow k_{23} \qquad (4)$$

$$[M^{m+}\ A^{a-}]_{(aq)} \underset{k_{43}}{\overset{k_{34}}{\rightleftharpoons}} \left[M^{m+}\ O\begin{matrix}H\\H\end{matrix}\ A^{a-}\right]_{(aq)}$$

where the k_{ij} values ($j = i + 1$) represent the specific rate constants and the individual equilibrium stability constants may be defined as $K_{ij} = k_{ij}/k_{ji}$ for each of the three consecutive steps. Two processes are involved in the first step (I) between states 1 and 2. First, the free hydrated ions approach each other to within the approximate dimensions of their ionic atmospheres, and second, there is a rearrangement of ions and molecules within the ionic atmosphere to give state 2. The second step (II) is the loss of a water molecule from the primary coordination sphere of the anion. The anion has three modes of interaction with the water molecules of the cation. The anion may interact strongly with one hydrogen of a water molecule in the primary hydration sheath of the cation, or with two hydrogens on either the same or two adjacent water molecules. At any one time the three structures are in equilibrium with one another. The third step (III) is the replacement of a water molecule from the inner coordination sphere of the cation by the anion and the formation of a chemical bond between the ions. There is a concomitant increase in the degree of disorder of the water structure as a result of charge neutralization and this gain in entropy is very often the principal contributing factor to thermodynamic stability. This is particularly true in the case of unsymmetrical electrolytes in which the various states have a net charge.

If the equilibrium constants for the successive association steps in the mechanism are K_{12}, K_{23}, and K_{34}, respectively, then the overall

stability constant, K_T, is given by the following (taking W = H_2O and neglecting charges):

$$K_T = \frac{[MW_2A] + [MWA] + [MA]}{[M][A]}$$

$$= \frac{[MW_2A]}{[M][A]} \left\{ 1 + \frac{[MWA]}{[MW_2A]} + \frac{[MA]}{[MWA]} \cdot \frac{[MWA]}{[MW_2A]} \right\}$$

$$K_T = K_{12} [1 + K_{23} + K_{23}K_{34}] \qquad (5)$$

As a consequence, the structure of the complex species present in solution can not be identified by the overall stability constant. The utility of the conventional approach is limited to situations wherein the anion, for example, is kept constant and the change in K_T for a series of complexes with similar metal ions is a function of the cationic properties and therefore of K_{34}. It is apparent from equation (5) that a simple relationship does not exist between the various equilibrium constants and consequently, extreme caution must be used in drawing conclusions about the predominant species in solution from stability measurements alone. If enthalpy and entropy data are available, the conclusions are more justified.

The only route to the evaluation of the individual equilibrium constants is by kinetic measurements. Equilibrium is reached very rapidly and the problem is amenable only to modern relaxation methods. The complete mechanism shows a dependence of $K_{34} = k_{34}/k_{43}$ on the ratio of the concentration of inner to outer complex.

Evidence indicates that the rate determining step of the mechanism

is indeed step III[34,35]. Supporting this are several theoretical considerations:

(a) If the rates of diffusion of the aquated ions, to within two water molecules of each other, are calculated from the theory of diffusion controlled reactions, the relaxation time should lie in the order of 10^{-9} seconds.

(b) The ease of removal of water molecules from an anion should take place faster than from a corresponding cation since the interaction of the anion with the surrounding water molecules is usually weaker than for the cation.

(c) The water molecules coordinated to the cation should be held more strongly due to the large surface charge on the cation resulting from the small ionic radius.

Experimental evidence for the correlation of the slow step with step III is exhibited by the dependence of the rate on the cation for a series of similar 1:1 and 2:2 electrolytes[25]. Sulfate, EDTA, and NH_3 complexes of Cu(II), for example, are formed at nearly the same rate[22]. D_2O studies of complexation show no dependence of OH bonds on the observed relaxations[42]. That the rate constants are directly related to step III has been demonstrated by Connick[27] in a number of studies using ^{17}O labelled water in nmr studies of water exchange rates in the transition elements. The rates obtained are related to $^{17}OH_2$ molecules entering the first coordination shell of the paramagnetic cations. The rates of water exchange for the divalent ions when compared with Eigen's[25] values for the rates of formation of inner sulfate ion-pairs show a fairly close parallelism. In addition, Tamm[43] has

shown the existence of three relaxation processes in an ultrasonic study of $MgSO_4$ complexation.

Since the substitution rate is apparently independent of the nature of the entering ligand, the metal to water bond must be broken prior to the arrival of the ligand at the coordination site. Such a mechanism, designated S_N1, is consistent with the observation that the slow step is cation dependent.

The rates of complex formation of the alkali metals, the alkaline earth metals, and the transition metals closely follow changes in electronic structure. For the transition metals the rates follow the effects of ligand-field stabilization. The ligand-field effects on the stability of the trivalent rare earth complexes and on the rates of ligand substitution are considered small because of the deep penetration of the 4f-electrons into the electronic atmosphere of the ion. A maximum of 10% contribution to the stability has been suggested by Dunn[44]. It is reasonable, therefore, to expect them to behave like the alkaline earth ions because of their pseudonoble gas configuration. That they do not has been attributed to a change in coordination number in the series.

CHAPTER II

GENERAL THEORY OF RELAXATION METHODS

Suppose that the reaction whose rate we wish to measure comes to an equilibrium position, with concentration values X_1, which can be perturbed by a change of some external parameter such as temperature or pressure. If such a change of conditions is made suddenly, there is a time-lag while the system approaches a new equilibrium position, with concentration values X_2. The time-lag is expressed as a "relaxation time", τ, which is an inverse measure of the sum of the rate constants for the forward and reverse processes and is given for a single unimolecular relaxation process by

$$\tau^{-1} = k_f + k_b \qquad (6)$$

The range of reaction half-times accessible to one or another of the relaxation methods lies within the total range of 10^{-9} to over 1 second[45]. Some relaxation methods make use of a single displacement of temperature (T-jump), pressure (P-jump), or electric field (Wein Effect II)[26,45]; the reaction is then followed as it moves towards the new equilibrium. Other methods make use of a pulsed or periodic disturbance set up by ultrasonic waves or by a high frequency alternating field[26,45]; the power absorbed by reason of the time-lag in re-establishing the equilibrium conditions is measured. The pulse-technique of

sound absorption has been used in this work.

Assume that the equilibrium to be studied is periodically perturbed. If the equilibrium is set up relatively slowly, so that τ is much longer than the periodic frequency, the parameter representing the extent of reaction is little affected and remains practically at the value corresponding to no perturbation (line a in Figure 1). If the equilibrium is set up relatively very fast, the reaction parameter follows closely the variations of the perturbation and so alters in

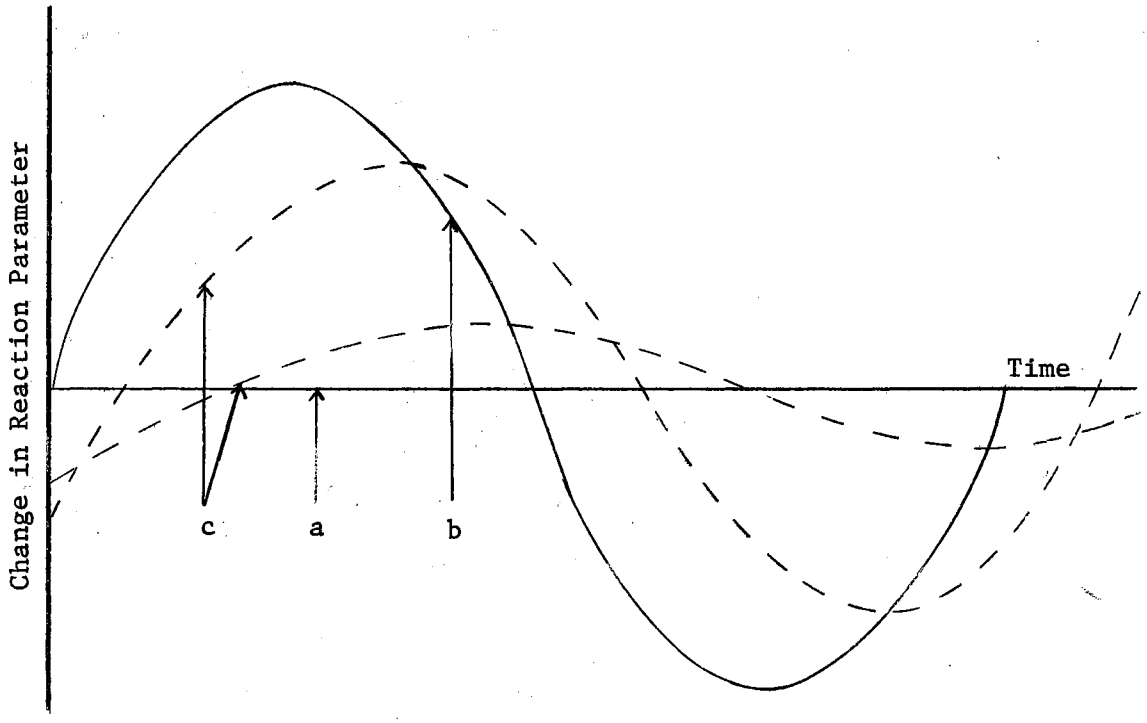

Figure 1. Periodic Disturbance of Chemical Equilibrium by External Parameter.

phase with it (curve b). If, however, the relaxation time of the equilibrium is comparable with the periodic time of the perturbation, the reaction parameter lags behind the perturbation, and therefore varies according to one of the dashed curves (such as c). This has a smaller

amplitude than curve b, and is out of phase with the variations of the perturbation. This phase difference leads to absorption of energy. As the frequency increases from zero the lag at first increases and with it the absorption per cycle; later the effect of the decreasing amplitude begins to dominate and the absorption decreases again. Mathematical treatment shows that at a certain frequency there is a maximum in the absorption per cycle given by $\omega\tau = 1$, where ω is the angular frequency in radians per second, equal to $2\pi f$ and f is the frequency in cycles per second. For a single relaxation process the absorption coefficient per wavelength, μ_λ, varies with frequency and is proportional to $\omega\tau/(1 + \omega^2\tau^2)$. This function has a maximum value of ½ when $\omega\tau = 1$. The curve has the form of the following equation, in which μ_{max} is the maximum value of μ_λ:

$$\mu_\lambda = 2\mu_{max} \frac{\omega\tau}{(1 + \omega^2\tau^2)} \tag{7}$$

If f_c is the frequency of the maximum absorption, then τ is given by $1/2\pi f_c$ and can be found from experiment.

Relaxation methods have a unique feature. Since the deviations from an equilibrium state are very small, the kinetics of a system can be described by a set of linear differential equations. For example, in the general reaction

$$A + B \underset{k_b}{\overset{k_f}{\rightleftharpoons}} AB \tag{8}$$

the rate equation is

$$-\frac{d\Delta c}{dt} = \frac{1}{\tau}\Delta c \tag{8}$$

where Δc is the deviation of the concentration of all components from their equilibrium values. If the chemical system is complex, a system of rate equations of the general form

$$\frac{d\Delta c}{dt} = \Sigma a_{ij}\,\Delta c_j \tag{9}$$

are obtained where a_{ij} are known functions of rate constants and equilibrium concentrations. If the system of simultaneous equations is solved a spectrum of relaxations is obtained and each relaxation has its own particular dependence on the equilibrium concentrations, but is not necessarily representative of a single step in the complex multistep mechanism, since there may be coupling between steps.

An ultrasonic wave propagates as an adiabatic pressure wave. Both temperature and pressure changes accompany the sound wave but in aqueous solutions, temperature fluctuations are nearly absent ($\Delta T \leq \pm 0.001^{\circ}$) because the thermal expansion of water is very small (zero at 4° C). The adiabatic compressibility of the fluid may be resolved into a virtually instantaneous portion plus a time dependent portion[46]:

$$\beta_s = \beta_r' + \beta_\infty \tag{10}$$

where β_∞ is the instantaneous compressibility and is given by the limiting value as the frequency approaches infinity and β_r' is the relaxational part of the compressibility which is frequency dependent. Whenever the frequency of pressure variation is such that a phase lag

exists between pressure and the specific volume the frequency dependence of the relaxational compressibility is

$$\beta_r' = \beta_r/(1 + \omega\tau) \tag{11}$$

where β_r is a real number. The phase lag causes dissipation of energy within each cycle

$$\text{Energy Lost Per Cycle} = \oint PdV \tag{12}$$

As the frequency rises from a low value, the shift in equilibrium will increasingly lag behind the pressure and the maximum energy is lost when

$$(\alpha_{chem}\,\lambda)_r = \frac{\pi\beta_r}{\beta_o}\left(\frac{\omega\tau}{1 + \omega^2\tau^2}\right) \tag{13}$$

where $\beta_o = \beta_r + \beta_\infty$ and α_{chem} is the excess absorption per wave length, λ, due to chemical relaxation.

CHAPTER III

INSTRUMENTATION AND PROCEDURES

The Calorimeter

The design of the microcalorimeter used in this investigation was essentially that used by Harris and Moore[47] in their study of complex formation of Ni(II) and Co(II) perchlorates in 1-butanol. However, for completeness the calorimeter with its modifications will be described in detail.

The several basic requirements for the design of a titration calorimeter satisfactory for thermometric studies of enthalpies of complexation are:

1. Maintenance-free operation.
2. Low thermal conductance properties and high chemical resistance.
3. Thorough and efficient mixing to attain rapid equilibrium.
4. Maintenance of titrant temperature at solution temperature throughout titration.
5. Sensitivity to small temperature changes, with no appreciable time delay in detection.
6. Electrical heat capacity calibration system.
7. Overall accuracy of within ± 1% for some suitable standard calibrating reaction involving a heat change of approximately one calorie.

8. Electrical stability and small noise to signal ratio.

A sketch of the internal construction of the calorimeter is shown in Figure 2. The illustrated parts were mounted in an isothermal air chamber. The calorimeter vessel and appendages were constructed from glass because of the fairly good structural stability and relatively low thermal conductance. All parts in contact with the solution were glass except the internal heater wire (A) and the titrant hypodermic needle (D). The system was found to give maintenance free operation. Cleaning was effected by rinsing with deionized water and reagent grade acetone. The reaction vessel itself was a small, silvered Dewar flask of approximately 60 ml. total volume. To improve thermal equilibrium the Dewar flask was placed in a double-walled, glass water jacket maintained at 25 ± 0.05° and the intervening space filled with insulating material. The temperature of the water jacket was maintained with a circulating heater (Haake Model FSe) using an external ice bath for cooling of the pump reservoir. Access to the inside of the calorimeter for electrical contacts, stirrer, and delivery tube was made through a standard taper ground glass fitting (T 40/50 mm.) The titrant was added from an ultra precision micrometer syringe (G) (R. Gilmont No. S-3200, 0.0001 ml. divisions, 0.02% accuracy, 2.5 ml. capacity) via a twelve inch Wilkens Instrument and Research Teflon 18 gauge hypodermic needle with a 22 gauge tip inserted into the end. A 1 ml. plastic syringe barrel, used as a "piggy back" reservoir (F), was attached to a B-D MS01 syringe stopcock (E) positioned such that the syringe could be removed for refilling without disturbing the calorimeter operation.

Mixing of the solution was accomplished by a glass stirring rod (~3 mm. diameter) with molded paddles on the end (C). The rod was

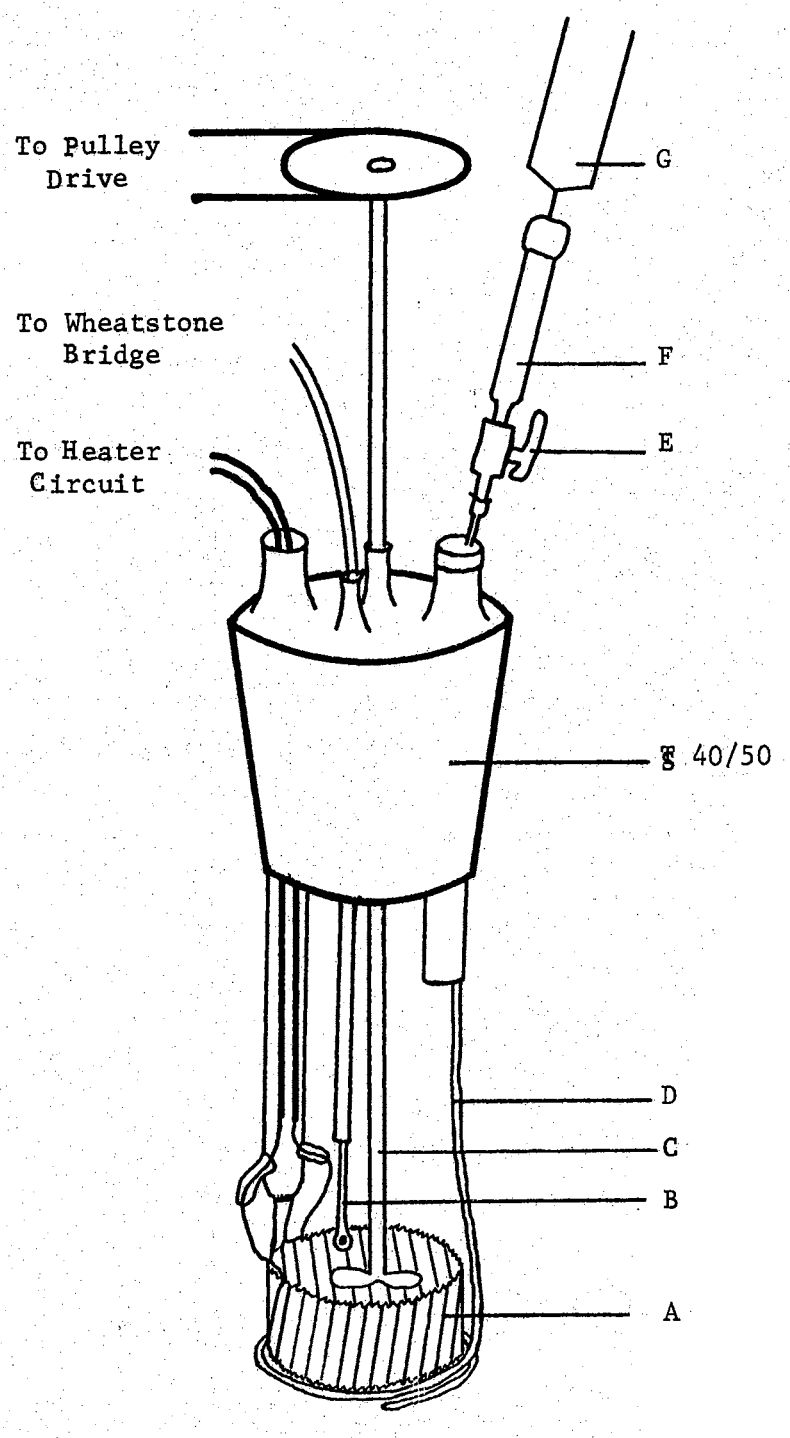

Figure 2. The Internal Parts of the Calorimeter

mounted in a Teflon bearing and connected to a stainless steel rod and pulley system mounted on top of the isothermal air chamber. An electronically controlled motor (G. K. Heller, Model GT21) was used to drive the stirrer at constant speed. Qualitative tests with dyes indicated complete mixing within 3 to 5 seconds.

Although all solutions were thermostated at 25° prior to introduction into the Dewar flask or syringe, an added precaution was taken to guarantee that the titrant temperature remained equal to that of the solution. The Teflon delivery needle (D) was coiled around the internal heater form below the surface of the solution enabling the titrant to equilibrate before additions were made to the solution.

A Sargent Coulometric Current Source, Model IV, was used for electrical calibration[48]. This unit provided a stabilized current at six values over the range 4.825 to 193.0 milliamperes regulated to ± 0.1%. Time of heating was measured directly on the incorporated timer of the instrument in units of 0.1 seconds with estimation possible to 0.02 seconds. Ideally the electrical energy input during calibration should approximate to the change in the chemical energy of the system under study. As a rule, a current of 48.25 ma. passed for a period of approximately 100 seconds was satisfactory. The heater wire, which was wound on a glass form, was of 0.0034 inch diameter platinum with a total resistance of 25.70 ohms. Connection to the current source was made by heavy copper wire leads.

Temperature changes were monitored using a 2000 ohm ± 1% thermistor (B) (Fenwal Electronics, Isocurve GB32PM12) as one arm of a Wheatstone bridge (Leeds and Northrup, No. 4760). The thermistor had a temperature coefficient of -3.87% per °C and was operated at a potential

of 1.45 volts. The out-of-balance signal was fed to an intermediate D.C. amplifier (Leeds and Northrup, No. 9834 Null Detector) and the virtually noise-free output from the amplifier displayed on a Sargent SR recorder with the range plug removed and the chart paper driven at one inch per minute. The full scale range of 125 mV. was just capable of handling the signal when the amplifier was set on a sensitivity of 2. The resultant bridge sensitivity was of the order of 0.17 calories per centimeter of pen displacement. Measurements were made to the nearest 0.01 cm. or ± 0.0001°. The displacement had been shown by preliminary experiments to be a linear function of temperature.

The heat capacity was calculated from the formula

$$h_c = \frac{i^2 R_h t}{4.184d} = \text{Number of calories per centimeter of pen travel} \quad (14)$$

where i = current across the heater in amperes

R_h = resistance of heater in ohms

t = time of current flow in seconds

d = pen displacement in centimeters

4.184 = number of joules per calorie

Thermometric Titration Procedure

In normal operation the null detector was never turned off since warm-up and adjustment required several hours. At least thirty minutes prior to using the calorimeter the thermistor battery and Coulometric Current Source were switched on. The titrant delivery system was filled and additional titrant forced through the reservoir and needle to expel

any trapped air. Care was also taken to exclude air when filling the micrometer syringe and when inserting it through the rubber septum of the "piggy back" reservoir. The tip of the titrant needle was then rinsed with deionized water and reagent grade acetone.

A 32.48 ml. aliquot of solution was added to the clean, dry Dewar vessel. The calorimeter vessel was finally completely assembled in the water jacket and circulation from the constant temperature bath begun. Stirring was then initiated and thermal equilibrium of the system was considered to have been attained when a nearly horizontal ($dT/dt \simeq 0$) baseline was established on the recorder. Time for equilibration was normally of the order of one hour. For each run heat capacity measurements were made before and after the titration, which consisted of four additions of 0.100 ml. aliquots of titrant at three to five minute intervals. Since the heat capacity changed only slightly during a run, the two heat capacity measurements were averaged to determine the energy change of the system.

To determine the magnitude of the pen deflection, d, for each addition, the recorded temperature base lines were extrapolated back to the mid-point of the inflection. The distance between the points of intersection of a vertical line through the midpoint of the inflection with the base lines was taken to be equal to d. This distance, in centimeters, multiplied by the heat capacity, in calories per centimeter, gives the number of calories change for each increment of titrant. A schematic drawing of an enthalpogram is shown in Figure 3.

Performance of the calorimeter was checked by measuring the heat of neutralization of 9.643×10^{-3} M HCl with 1.240 M NaOH as titrant. A value of -13.33 ± 0.04 kcal./mole (the uncertainty is given as the

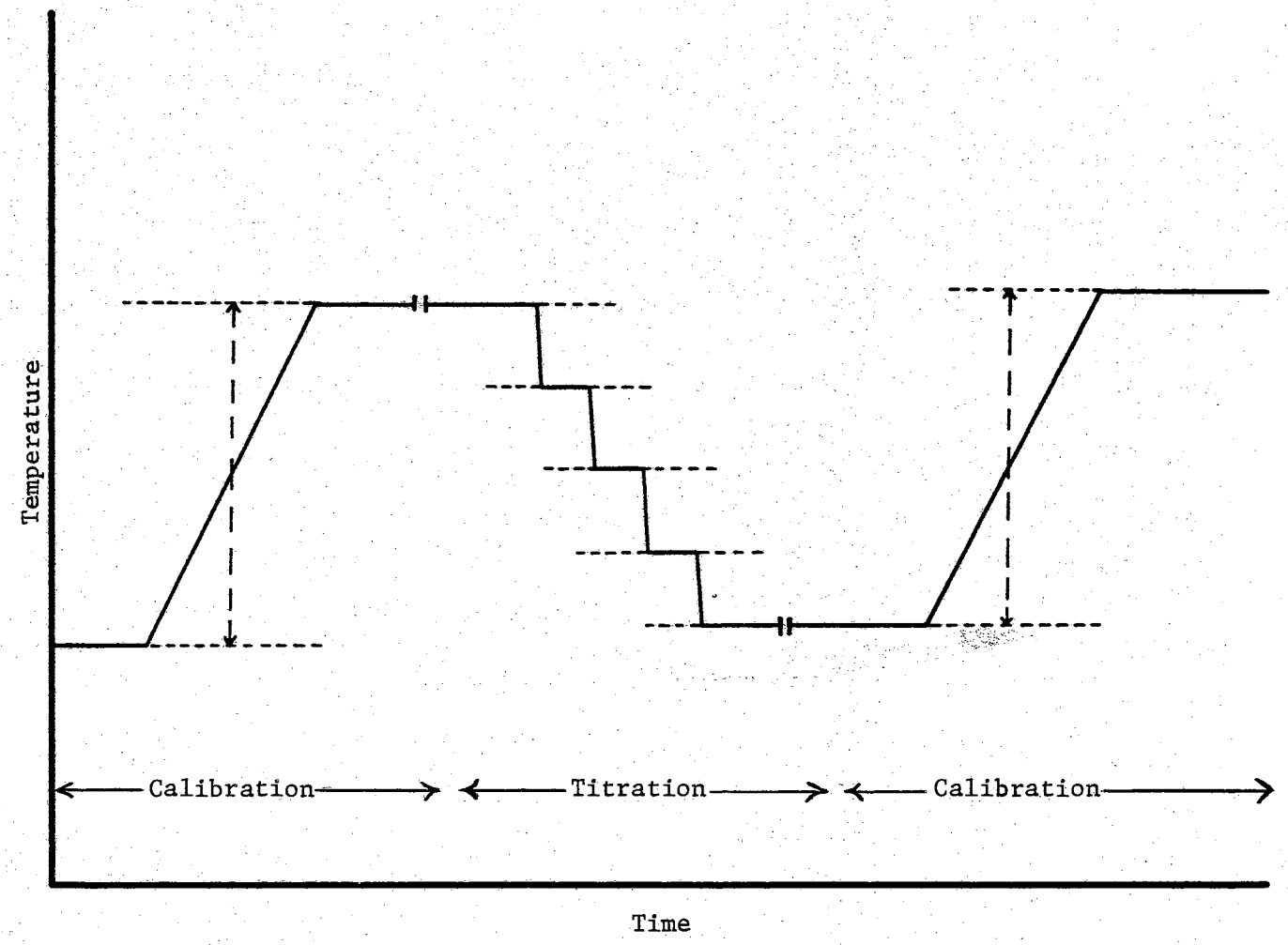

Figure 3. Schematic Diagram of a Typical Enthalpogram

average deviation for five runs) at 25° was obtained after correcting for the heat of dilution, which agrees to within 0.1% of the value of -13.34 kcal./mole reported by Hale, Izatt, and Christensen[49].

The Ultrasonic Apparatus

The pulse technique can be used in the frequency range 1-300 MHz. Since the absorption is proportional to the square of the frequency, the absorption is very small below 1 MHz. At very high frequencies, the efficiency of the crystal transducer is greatly reduced. The equipment used in this study has a frequency range of 5 to 75 MHz.

The Electronic System

A block diagram of the apparatus is shown in Figure 4. The signal is initiated by a square wave pulse generator supplying two output pulses at about 60 pulses per second which are separated by a variable delay. The two pulses are identical in amplitude and polarity. The first pulse drives a pulse amplifier which supplies approximately 500 volts amplitude to the transmitters. These in turn put out 150 volts peak to peak into a circuit impedance of 75 ohms to drive a crystal transducer. The second pulse drives a transistor pulse amplifier. This pulses a particular comparison pulse oscillator, and the output from the selected unit is passed through a set of precision attenuators. The outputs of the receiving transducer and the attenuators are combined in a passive addition circuit and taken to a video amplifier. The resultant signal is then displayed on an oscilloscope, Tektronix 536, equipped for fast rise time.

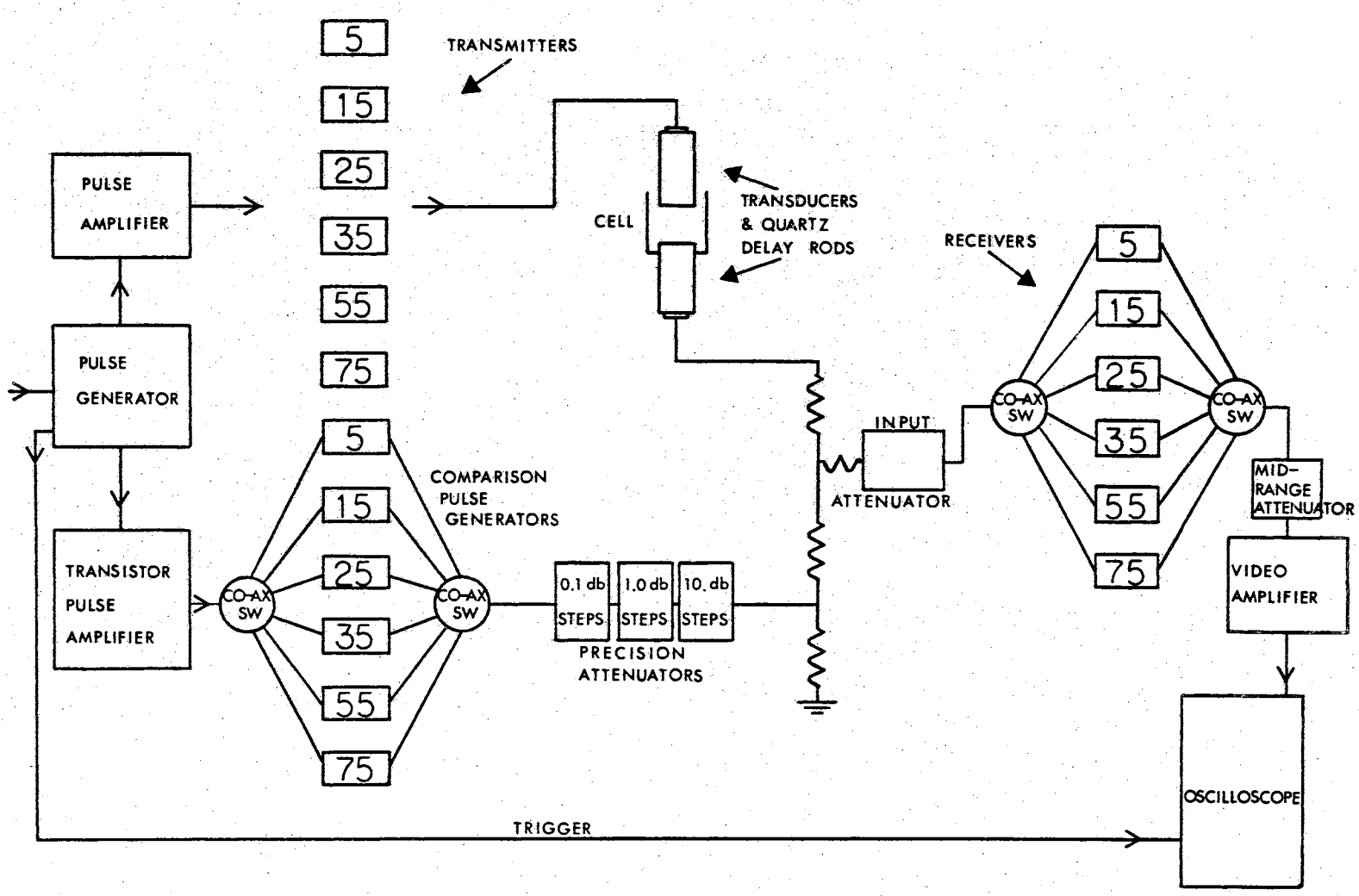

Figure 4. Block Diagram of Electrical System

The Mechanical System

The mechanical system is pictured in Figure 5. It consists of three parallel stainless steel platforms anchored to a stainless steel back. On the lower platform is positioned a table, fastened by a spring through the center and two spin off nuts on either side. The table is supported by three adjustable leveling feet, and is actually a large chuck into which a quartz rod can be inserted, electrical contacts with the rod being made on the sides of the chuck and through the bottom by a spring leaf assembly; the external connection is made through a BNC connector mounted on the side of the table. The center platform has a moveable chuck (electrical connections through the sides and base) tensioned by springs so as to maintain position if moved vertically. The upper platform has a micrometer firmly mounted above the upper chuck. The micrometer moves the upper chuck through an intermediate stainless steel ball to achieve calibrated vertical motion of the receiver transducer.

The Transducer Assembly

Two delay rods of Spectrosil B grade fused quartz were obtained from Thermal Syndicates Ltd., England. The emitter and lower rod has the specifications, length - 80 mm ± 1.0 mm, diameter - 30 mm ± 0.5 mm, one end ground to a taper, the semi angle being 5 degrees leaving the diameter of one end 24 mm. The tapered end fits a water jacket. The detector rod dimensions are 80 ± 1 mm in length and 20 mm ± 0.5 mm in diameter. Both cylinders have end faces optically flat to 1/4 of the wavelength of green light and are parallel to 6 seconds of arc.

Each rod was platinum plated on one end and to approximately 30mm

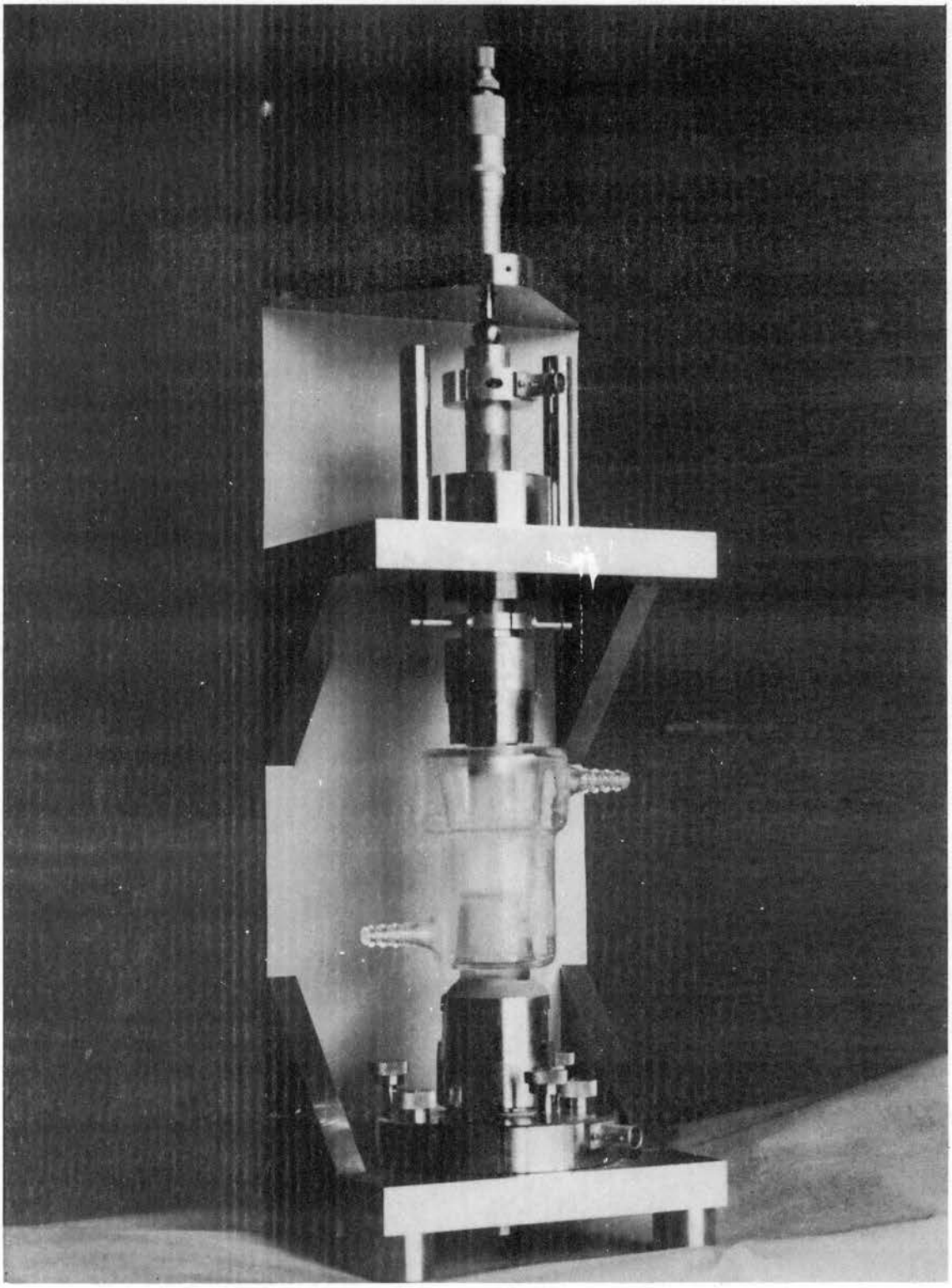

Figure 5. Mechanical System

along the side by repeated application and heating to 700 ^{o}C of Liquid Bright Platinum (DuPont #7447) until a conducting surface of approximately 1 ohm resistance between face and side was achieved.

The piezoelectric transducer elements are X-cut crystals with a fundamental resonant frequency of 5000 KHz with a tolerance of ± 70 KHz (Marconi's W. T. Co., Ltd.). The crystals were attached to the delay rods using hot paraffin wax--the crystals being "rung in" until there was essentially a monomolecular bond between the crystal and rod. The outer face of the crystal was coated with liquid silver conducting paint to achieve electrical contact. The rods were checked for excess attenuation due to poor bonding and the "ringing in" process repeated until the lowest value of attenuation was obtained.

Experimental Procedure

The solution under study was placed in the thermostated cell. The delay rods were made parallel by adjusting the lower table until the first pulse displayed on the oscilloscope was maximized at every frequency. This was done with the quartz rods near maximum separation. The transmitter pulse was tuned to a maximum at a given frequency. To check that the comparison pulse generator was operating at the same frequency, the two pulses were overlapped, and the comparison pulse frequency tuned until beating was observed in the oscilloscope display. It was not possible to measure the precise separation of the delay rods so the total sound absorbed, in decibels, was measured as a function of the change in separation, in centimeters. More precisely, a reading was taken by selecting a value on the precision attenuators which gave a suitable height for the comparison pulse. The transmitted

pulse was matched to the same height with the micrometer drive of the mechanical system. Where possible, seven measurements of attenuation and distance were taken in replicate. The sound absorption coefficient, α_T, in decibels per centimeter, for each frequency was obtained from the slope of the plot of distance versus attenuation.

For the measurement of rate constants as a function of temperature a dual reservoir temperature control system was used. For studies at 5° an insulated, copper-lined tank of $\sim$ 120 liters volume was maintained at $\sim 4.5^{\circ}$ by means of electrical refrigeration. Water from this tank was circulated through an external copper tubing coil placed in a polystyrofoam tank of $\sim$ 32 liters volume. Stirring of the large tank and circulation of coolant was accomplished by means of a variable flow, impeller-type pump (Flotec R2B1-1000). Water in the smaller tank was heated as necessary and circulated around the reaction cell by a Bronwell Constant Temperature Circulator. The temperature was maintained to $\pm$ 0.05 degrees at all temperatures.

The smaller tank containing the peripheral apparatus was covered by the same polystyrofoam material and the system sealed as tightly as possible. At 45° no external cooling was necessary due to normal heat losses to the surroundings. The reaction cell itself was wrapped in insulating material and all connections were covered with Armstrong Armaflex insulating tubing.

It was found that approximately thirty minutes were required for the 20-25 ml. of sample solution in the cell to come to thermal equilibrium. To reduce the loss of solvent by evaporation during this equilibration period (esp. at 45°), modeling clay was used to seal the cell with the receiving transducer element placed in the position of

minimum separation. During a typical determination of α_T as a function of frequency the receiving transducer element was always moved such as to increase the distance of separation, thereby maintaining better thermal equilibrium between the delay rod and the solution. A series of duplicate measurements at all six frequencies could usually be made within 45-60 minutes.

CHAPTER IV

EXPERIMENTAL AND TREATMENT OF DATA

Solutions for Calorimetry

Lanthanide nitrate hydrates of 99.9% purity (American Potash and Chemical Co.) were used in the preparation of approximately 0.05F solutions. Cation concentration was determined by titration of the nitric acid, produced by cation exchange on strongly acidic Dowex 50 W-X8, 20-50 mesh resin, with standard sodium hydroxide. The concentration of the stock sodium sulfate titrant solution was determined gravimetrically as barium sulfate to be 0.6411F.

Calorimetric Data

The energy change in the calorimeter for the reaction

$$Ln^{3+}(aq) + SO_4^{2-}(aq) \rightleftharpoons LnSO_4^{+}(aq) + Q_{cal} \qquad (15)$$

in dilute solution consists of two main parts. The observed energy change, Q_{cal}, is the summation of Q_{dil}, the heat of dilution of the Na_2SO_4 titrant, and Q_{rx}, the heat of complex formation, and may be written

$$Q_{cal} = Q_{dil} + Q_{rx} \qquad (16)$$

Contributions from the heat of dilution of the $LnSO_4^+$ complex and the heat of dilution of lanthanide nitrate were considered to be insignificantly small since the total increase in volume was only 0.400 ml. Q_{dil} was determined to be 0.65 kcal/mole endothermic by titration of the Na_2SO_4 stock solution into a $NaNO_3$ solution of similar ionic strength to that of the $Ln(NO_3)_3$. After this work was completed, attention was drawn to the need to correct for the heat of association of $NaSO_4^-$, which would be different in the dilution and complexation experiments[50]. The correction would not be very large since the total sodium sulfate added was only 0.256×10^{-3} mole. A calculation, which was necessarily very approximate because of the high ionic strength of the titrant, showed that the difference in the heat change on adding Na_2SO_4 to $NaNO_3$ and to $Ln(NO_3)_3$ was at most only 0.2 kcal/mole. The computed ΔH_T^o values could therefore be approximately 0.2 kcal/mole more endothermic than for those calculated where the correction had been made. In the presence of the very stable $LnSO_4^+$ complexes the concentration of $NaSO_4^-$ would be very small and could be neglected in the material balance equations.

The concentration of the 1:1 complex, $LnSO_4^+$, was calculated from the material balance equations for total sulfate

$$a = [HSO_4^-] + [SO_4^{2-}] + [LnSO_4^+] \qquad (17)$$

and total metal

$$m = [Ln^{3+}] + [LnSO_4^+] \qquad (18)$$

and from the thermodynamic stability constant expression

$$K = \gamma_1[LnSO_4^+]/\gamma_2\gamma_3[Ln^{3+}][SO_4^{2-}] \quad (19)$$

where γ_i is the mean activity coefficient of the ion of charge i. From the measured pH of the solution and the dissociation constant of HSO_4^-, the concentration of bisulfate ion was calculated to be insignificantly small. Consequently, the proton released by displacement of the equilibrium

$$HSO_4^- \rightleftharpoons H^+ + SO_4^{2-} \quad (20)$$

to the right, by removal of sulfate ion on complexing, is negligible and no correction to the measured heat was necessary. The stability constants from conductimetric experiments were used[10]; undetermined constants were obtained by interpolation. Mean activity coefficients were calculated by standard iteration to constant γ_i around equations (17), (18), and (19), the expression for ionic strength (21),

$$\mu = \tfrac{1}{2}\{[Na^+] + [NO_3^-] + 9[Ln^{3+}] + 4[SO_4^{2-}] + [LnSO_4^+]\} \quad (21)$$

and the Davies[57] equation (22), where z_i is the charge on

$$-\log \gamma_i = 0.509\, z_i^2 \{\mu^{\frac{1}{2}}/(1 + B\mathring{a}\mu^{\frac{1}{2}}) - 0.3\mu\} \quad (22)$$

the ion i (see Appendix A for computer program). The Bjerrum distance, q, for ion pair formation is 21.4 Å for a 3:2 electrolyte in aqueous solution at 25° so the usual $\mathring{a}$ value of 3-5 Å is probably too small.

An arbitrary value of $\mathring{a}$ (~8.86 Å) equal to the sum of the ionic radii plus two water molecule diameters, was used to be consistent with the kinetic model[41]. This $\mathring{a}$ value is perhaps a little too large in that an $\mathring{a}$ value of 7.3 Å was found to give the best results for the stability constant of the lanthanum cobalticyanide 1:1 complex[52]. However, the calculated heats differed by only 6% when $\mathring{a}$ values of 5.0 Å and 8.86 Å were used in the present work (see equation (41) for evaluation of B).

Although the stability constant data[10] could be in error by as much as 15%, since the conductimetric measurements were made on solutions of stoichiometric ion concentrations and the formation of a higher sulfate complex is possible, it was found that changing the value of K in the calculations by as much as 30% (literature values for $K_{EuSO_4^+}$ are 3.63×10^3 and 5.25×10^3 respectively[12]) caused less than 1.0% change in the calculated values for ΔH. Izatt and coworkers[11] had, in a much more elegant treatment of data from entropy titration experiments, previously arrived at the same conclusion, that as K becomes very large ΔH becomes independent of the value of K. Consequently, using their stability constants for the lanthanide monosulfates made essentially no difference to the calculated ΔH values. Higher complexation was avoided by keeping the lanthanide ion in excess, at least 50:1, over sulfate. There is no evidence in the literature for the existence of $Ln_2SO_4^{4+}$ or higher complexes. On the average, only 15% of the analytical metal ion concentration was in complex form while approximately 97% of the total sulfate ion was complexed. An attempt was made to determine the stability constant for $NdSO_4^+$

independently by a corresponding solutions analysis of the heat of formation as a function of concentration. However, the stability constant is too large to make such an analysis practical. Nevertheless, some confidence in the use of the empirical equation (22) to calculate activity coefficients was gained from the fact that the heats of complexation were reproducible from measurements at different metal concentrations. The uncertainty in ΔH is estimated from the standard deviation to be ± 0.4 kcal/mole. A typical set of experimental data are given for terbium sulfate in Table I. The heats of complexation for all the systems are given in Table II. A sample calculation illustrating how ΔH_T^o is obtained from the experimental data is given below for the data of Table I on terbium sulfate.

TABLE I

Terbium Sulfate

C_{Tb} = 0.0526 F; C_{SO_4} = 0.6411 F; Heat capacity, $\bar{h}_c$ = 0.178 cal./cm.;

$[TbSO_4^+]_{Total} = 0.758 \times 10^{-2}$ F; $\Delta H_{dil.\ Na_2SO_4}$ = 0.65 kcal./mole.

Volume (ml.)	Pen Displacement d (cm.)	$q_{cal} = d \times \bar{h}_c$ (cal)
32.48	----	-----
32.58	1.72	0.306
32.68	1.65	0.294
32.78	1.70	0.303
32.88	1.66	0.295

TABLE II

ENTHALPIES OF COMPLEXATION OF YTTRIUM AND THE LANTHANIDE MONOSULFATES

Ion	$10^2 F.C_M$	Total Volume (ml.)	$10^3 F[MSO_4^+]$	Heat Capacity $\bar{h}_c$ (cal/cm.)	Deflection D(cm.)	$Q=\bar{h}_c \times D$(cal.)	ΔH^o_{corr} (kcal/mole)	Mean ΔH^o_{corr} (kcal/mole)
La	5.44	32.95	7.57	0.171	6.19	1.06	3.60	
	5.44	33.12	7.53	0.174	6.03	1.05	3.56	
	5.44	33.34	7.48	0.171	5.81	1.00	3.34	3.50
Ce	4.88	33.27	7.44	0.172	6.64	1.14	3.98	
	4.88	33.40	7.41	0.176	6.34	1.12	3.87	
	4.88	33.11	7.48	0.170	6.00	1.02	3.48	3.78
Pr	4.54	33.11	7.52	0.176	6.02	1.06	3.63	
	4.54	32.88	7.52	0.174	6.78	1.18	4.13	
	4.54	32.88	7.52	0.171	6.72	1.15	4.00	3.92
Nd	4.54	32.88	7.52	0.173	7.27	1.26	4.44	
	4.54	32.88	7.52	0.174	6.52	1.13	3.93	
	4.54	32.88	7.52	0.180	6.67	1.20	4.19	
	2.27	32.98	8.73	0.170	8.07	1.37	4.11	
	1.14	32.98	7.32	0.161	7.08	1.14	4.08	4.15

TABLE II (Continued)

Ion	$10^2 F.C_M$	Total Volume (ml.)	$10^3 F[MSO_4^+]$	Heat Capacity $\bar{h}_c$ (cal/cm.)	Deflection D(cm.)	$Q=\bar{h}_c \times D$(cal.)	ΔH^o_{corr} (kcal/mole)	Mean ΔH^o_{corr} (kcal/mole)
Sm	5.20	32.88	7.59	0.173	6.56	1.14	3.91	
	5.20	32.88	7.59	0.175	7.56	1.32	4.66	
	5.20	32.88	7.59	0.172	7.38	1.27	4.45	4.34
Eu	4.79	32.88	7.55	0.175	7.56	1.32	4.67	
	4.79	32.88	7.55	0.168	6.85	1.15	3.99	
	4.79	32.88	7.55	1.167	6.53	1.09	3.74	4.13
Gd	4.72	32.88	7.55	0.177	6.52	1.16	4.01	
	2.40	32.88	7.16	0.175	6.73	1.18	4.19	
	4.72	32.88	7.55	0.178	6.61	1.18	4.10	4.10
Tb	5.26	32.88	7.58	0.166	6.94	1.15	3.97	
	5.26	32.88	7.58	0.178	6.73	1.20	4.15	
	5.26	32.88	7.58	0.175	6.54	1.15	3.95	4.02
Dy	5.12	32.88	7.55	0.166	6.12	1.02	3.43	
	5.12	32.88	7.55	0.169	6.31	1.06	3.63	
	5.88	32.88	7.54	0.169	6.40	1.08	3.67	3.58

TABLE II (Continued)

Ion	$10^2 F.C_M$	Total Volume (ml.)	$10^3 F[MSO_4^+]$	Heat Capacity $\bar{h}_c$ (cal/cm.)	Deflection D(cm.)	$Q=\bar{h}_c$ x D(cal.)	ΔH^o_{corr} (kcal/mole)	Mean ΔH^o_{corr} (kcal/mole)
Ho	4.63	32.88	7.50	0.173	6.05	1.05	3.60	
	4.63	32.88	7.50	0.166	6.39	1.06	3.65	
	4.63	32.88	7.50	0.164	6.06	0.99	3.37	3.54
Er	3.89	32.88	7.41	0.168	6.59	1.10	3.88	
	3.89	32.88	7.41	0.164	5.87	0.96	3.31	
	3.89	32.88	7.41	0.163	5.42	0.88	2.98	3.39
Tm	4.47	32.88	7.48	0.163	5.61	0.92	3.07	
	4.47	32.88	7.48	0.166	5.88	0.97	3.31	
	4.47	32.88	7.48	0.164	5.56	0.92	3.07	3.15
Yb	3.36	32.88	7.32	0.162	5.26	0.85	2.90	
	3.36	32.88	7.32	0.164	5.34	0.88	2.99	
	3.36	32.88	7.32	0.160	5.19	0.83	2.81	2.90
Lu	4.35	32.88	7.47	0.169	6.57	1.11	3.87	
	4.35	32.88	7.47	0.174	6.00	1.04	3.60	
	4.35	32.88	7.47	0.164	5.71	0.93	3.15	3.54

TABLE II (Continued)

Ion	$10^2 F.C_M$	Total Volume (ml.)	$10^3 F[MSO_4^+]$	Heat Capacity $\bar{h}_c$ (cal/cm.)	Deflection D(cm.)	$Q=\bar{h}_c$ x D(cal.)	ΔH^o_{corr} (kcal/mole)	Mean ΔH^o_{corr} (kcal/mole)
Y	4.84	32.88	7.44	0.169	6.09	1.03	3.56	
	4.84	32.88	7.44	0.161	5.71	0.92	3.11	
	4.84	32.88	7.44	0.161	5.80	0.93	3.17	3.28

Sample Calculation

To 32.48 ml. of 0.0526 F $Tb(NO_3)_3$ a total of 0.400 ml. of 0.6411 F Na_2SO_4 was added producing a total pen deflection of 6.73 cm. The average heat capacity for this run was determined to be 0.178 cal/cm. The total number of calories absorbed was

$$q_{cal} = d \cdot \bar{h}_c \tag{23}$$

$$= 6.73 \text{ cm} \times 0.178 \text{ cal/cm} = 1.198 \text{ cal.}$$

The concentration of complex, $[TbSO_4^+]$, was calculated to be 0.758×10^{-2} M, thus

$$\Delta H = 1.198 \text{ cal}/(0.758 \times 10^{-2} \text{ mol}/\ell \times 0.03288\ \ell)$$

$$= 4.80 \text{ kcal/mole}$$

The heat of dilution of the Na_2SO_4 titrant was 0.65 kcal/mole, therefore,

$$\Delta H_T^o = 4.80 - 0.65 = 4.15 \text{ kcal/mole}$$

Solutions for Kinetics

Rare earth oxides with a purity of 99.9% (American Potash and Chemical Co.) were used in the preparation of the corresponding hydrated rare earth sulfates. The oxides were dissolved in 6N HCl and then 6N H_2SO_4 was added to yield a quantitative amount of the sulfate. The sulfates were then precipitated by the addition of a large excess

of absolute ethyl alcohol. After removal of excess alcohol, the sulfates were analyzed for cation exchange on strongly acidic Dowex 50W-X8, 20-50 mesh resin. The resulting solutions were titrated to the phenolphthalein end point with standardized sodium hydroxide.

The salts were weighed as the 8-hydrate and stock solutions of approximately 0.02 M prepared; other concentrations were obtained by dilution. The concentrations were analyzed by cation exchange as before. Five ml. aliquots of the solutions were passed through columns loaded with strongly acidic Dowex 50W-X8, 20-50 mesh resin and washed with 150 ml. of deionized water. The resulting sulfuric acid was titrated to the phenolphthalein end point with standardized sodium hydroxide.

Velocity of Sound in Water

In order to determine the wavelength of sound at each temperature, for each of the six frequencies, it was necessary to measure the velocity. The "beating" of superimposed pulses, which have travelled through the liquid a different number of times, can be used to measure the wavelength, λ, of the ultrasonic wave in the liquid[53]. The velocity, c, in meters per second, is obtained from $c = \lambda f$, where λ is the wavelength in meters per cycle and f is the frequency in cycles per second. The beats are space rather than time beats in the sense that the pulse goes through consecutive maxima and minima when the liquid path length is changed. A satisfactory condition is realized by broadening the pulse so that the end of the direct pulse radiated from the oscillator (A) beats with the first ultrasonic pulse (B), which has travelled through the liquid once. A schematic diagram of the

oscilloscope trace is shown in Figure 6. The difference in the micrometer readings between two adjacent maxima equals the ultrasonic wavelength, because the phase of the oscillations within the radiated pulse

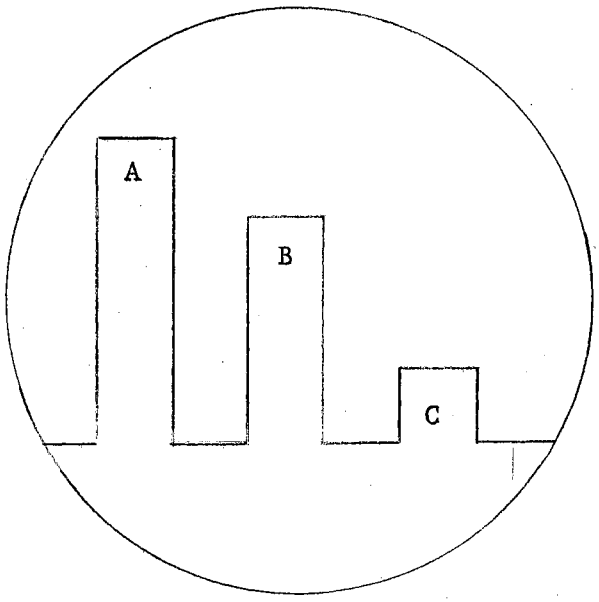

Figure 6. Oscilloscope Trace. A - direct pulse radiated from oscillator; B - first ultrasonic pulse; C - second ultrasonic pulse which has undergone double reflection in the liquid.

remains constant while that of the ultrasonic pulse picked up by the receiving crystal goes through 360° each time the path length is changed by one wavelength. Alternately, the first and second pulses of the wave train may also be used. The first pulse (B) having travelled through the liquid once, while the second (C) travels through the liquid three times. If the liquid path length is x cm for B, then the difference in ultrasonic path length for pulses B and C is 2x, so that successive maxima occur for changes in the micrometer reading equal to

$\lambda/2$.

The accuracy of velocity measurements depends upon how many beats can be counted before the absorption of the liquid or the separation of the interfering pulses makes them indistinct. All velocity measurements were made at 25 MHz and at least 50 beats were counted in determining the wavelength. The values of the velocity at 5°, 25°, and 45° are calculated from c = (Δx)(frequency)/no. beats and are given in Table III. These values agree in all cases to within 0.2% of those reported by Randall[54] from measurements at 750 Kc.

TABLE III

VELOCITY OF SOUND AS A FUNCTION OF TEMPERATURE

Temp., °C	c, meters/second
5	1425
25	1500
45	1540

Determination of Stability Constants

In sound absorption experiments priority has been given to those systems which have previously been characterized by other methods from the point of view of the equilibrium constant of the complete reaction, K_T. For the lanthanide sulfates this information was available only at 25°[10]. Values of K_T at 5° and 45° for the ions Ce(III) through Ho(III) were calculated from the known K_T values at 25° and the enthalpies of complexation, ΔH^o_T, measured calorimetrically[13] under conditions

similar to the kinetic experiments[34,35], using the familiar van't Hoff Isochore expression

$$\frac{d(\log K_T)}{d(1/T)} = -\Delta H_T^o/2.303R \qquad (24)$$

The assumption is made that the enthalpy is constant over the temperature range. A non-constant ΔH_T^o would lead to curvature in the plot of log K_T versus 1/T which would introduce some error into the calculated values of K_T. Such curvature has indeed been reported for $CrNCS^{2+}$[55] and $Co(NH_3)_5Cl^{2+}$[56] complexes. However, both are outer-sphere complexes and there is good reason to believe that it is a consequence of a purely long-range electrostatic interaction. Moreover, from the earlier remark that ΔH_T^o is insensitive to K_T[11,13], this method of calculating K_T at different temperatures might well make the difference between a calculated K_T and an experimentally measured K_T inconsequential. The calculations are based on the assumption of a constant ΔH_T^o and as such it should be appreciated that the results and observations made on the results are limited by this approximation until a more direct measure of the stability constants are made. Values for these constants for the salts studied are given in Table IV.

Kinetic Data

The attenuation of a plane progressive wave traversing a solution is given by the equation

$$I = I_o \exp(-2\alpha_T x) \qquad (25)$$

TABLE IV

STABILITY CONSTANTS AS A FUNCTION OF TEMPERATURE

	$K_T \times 10^{-3}$		
Salt/Temp	5°	25°	45°
Ce^{3+}	2.44	3.85	5.74
Pr^{3+}	2.59	4.17	6.32
Nd^{3+}	2.62	4.35	6.74
Sm^{3+}	2.69	4.55	7.21
Eu^{3+}	2.75	4.55	7.06
Gd^{3+}	2.77	4.55	7.03
Tb^{3+}	2.65	4.32	6.61
Dy^{3+}	2.65	4.08	5.97
Ho^{3+}	2.51	3.85	5.60

where I is the sound intensity at distance x, I_o is the sound intensity at distance zero, and α_T is the absorption coefficient of the solution. The experimentally measured absorption is α_T and α_{chem}, due to chemical relaxation, is obtained by subtracting the solvent contribution, α_{H_2O}

$$\alpha_{chem} = \alpha_T - \alpha_{H_2O} \tag{26}$$

Equation (26) implies strict additivity of absorption contributions. The addition of a solute to a solvent can decrease the observed absorption due to the solvent even in moderately dilute solutions. This means an error is introduced in treating the absorption of electrolytes in solution as the sum of the absorption due to the solvent and that due to the chemical relaxation processes. In most instances where chemical relaxation is involved, the overall absorption is considerably greater than that for the solvent alone and the error introduced is small. Measurements are expressed as absorption per wavelength μ_λ or $\alpha_{chem}\lambda$ where λ is determined by the ratio c_w^t/f and c_w^t is the velocity of sound in pure water at t ^oC. In dilute solutions the sound velocity does not change markedly from c_w^t .

The maximum of a relaxation curve may not always be observed within the available frequency range because theoretically a complete single relaxation occurs over one decade in frequency. The curve could be extrapolated to give a rough estimate of the maximum frequency, however, a more quantitative result is obtained if the equation for chemical relaxation

$$\alpha_T/f^2 = \frac{A'}{1 + (f/f_c)^2} + B' \qquad (27)$$

is used where B' is the absorption due to the solvent and A' is the amplitude of the chemical absorption. Equation (27) can be rearranged to read

$$\alpha_T/f^2 + \alpha_T/f_c^2 = A' + B' + \frac{B'f^2}{f_c^2}$$

or

$$\alpha_T/f^2 - B' = -\left(\frac{\alpha_T - B'f^2}{f_c^2}\right) + A'$$

but since $B' = \alpha_{H_2O}/f^2$ the expression can be further simplified to

$$\alpha_{chem}/f^2 = -\alpha_{chem}/f_c^2 + A' \qquad (28)$$

A plot of the left hand side versus α_{chem} gives A' as the intercept and $-1/f_c^2$ as the slope and hence the characteristic relaxation frequency f_c. It was found, however, that scatter in the data on such a plot provided enough latitude to draw more than one straight line. A least-squares solution was not considered desirable for curve fitting since more emphasis was generally placed on data points in the immediate vicinity of the maximum frequency. Consequently estimates of f_c from equation (28) were used in equation (7), the theoretical relaxation curve expression, to get the best fit of the observed and calcu-

lated $\alpha_{chem}\lambda$ values. Tables V-XII give the values for α_{chem}/f^2 for all of the solutions studied. Representative plots of α_{chem}/f^2 versus α_{chem} and $\log(\alpha_{chem}\lambda)$ versus log f for $SmSO_4^+$ at 5° are shown in Figures 7 and 8.

The Reaction Mechanism

The analysis of the data is based on the three-step complex formation mechanism[41]

$$\begin{array}{ccc} Ln^{3+}(aq) + SO_4^{2-}(aq) & \underset{k_{21}}{\overset{k_{12}}{\rightleftharpoons}} & [Ln^{3+}(H_2O)_2SO_4^{2-}](aq) \\ & & \Big\uparrow k_{32} \quad k_{23} \Big\downarrow \\ [Ln^{3+}SO_2^{2-}](aq) & \underset{k_{43}}{\overset{k_{34}}{\rightleftharpoons}} & [Ln^{3+}(H_2O)SO_4^{2-}](aq) \end{array} \qquad (29)$$

For a complete kinetic solution the spectra should consist of three relaxations corresponding to the three steps of the mechanism, with corresponding relaxation times given by the equations

$$1/\tau_I = 2\pi f_{cI} = k_{21} + k_{12}' \qquad (30)$$

$$1/\tau_{II} = 2\pi f_{cII} = k_{32} + \left(\frac{k_{12}'}{k_{12}' + k_{21}}\right) k_{23} = k_{32} + k_{23}' \qquad (31)$$

$$1/\tau_{III} = 2\pi f_{cIII} = k_{43} + \left(\frac{k_{23}'}{k_{23}' + k_{32}}\right) k_{34} = k_{43} + k_{34}' \qquad (32)$$

TABLE V

MEASURED CHEMICAL ABSORPTION AS A FUNCTION OF FREQUENCY AND CONCENTRATION FOR $Ce_2(SO_4)_3$

	$\alpha_{chem}/f^2 \times 10^{16}$ $\frac{db \cdot sec^2}{cm}$		
	25°		
f(MHz)	0.01617 F		
5	324.		
15	175.		
25	93.4		
35	60.7		
55	28.8		
75	17.7		
	45°		
f(MHz)	0.01617 F	0.01078 F	0.00539 F
5	168.	108.	64.0
15	121.	83.5	50.2
25	86.4	59.2	32.0
35	67.3	42.0	21.1
55	36.6	22.4	9.4
75	21.3	14.3	7.8
	$HO_2(SO_4)_3$ at 45°		
f(MHz)	0.02048 F	0.01536 F	0.01024 F
5	268.	204.	132.
15	172.	135.	88.4
25	102.	78.7	53.4
35	66.8	50.8	33.5
55	31.6	23.6	16.1
75	19.1	14.3	9.2

TABLE VI

MEASURED CHEMICAL ABSORPTION AS A FUNCTION OF FREQUENCY AND CONCENTRATION FOR $Pr_2(SO_4)_3$

$\alpha_{chem}/f^2 \times 10^{16}$ $\frac{db \cdot sec^2}{cm}$

5^o

f(MHz)	0.01960 F	0.01470 F	0.00980 F
5	664.	512.	376.
15	258.	194.	136.
25	124.	90.9	61.0
35	68.9	50.8	34.6
55	32.9	22.5	14.8
75	21.5	13.9	8.4

25^o

f(MHz)	0.01470 F	0.00980 F
5	308.	216.
15	172.	120.
25	101.	68.8
35	65.6	43.9
55	32.3	22.1
75	19.8	12.9

45^o

f(MHz)	0.01470 F	0.00980 F	0.00490 F
5	144.	124.	60.0
15	110.	80.0	45.3
25	83.7	60.2	33.6
35	65.9	45.7	25.2
55	38.7	26.3	13.5
75	24.7	14.9	8.0

TABLE VII

MEASURED CHEMICAL ABSORPTION AS A FUNCTION OF FREQUENCY AND CONCENTRATION FOR $Nd_2(SO_4)_3$

	$\alpha_{chem}/f^2 \times 10^{16}$ $\frac{db \cdot sec^2}{cm}$		
	5°		
f(MHz)	0.02034 F	0.01526 F	0.01017 F
5	596.	488.	344.
15	295.	219.	156.
25	150.	111.	73.0
35	85.4	59.3	40.9
55	43.3	26.5	18.2
75	25.7	18.6	11.3
	25°		
f(MHz)	0.01526 F		0.00508 F
5	260.		116.
15	171.		61.8
25	108.		36.9
35	74.2		23.7
55	37.7		12.9
75	23.5		8.6
	45°		
f(MHz)	0.01526 F	0.01017 F	0.00508 F
5	148.	72.0	60.0
15	105.	73.7	42.7
25	81.3	56.6	31.4
35	68.1	46.3	26.0
55	43.6	27.2	14.3
75	27.0	16.5	8.8

TABLE VIII

MEASURED CHEMICAL ABSORPTION AS A FUNCTION OF FREQUENCY AND CONCENTRATION FOR $Sm_2(SO_4)_3$

$\alpha_{chem}/f^2 \times 10^{16}$ $\frac{db \cdot sec^2}{cm}$

f(MHz)	0.00949 F	0.00474 F	0.00237 F
	5°		
5	208.	151.	69.2
15	150.	81.3	44.4
25	102.	52.2	25.1
35	68.9	34.0	15.8
55	34.4	16.6	7.7
75	20.4	10.0	5.8
	25°		
f(MHz)	0.00976 F	0.00488 F	0.00244 F
5	105.	73.6	43.6
15	91.6	52.0	28.9
25	72.8	38.6	19.5
35	53.9	29.1	13.6
55	33.7	16.5	7.5
75	19.1	10.5	4.4
	45°		
f(MHz)	0.01460 F	0.00976 F	0.00488 F
5	160.	80.0	64.0
15	71.1	53.5	37.4
25	63.6	43.7	24.5
35	52.5	37.0	20.8
55	39.0	25.4	13.2
75	25.4	16.8	8.5

TABLE IX

MEASURED CHEMICAL ABSORPTION AS A FUNCTION OF FREQUENCY AND CONCENTRATION FOR $Eu_2(SO_4)_3$

$\alpha_{chem}/f^2 \times 10^{16}$ $\frac{db \cdot sec^2}{cm}$

5°

f(MHz)	0.02002 F	0.01502 F	0.01001 F
5	378.	304.	218.
15	272.	203.	150.
25	174.	131.	83.5
35	128.	84.8	58.4
55	63.1	41.8	32.4
75	37.1	24.0	18.3

25°

f(MHz)	0.01502 F	0.00500 F
5	160.	80.0
15	125.	49.8
25	93.6	33.8
35	74.8	25.4
55	45.6	15.2
75	29.0	9.5

45°

f(MHz)	0.01502 F	0.01001 F	0.00569 F
5	140.	52.0	40.2
15	73.3	54.4	34.0
25	62.4	40.5	28.5
35	54.4	40.0	24.3
55	39.0	26.5	16.2
75	27.8	16.5	10.9

TABLE X

MEASURED CHEMICAL ABSORPTION AS A FUNCTION OF FREQUENCY AND CONCENTRATION FOR $Gd_2(SO_4)_3$

	$\alpha_{chem}/f^2 \times 10^{16}$ $\frac{db \cdot sec^2}{cm}$		
	5°		
f(MHz)	0.01528 F	0.01019 F	0.00510 F
5	288.	208.	80.0
15	194.	136.	56.4
25	130.	88.8	33.1
35	73.4	53.0	20.7
55	38.0	27.1	9.8
75	21.5	15.8	4.9
	25°		
f(MHz)	0.01528 F		
5	180.		
15	128.		
25	93.0		
35	70.8		
55	43.5		
75	25.5		
	45°		
f(MHz)	0.01528 F	0.01019 F	0.00510 F
5	80.0	76.0	68.0
15	74.2	59.1	31.6
25	66.2	48.2	26.1
35	57.1	41.4	22.9
55	40.2	27.1	14.0
75	28.2	19.2	9.5

TABLE XI

MEASURED CHEMICAL ABSORPTION AS A FUNCTION OF FREQUENCY AND CONCENTRATION FOR $Tb_2(SO_4)_3$ [55]

	$\alpha_{chem}/f^2 \times 10^{16}$ $\frac{db \cdot sec^2}{cm}$		
	5°		
f(MHz)	0.01008 F	0.00543 F	0.00310 F
5	208.	116.	40.1
15	126.	65.3	18.4
25	71.0	37.9	9.1
35	42.3	20.0	5.4
55	15.2	10.5	2.8
75	11.2	6.2	2.0
	25°		
f(MHz)	0.01500 F		0.00499 F
5	192.		103.
15	140.		57.6
25	91.2		34.6
35	63.8		22.3
55	36.8		11.2
75	20.6		7.4
	45°		
f(MHz)	0.01551 F	0.01008 F	0.00543 F
5	120.0	97.0	50.0
15	84.9	75.1	34.7
25	72.5	47.0	30.6
35	60.2	37.6	21.4
55	31.7	22.6	12.6
75	25.8	15.8	7.1

TABLE XII

MEASURED CHEMICAL ABSORPTION AS A FUNCTION OF FREQUENCY AND CONCENTRATION FOR $Dy_2(SO_4)_3$

$\alpha_{chem}/f^2 \times 10^{16}$ $\frac{db \cdot sec^2}{cm}$

5^o

f(MHz)	0.02023 F	0.01517 F	0.01012 F
5	668.	404.	304.
15	206.	159.	107.
25	96.3	73.0	48.8
35	56.1	41.3	25.5
55	26.3	18.2	11.4
75	13.2	10.7	6.6

25^o

f(MHz)	0.01517 F
5	310.
15	158.
25	85.6
35	53.6
55	27.3
75	15.9

45^o

f(MHz)	0.01517 F	0.01012 F	0.00506 F
5	124.	116.	108.
15	113.	78.2	43.6
25	79.0	53.9	27.5
35	57.2	41.0	20.8
55	32.8	22.6	11.8
75	19.9	13.9	7.1

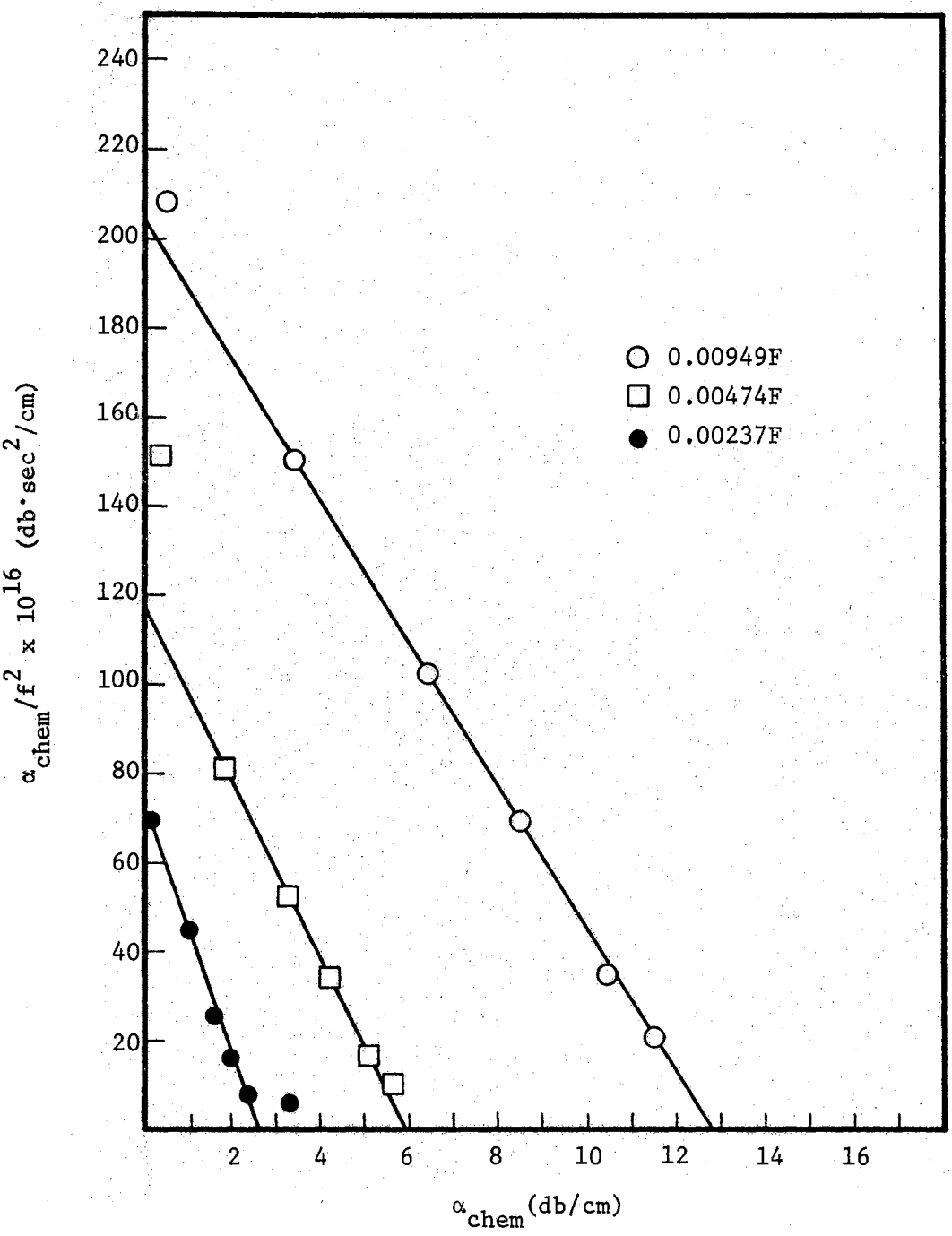

Figure 7. Plot of α_{chem}/f^2 Versus α_{chem} for $Sm_2(SO_4)_3$ at 5°. The Slope is Equal to $-1/f^2_{cIII}$ and the Intercept is A'.

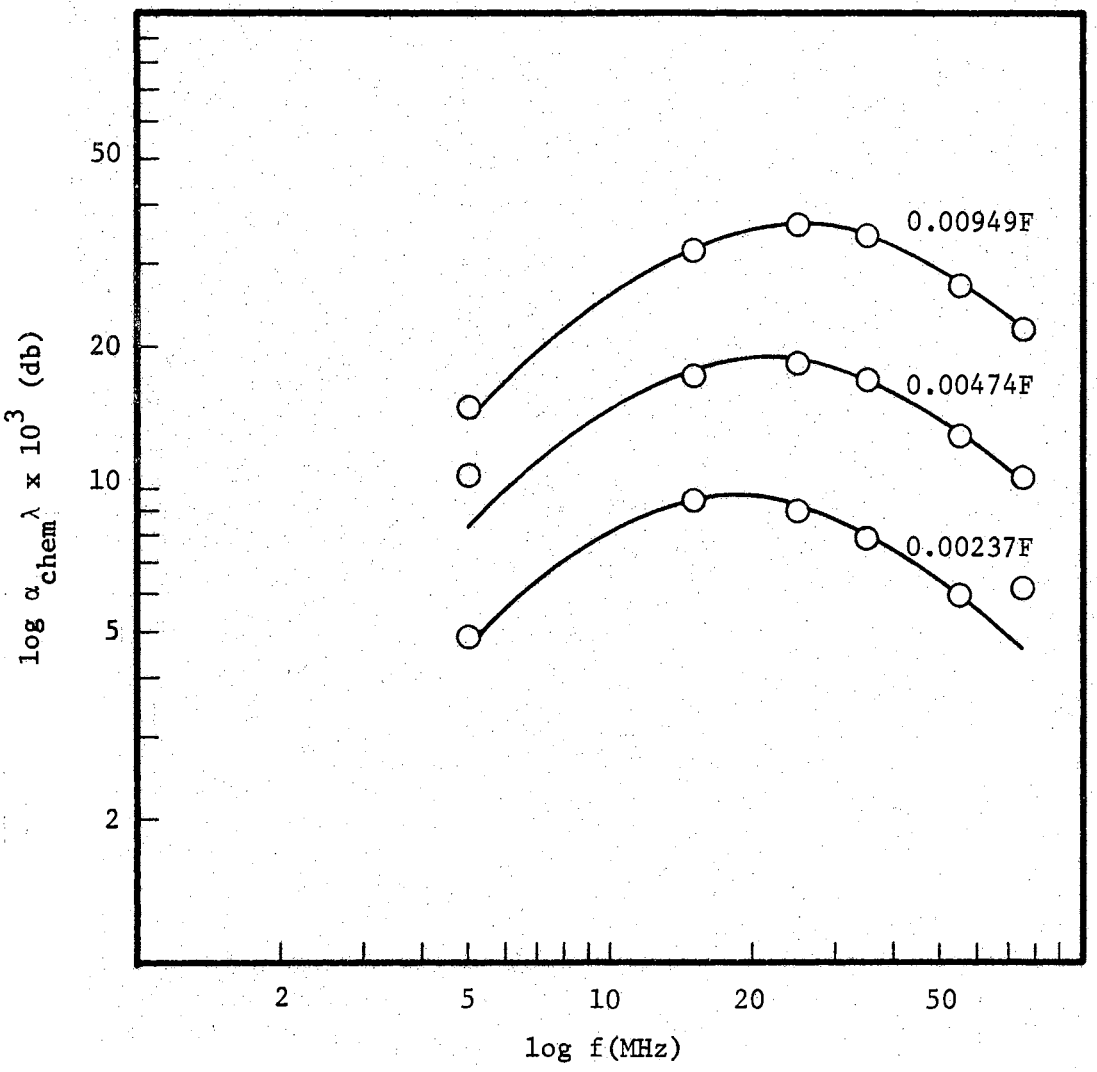

Figure 8. Sound Absorption Curves for Solutions of $Sm_2(SO_4)_3$ at 5°.

where τ_i = relaxation time and f_{ci} = frequency of maximum absorption for step i; k_{12}' involves a correction for activities of the ions since step I is bimolecular. For small perturbations

$$k_{12}' = k_{12}^{o}\, \pi_f \{[Ln^{3+}] + [SO_4^{2-}] + [SO_4^{2-}](\frac{\partial \ln \pi_f}{\partial \ln [Ln^{3+}]})\} \quad (33)$$

where k_{12}^{o} is the rate constant at zero ionic strength, π_f is the activity coefficient quotient $\gamma_{3+}\, \gamma_{2-}/\gamma_{\pm}$, and $[Ln^{3+}]$ and $[SO_4^{2-}]$ represent the equilibrium free ion concentrations in solution. If the concentration of solute is C_i mole/ℓ. of $Ln_2(SO_4)_3$ and β is the degree of association at equilibrium, the total concentration of the 1:1 associated species is $2\beta C_i$ mole/ℓ. The ion concentrations are therefore $[Ln^{3+}] = 2(1 - \beta)C_i$ mole/ℓ. and $[SO_4^{2-}] = (3 - 2\beta)C_i$ mole/ℓ., respectively. Equation (33) then becomes

$$k_{12}' = k_{12}^{o}\, \pi_f C_i \{(5 - 4\beta) + [(3 - 2\beta)\frac{\partial \ln \pi_f}{\partial \ln \beta}]_{C_i}\} \quad (34)$$

The rate expressions can be rewritten in terms of concentration and equilibrium constants:

$$2\pi f_{cI} = k_{21} + k_{12}^{o}\, [\theta(C)] \quad (35)$$

$$2\pi f_{cII} = k_{32} + [\frac{\theta(C)}{K_{12}^{-1} + \theta(C)}]\, k_{23} \quad (36)$$

$$2\pi f_{cIII} = k_{43} + [\frac{\theta(C)}{(K_{12}K_{23})^{-1} + (1 + K_{23}^{-1})[\theta(C)]}]\, k_{34}$$

$$= k_{43} + \Phi(C)\, k_{34} \tag{37}$$

where K_{12}, K_{23}, and K_{34} are thermodynamic equilibrium constants for steps (I), (II), and (III) respectively, defined as $K_{12} = k_{12}/k_{21}$, $K_{23} = k_{23}/k_{32}$, $K_{34} = k_{34}/k_{43}$, and

$$\theta(C) = \pi_f C_i \{(5 - 4\beta) + [(3 - 2\beta) \frac{\partial \ln \pi_f}{\partial \ln \beta}]_{C_i}\} \tag{38}$$

β was calculated for each value of C_i by a standard iteration procedure, similar to that discussed in the calorimetric section, by using the total thermodynamic equilibrium constants, where available, derived from conductivity measurements[10] or calculated as previously described. The activity coefficients γ_{3+}, γ_{2-}, and $\gamma_{\pm}$ were evaluated using a modified form of the Davies equation[51],

$$- \log \gamma_i = A z_i^2 \{\frac{\mu^{\frac{1}{2}}}{1 + Ba^{o}\mu^{\frac{1}{2}}} - 0.3\mu\} \tag{39}$$

where μ is the ionic strength $= 3C_i + 12(1 - \beta)C_i$, A and B are the parameters in the Debye-Hückel Theory of Electrolytes[58] which, in the purely electrostatic model, describe long-range and short-range interactions respectively, and are given by

$$A = (\frac{2\pi N_L}{1000})^{\frac{1}{2}} \cdot \frac{e^3}{2.303k^{3/2}} \cdot \frac{1}{(\varepsilon T)^{3/2}} = \frac{1.8246 \times 10^6}{(\varepsilon T)^{3/2}} (\frac{\ell \cdot {}^{o}K^3}{\text{mole}})^{\frac{1}{2}} \tag{40}$$

$$B = (\frac{8\pi N_L e^2}{1000k})^{\frac{1}{2}} \frac{1}{(\varepsilon T)^{\frac{1}{2}}} = \frac{50.29 \times 10^8}{(\varepsilon T)^{\frac{1}{2}}} (\frac{\ell \cdot {}^{o}K}{\text{mole} \cdot \text{cm}})^{\frac{1}{2}} \tag{41}$$

where ε is the macroscopic dielectric constant of the solvent, N_L is Avogadro's number, e is the electronic charge, k is the Boltzmann constant, T is the absolute temperature, and $\overset{o}{a}$ is the distance of closest approach of the ions. To be consistent with the theoretical calculation of K_{12}, required in the solution of equation (37), $\overset{o}{a}$ was taken as the sum of the ionic radii plus two water molecule diameters, or $r_{Ln^{3+}} + 7.82\ \overset{o}{A}$. The solution of the derivative term in the expression for $\theta(C)$ was evaluated according to[46]

$$\partial \ln \pi_f / \partial \ln \beta = \partial \ln \pi_f / \partial \mu \cdot \partial \mu / \partial \ln \beta \qquad (42)$$

From the Davies equation (39), where γ_i is a function of μ, it can be shown by partial differentiation that

$$\partial \ln \gamma_i / \partial \mu = -Mz_i^2 \left[(1 + B\overset{o}{a}\mu^{\frac{1}{2}})^{-2} (\tfrac{1}{2}\mu^{-\frac{1}{2}}) - 0.3 \right] \qquad (43)$$

and since

$$\partial \ln \pi_f / \partial \mu = \frac{\partial \ln \gamma_{3+}}{\partial \mu} + \frac{\partial \ln \gamma_{2-}}{\partial \mu} - \frac{\partial \ln \gamma_{\pm}}{\partial \mu} \qquad (44)$$

that

$$\partial \ln \pi_f / \partial \mu = -MA(z^2_{Ln^{3+}} + z^2_{SO_4^{2-}} - z^2_{LnSO_4^{+}}) \left[\frac{1}{2\mu^{\frac{1}{2}}(1 + B\overset{o}{a}\mu^{\frac{1}{2}})} - 0.3 \right] \qquad (45)$$

Partial differentiation of the expression for the ionic strength with respect to $\ln \beta$ gives

$$\partial \mu / \partial \ln \beta = \beta \cdot \partial \mu / \partial \beta = \beta C_i (z^2_{Ln^{3+}} + z^2_{SO_4^{2-}} - z^2_{LnSO_4^{+}}) \qquad (46)$$

Equations (45) and (46) may then be combined to give

$$\frac{\partial \ln \pi_f}{\partial \ln \beta} = - MA\beta C_i \left(z^2_{Ln^{3+}} + z^2_{SO_4^{=}} - z^2_{LnSO_4^{+}}\right)\left[\frac{1}{2\mu^{\frac{1}{2}}(1 + B\mathring{a}\mu^{\frac{1}{2}})^2} - 0.3\right] \quad (47)$$

where M = 2.302585 and the other parameters are as previously defined (see Appendix B for computer program).

If it can be argued that the chemical relaxation is a result of step III, the rate constants, and hence K_{34}, can be obtained from a graphical solution of equation (37). The unknowns in this equation are K_{12}^{-1} and K_{23}^{-1}. K_{12}^{-1} was calculated using the Bjerrum equation[58]

$$K_{12} = \frac{4\pi N_L \mathring{a}^3}{1000} b^3 Q(b) \quad (48)$$

where

$$b = \frac{|z_{Ln^{3+}} z_{SO_4^{2-}}|e^2}{\epsilon k T \mathring{a}} \quad (49)$$

and

$$Q(b) = \int_2^b b^{-4} e^b \, db \quad (50)$$

and was essentially independent of the small changes in $\mathring{a}$ for the series. In the original work at 25° K_{23}^{-1} was taken to be 0.51, the value for $MgSO_4$.[59] Additional calculations showed that k_{43} was insensitive to K_{23}^{-1} within the range of 0.1 to 1.0, but that the value of k_{34} increased proportionately.

The overall thermodynamic association constant, K_T, is related to the equilibrium steps by the expression (see Chapter I)

$$K_T = K_{12} (1 + K_{23} + K_{23}K_{34}) \quad (5)$$

In subsequent work[35] at 25°, a reiterative procedure using equations (37) and (5) was used to calculate a value of K_{23}^{-1} for samarium to give good agreement between K_T obtained kinetically with that obtained conductimetrically. This value, $K_{23}^{-1} = 0.72$, was then used in the determination of k_{34} and k_{43} for the remaining ions. The agreement between the kinetic and conductimetric values was acceptable in most cases.

From equation (37) the plot of $2\pi f_{cIII}$ gives k_{34} as slope and k_{43} as intercept. The evaluation of k_{43} is complicated by the fact that the intercept at $\Phi(C) = 0$ is negative. However, when A' from equation (28) is plotted as a function of $\Phi(C)$ a zero value of A' is obtained at a finite value of $\Phi(C)$, indicating that a certain limiting concentration of complex must be present in solution before absorption in excess of the solvent is observed. This limiting value of $\Phi(C)$ was used to determine the value of k_{43}. A typical plot for these functions for $SmSO_4^+$ at 5° is shown in Figure 9.

It was observed in this study that A' was not a particularly linear function of $\Phi(C)$, especially at concentrations below approximately 0.005 M. Scrutiny of the previous data at 25° suggested that some of these solutions should be investigated at higher concentrations, i.e. greater than 0.010 M. Thus, in addition to the studies at 5° and 45°, measurements were made for Ce(III), Pr(III), Nd(III), Sm(III), Eu(III), Gd(III), Tb(III), and Dy(III) at higher concentrations

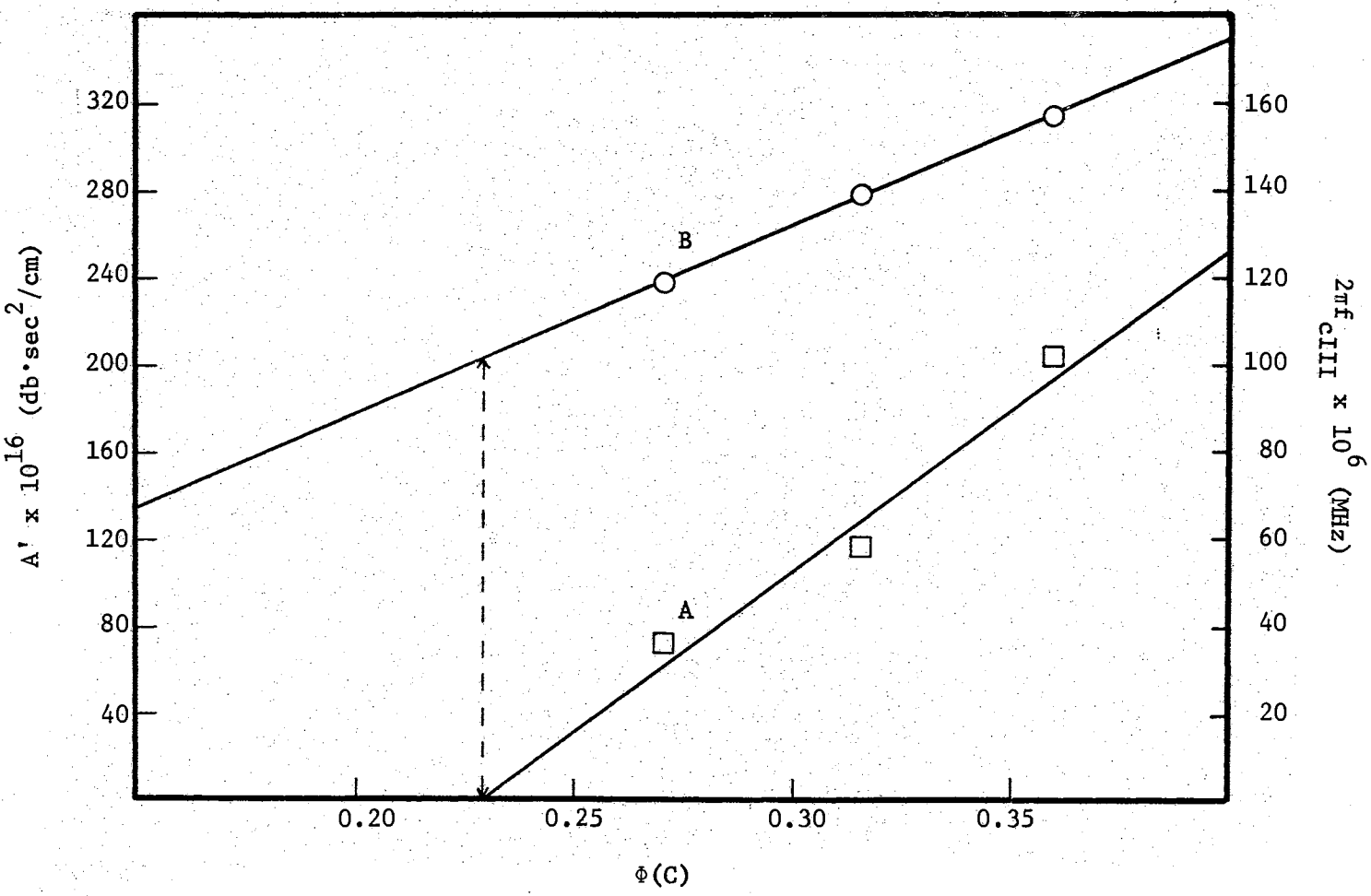

Figure 9. Plots of $2\pi f_{cIII}$ Versus $\Phi(C)$ (Line B) and A' Versus $\Phi(C)$ (Line A). The Slope of Line B is Equal to k_{34} and the Zero Value of Line A Gives k_{43}.

than in previous studies (see Tables V-XII).

In an attempt to improve the treatment of the data a computer program was written (Appendix C), which used the values of $\theta(C)$, $\Phi(C)$, $2\pi f_{cIII}$, and A' at three concentrations (see Tables XIII-XV) to calculate least-squares lines through the data, and evaluate k_{34}, k_{43}, K_{34}, and K_{23}. A reiterative procedure was used based on equation (37), which gives the expression for $\Phi(C)$ also and the equation for K_T (5). The process was iterated until the difference between consecutive values of K_{23}^{-1} was less than 0.0001. On the average, 5 iterations were sufficient to give the necessary kinetic parameters. These values are given in Table XVI.

Activation parameters applicable at 25^o for the third step in the mechanism were then obtained from the kinetic constants at 5^o, 25^o, and 45^o. From transition-state theory $K^{\ddagger}$ values for the forward and for the reverse reactions may be calculated from

$$K^{\ddagger} = \left(\frac{h}{kT}\right) k_{ij} \qquad (51)$$

where h and k have their usual meaning and k_{ij} is the forward or the reverse rate constant respectively for step III at 25^o[60]. The free energies of activation, $\Delta G^{\ddagger}$, are given by

$$\Delta G^{\ddagger} = - RT \ln K^{\ddagger} \qquad (52)$$

Activation energies, E_a, for both forward and reverse processes are obtained from the slopes of the plots of $\log k_{34}$ and $\log k_{43}$ versus $1/T$ according to

TABLE XIII

RELAXATION FREQUENCY DATA AT 5°

Ion	Conc. x 10^2(F)	$2\pi f_{cIII}$(MHz)	A' x 10^{16} ($\frac{db \cdot sec^2}{cm}$)	θ(C) x 10^2	Φ(C) (Final)
Pr^{3+}	1.960	74.7	670.0	0.418	0.496
	1.470	71.0	538.0	0.344	0.476
	0.980	67.8	397.0	0.269	0.448
Nd^{3+}	2.034	82.9	680.0	0.428	0.417
	1.526	77.2	544.0	0.352	0.398
	1.017	72.8	411.0	0.274	0.372
Sm^{3+}	0.949	157.0	204.0	0.262	0.360
	0.474	138.8	117.0	0.180	0.316
	0.237	118.7	72.5	0.128	0.271
Eu^{3+}	2.002	147.0	383.0	0.418	0.407
	1.502	139.4	296.0	0.344	0.389
	1.001	127.5	231.5	0.269	0.362
Gd^{3+}	1.528	151.3	270.0	0.347	0.416
	1.019	140.7	199.0	0.271	0.389
	0.510	121.2	88.5	0.186	0.343
Tb^{3+}	1.008	105.5	226.0	0.352	0.335
	0.543	92.3	132.5	0.270	0.309
	0.310	80.0	44.0	0.193	0.273

TABLE XIII (Continued)

Ion	Conc. x 10^2(F)	$2\pi_{cIII}$(MHz)	A' x 10^{16} ($\frac{db \cdot sec^2}{cm}$)	θ(C) x 10^2	Φ(C) (Final)
Dy^{3+}	2.023	73.5	550.0	0.421	0.266
	1.517	69.1	455.0	0.347	0.251
	1.012	61.5	358.0	0.271	0.231

TABLE XIV

RELAXATION FREQUENCY DATA AT 25°

Ion	Conc. x 10^2(F)	$2\pi_{cIII}$(MHz)	A' x 10^{16} ($\frac{db \cdot sec^2}{cm}$)	θ(C) x 10^2	Φ(C) (Final)
Ce^{3+}	1.617	114.6	283.2	0.335	0.489
	0.980	105.3	227.5	0.247	0.455
	0.490	92.5	149.0	0.169	0.406
Pr^{3+}	1.470	141.9	224.5	0.312	0.554
	0.980	130.9	168.5	0.244	0.526
	0.538	120.0	97.0	0.176	0.483
Nd^{3+}	1.526	160.1	216.0	0.318	0.527
	0.961	147.6	164.5	0.240	0.495
	0.508	129.4	92.8	0.170	0.449
Sm^{3+}	0.976	239.3	103.0	0.241	0.493
	0.488	208.5	61.0	0.165	0.443
	0.244	177.7	35.0	0.116	0.389
Eu^{3+}	1.502	265.6	126.0	0.312	0.528
	0.980	248.4	98.5	0.241	0.500
	0.500	218.5	51.2	0.167	0.454
Gd^{3+}	1.528	222.9	140.0	0.315	0.507
	0.950	207.0	87.7	0.237	0.474
	0.470	171.0	48.0	0.162	0.424

TABLE XIV (Continued)

Ion	Conc. x 10^2(F)	$2\pi_{cIII}$(MHz)	A' x 10^{16} ($\frac{db \cdot sec^2}{cm}$)	θ(C) x 10^2	Φ(C) (Final)
Tb^{3+}	1.500	172.7	167.0	0.312	0.466
	0.998	157.0	129.6	0.244	0.439
	0.499	133.1	65.5	0.168	0.391
Dy^{3+}	1.517	116.0	269.0	0.316	0.455
	0.970	104.2	166.0	0.242	0.425
	0.650	92.9	70.5	0.194	0.398
Ho^{3+}	1.536	72.0	380.0	0.320	0.374
	1.076	66.6	320.0	0.257	0.352
	0.538	55.9	202.5	0.176	0.309

TABLE XV

RELAXATION FREQUENCY DATA AT 45°

Ion	Conc. x 10^2(F)	$2\pi_{cIII}$(MHz)	A' x 10^{16} ($\frac{db \cdot sec^2}{cm}$)	θ(C) x 10^2	Φ(C) (Final)
Ce^{3+}	1.617	197.8	145.0	0.306	0.501
	1.078	182.7	103.0	0.239	0.474
	0.539	151.3	66.5	0.163	0.426
Pr^{3+}	1.470	234.2	124.0	0.286	0.534
	0.980	212.9	95.5	0.224	0.507
	0.490	182.7	61.8	0.154	0.458
Nd^{3+}	1.526	265.6	115.0	0.291	0.608
	1.017	240.5	83.0	0.228	0.582
	0.508	215.4	51.0	0.156	0.533
Sm^{3+}	1.460	331.0	77.0	0.281	0.632
	0.976	305.0	57.2	0.221	0.607
	0.488	270.0	31.7	0.151	0.559
Eu^{3+}	1.502	364.9	74.3	0.286	0.618
	1.001	341.6	53.6	0.224	0.592
	0.569	304.0	37.1	0.164	0.553
Gd^{3+}	1.528	348.5	79.5	0.289	0.654
	1.019	314.0	61.5	0.226	0.629
	0.510	297.0	33.5	0.155	0.582

TABLE XV (Continued)

Ion	Conc. x 10^2(F)	$2\pi_{cIII}$(MHz)	A' x 10^{16} ($\frac{db \cdot sec^2}{cm}$)	θ(C) x 10^2	Φ(C) (Final)
Tb^{3+}	1.551	280.2	79.0	0.292	0.585
	1.008	248.7	65.6	0.226	0.557
	0.543	233.0	42.0	0.161	0.514
Dy^{3+}	1.517	203.5	126.0	0.290	0.581
	1.012	186.5	98.0	0.227	0.555
	0.506	166.4	57.5	0.156	0.507
Hb^{3+}	2.048	138.8	234.0	0.354	0.574
	1.536	128.7	200.0	0.293	0.556
	1.024	123.1	141.0	0.230	0.530

TABLE XVI

VALUES OF RATE CONSTANTS AND ASSOCIATION CONSTANTS AS FUNCTIONS OF TEMPERATURE

Ion	Temp.(°C)	$k_{34} \times 10^{-8}(sec^{-1})$	$k_{43} \times 10^{-8}(sec^{-1})$	K_{34}	K_{23}	$K_{12} \times 10^{-2}(\ell/mole)$	$K_T \times 10^{-3}(\ell/mole)$
Ce^{3+}	[a] 5	0.98	0.37	2.65	1.55	3.91	2.44
	25	2.65	0.68	3.90	1.62	4.31	3.85
	45	6.26	1.15	5.44	1.67	4.88	5.74
Pr^{3+}	5	1.46	0.58	2.54	1.58	3.92	2.59
	25	3.08	1.03	3.00	2.16	4.32	4.17
	45	6.70	1.32	5.06	1.97	4.89	6.32
Nd^{3+}	5	2.26	0.57	3.97	1.14	3.93	2.62
	25	3.94	1.06	3.71	1.92	4.33	4.35
	45	6.72	1.75	3.83	2.64	4.90	6.74
Sm^{3+}	5	4.28	1.01	4.23	1.11	3.96	2.69
	25	5.94	1.50	3.97	1.90	4.36	4.55
	45	8.23	2.28	3.62	2.95	4.93	7.21
Eu^{3+}	5	4.36	0.99	4.39	1.10	3.96	2.75
	25	6.45	1.86	3.46	1.84	4.37	4.55
	45	9.44	2.48	3.81	2.76	4.94	7.06
Gd^{3+}	5	4.12	1.07	3.86	1.23	3.97	2.77
	25	6.37	1.48	4.30	1.78	4.37	4.55
	45	7.76	2.49	3.11	3.21	4.95	7.03

TABLE XVI (Continued)

Ion	Temp. (°C)	$k_{34} \times 10^{-8}$ (sec^{-1})	$k_{43} \times 10^{-8}$ (sec^{-1})	K_{34}	K_{23}	$K_{12} \times 10^{-2}$ (ℓ/mole)	$K_T \times 10^{-3}$ (ℓ/mole)
Tb^{3+}	5	4.10	0.74	5.55	0.86	3.98	2.65
	25	5.21	1.07	4.85	1.51	4.39	4.32
	45	7.08	1.70	4.16	2.38	4.96	6.61
Dy^{3+}	5	3.45	0.39	8.77	0.58	3.99	2.65
	25	4.04	0.85	4.76	1.44	4.40	4.08
	45	4.96	1.35	3.68	2.35	4.97	5.97
Ho^{3+}	[a] 5	1.50	0.12	12.3	0.42	4.00	2.51
	25	2.46	0.38	6.56	1.02	4.41	3.85
	45	3.71	0.97	3.84	2.11	4.99	5.60

[a] Estimated From Graph.

$$\frac{d\ (\log k_{ij})}{d\ (1/T)} = -E_a/2.303\ R \qquad (53)$$

Enthalpies of activation, $\Delta H^{\ddagger}$, are calculated from

$$\Delta H^{\ddagger} = E_a - RT \qquad (54)$$

and the entropies of activation, $\Delta S^{\ddagger}$, by

$$\Delta S^{\ddagger} = (\Delta H^{\ddagger} - \Delta G^{\ddagger})/T \qquad (55)$$

The activation parameters are listed in Table XVII.

From plots of log K_{12}, log K_{23}, and log K_{34} versus 1/T the individual values for the change in enthalpy at 25° accompanying each step are determined from the respective slopes which are $-\Delta H_{ij}/2.303\ R$. The plots of log k_{ij} and log K_{ij} versus 1/T are shown in Figures 10-18. The value of ΔH_{12} was constant throughout the series at 0.97 kcal/mole and this plot is not shown. From equations (2), (3) and the values for the K_{ij} at 25°, the values of ΔG and ΔS may be obtained. The thermodynamic quantities obtained may then be summed according to Hess' Law to give the total change for each particular parameter. These individual values and their sums are compared with the values determined calorimetrically in Table XVIII.

Although there is considerable evidence to support a three-step mechanism, it has been suggested that the data be treated by a two-step mechanism in which steps I and II of equation (29) are combined into one step and are defined by one association constant, K_{13}. This

TABLE XVII

VALUES OF THE ACTIVATION PARAMETERS FOR THE REACTION $Ln^{3+}H_2O\ SO_4^{2-} \rightleftharpoons Ln^{3+}SO_4^{2-} + H_2O$ AT 25°

Ion	$K^{\ddagger} \times 10^5$	E_a(kcal/mole)	$\Delta H^{\ddagger}$(kcal/mole)	$\Delta G^{\ddagger}$(kcal/mole)	$\Delta S^{\ddagger}$(cal/mole·deg)
Ce^{3+}					
Forward	4.26	8.10	7.51	5.96	5.20
Reverse	1.09	4.97	4.38	6.77	- 8.02
Pr^{3+}					
Forward	4.96	6.69	6.10	5.87	0.77
Reverse	1.66	3.66	3.07	6.52	-11.57
Nd^{3+}					
Forward	6.34	4.80	4.21	5.73	- 5.10
Reverse	1.71	4.95	4.36	6.50	- 7.18
Sm^{3+}					
Forward	9.56	2.87	2.28	5.48	-10.73
Reverse	2.41	3.56	2.97	6.30	-11.17
Eu^{3+}					
Forward	10.38	3.40	2.81	5.45	- 8.85
Reverse	3.00	4.01	3.42	6.17	- 9.22
Gd^{3+}					
Forward	10.25	2.78	2.19	8.17	-20.06
Reverse	2.38	3.73	3.14	6.31	-10.63

TABLE XVII (Continued)

Ion	$K^{\ddagger} \times 10^5$	E_a (kcal/mole)	$\Delta H^{\ddagger}$ (kcal/mole)	$\Delta G^{\ddagger}$ (kcal/mole)	$\Delta S^{\ddagger}$ (cal/mole·deg)
Tb^{3+}					
Forward	8.38	2.40	1.81	5.56	-12.58
Reverse	1.73	3.67	3.08	6.50	-11.47
Dy^{3+}					
Forward	6.50	1.59	1.00	5.71	-15.80
Reverse	1.36	5.41	4.82	6.64	- 6.10
Ho^{3+}					
Forward	3.96	3.87	3.28	6.01	- 9.16
Reverse	0.60	8.90	8.31	4.39	-13.15

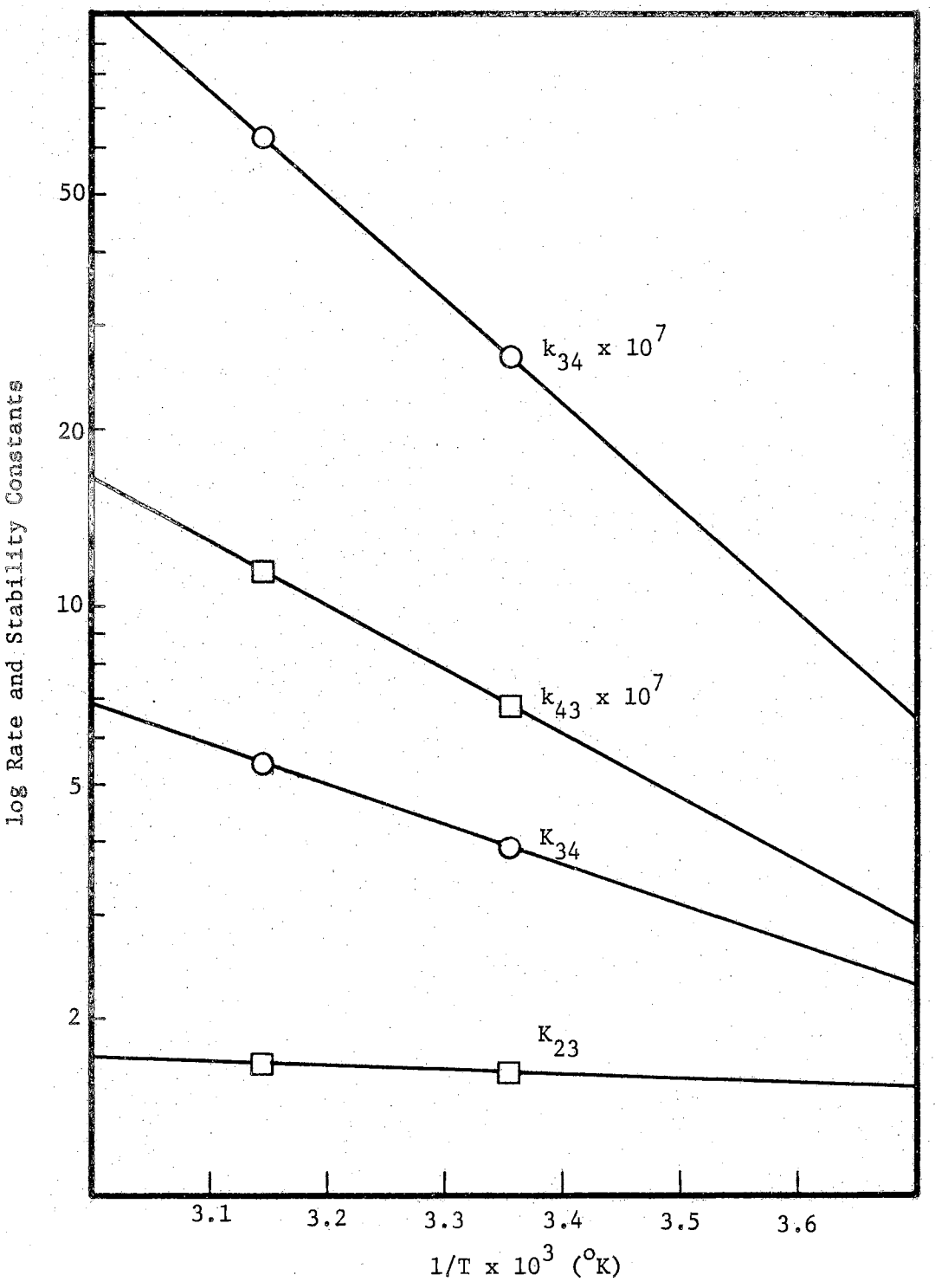

Figure 10. Plots of Rate Constants and Stability Constants for $Ce_2(SO_4)_3$ Versus 1/T (°K).

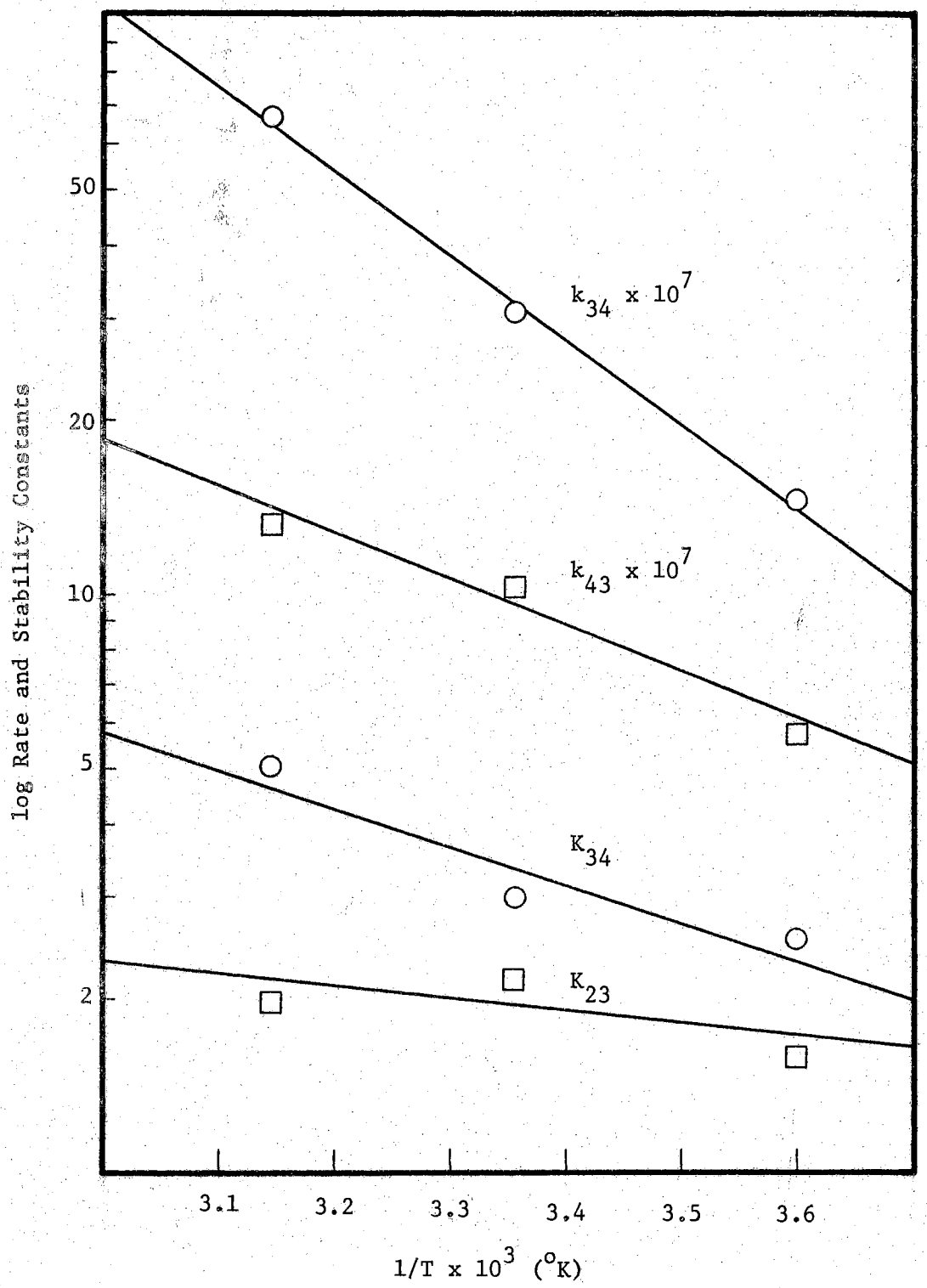

Figure 11. Plots of Rate Constants and Stability Constants for $Pr_2(SO_4)_3$ Versus 1/T (°K).

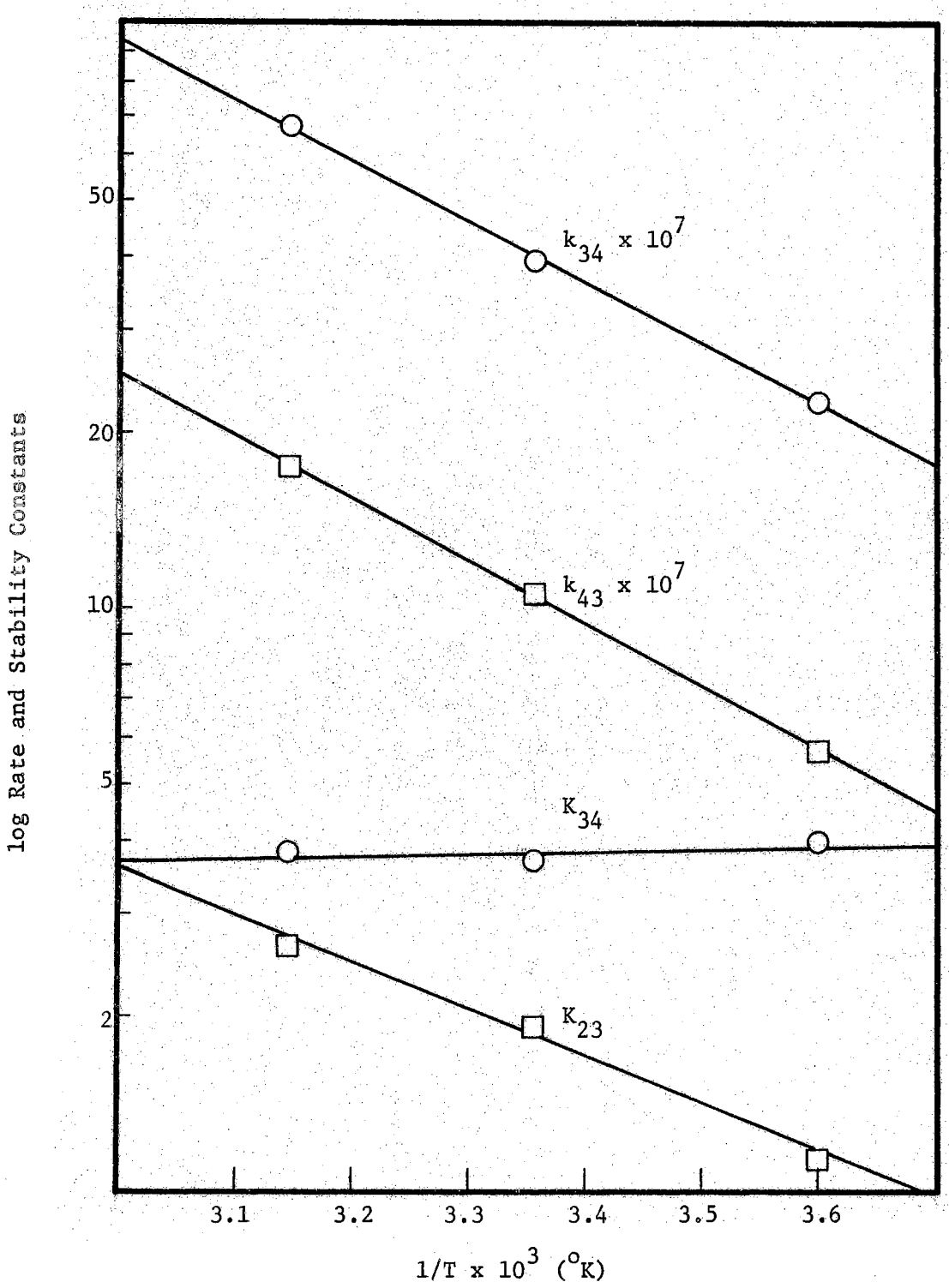

Figure 12. Plots of Rate Constants and Stability Constants for $Nd_2(SO_4)_3$ Versus 1/T (°K).

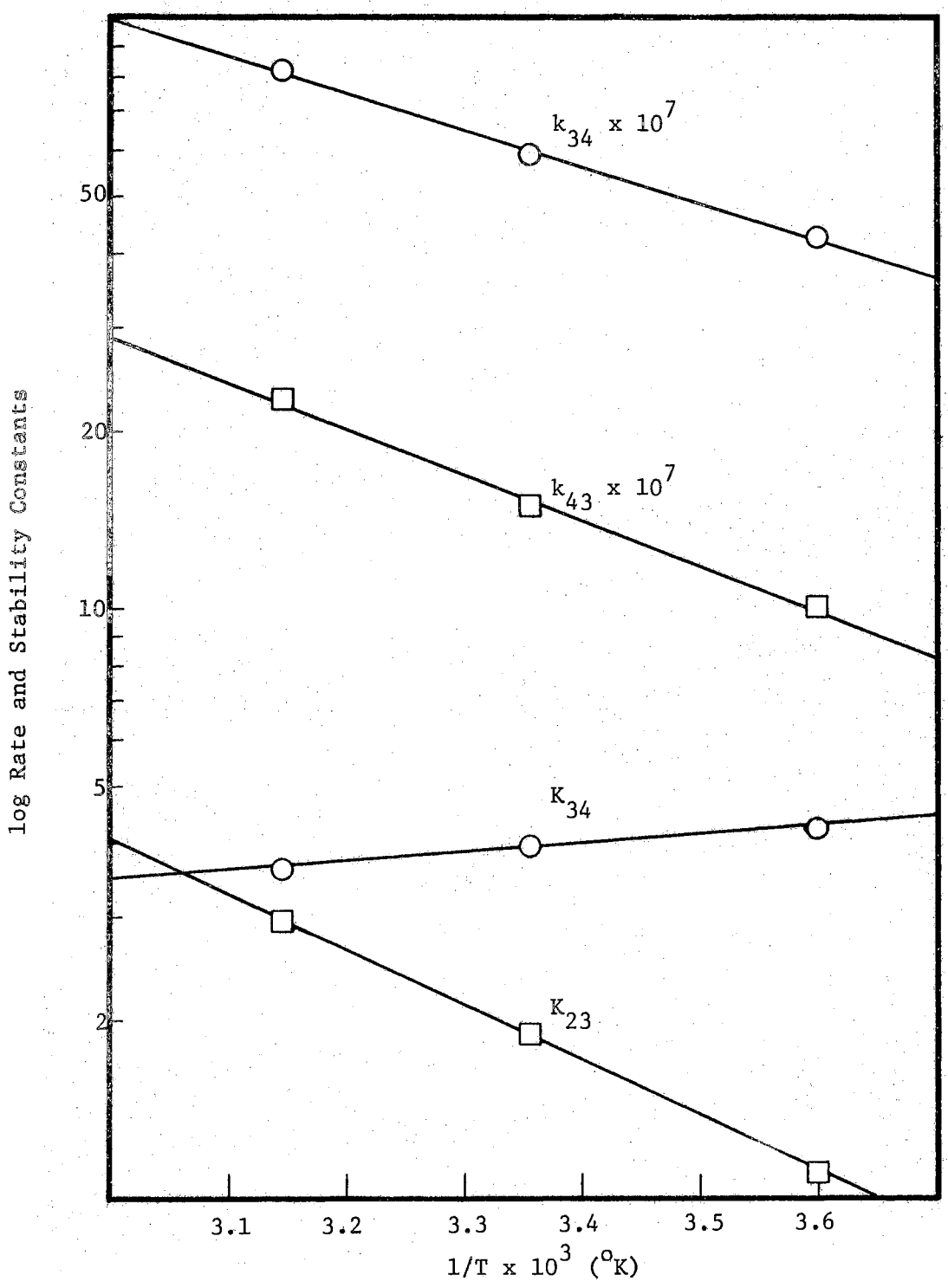

Figure 13. Plots of Rate Constants and Stability Constants for $Sm_2(SO_4)_3$ Versus 1/T (^oK).

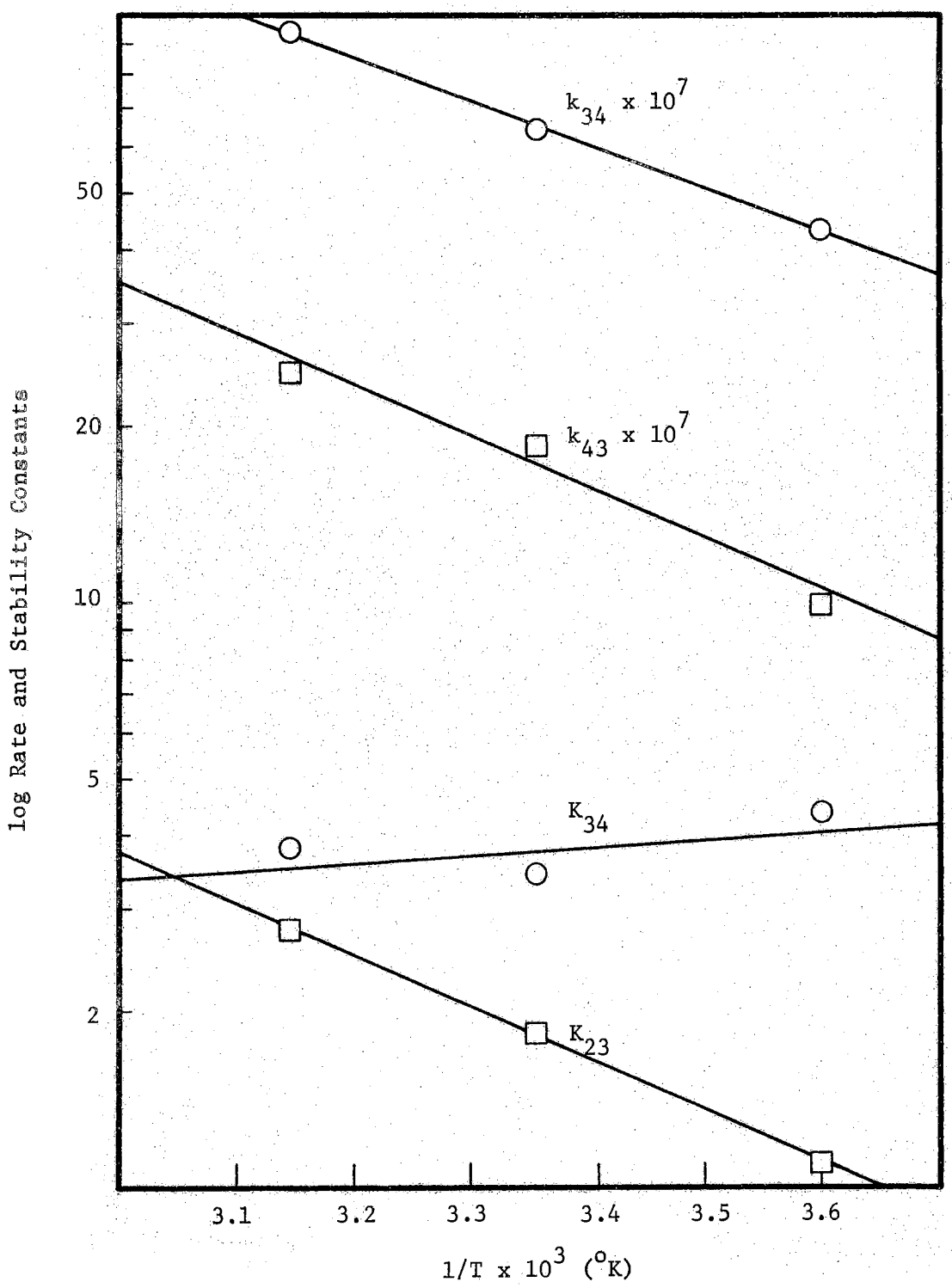

Figure 14. Plots of Rate Constants and Stability Constants for $Eu_2(SO_4)_3$ Versus 1/T (^oK).

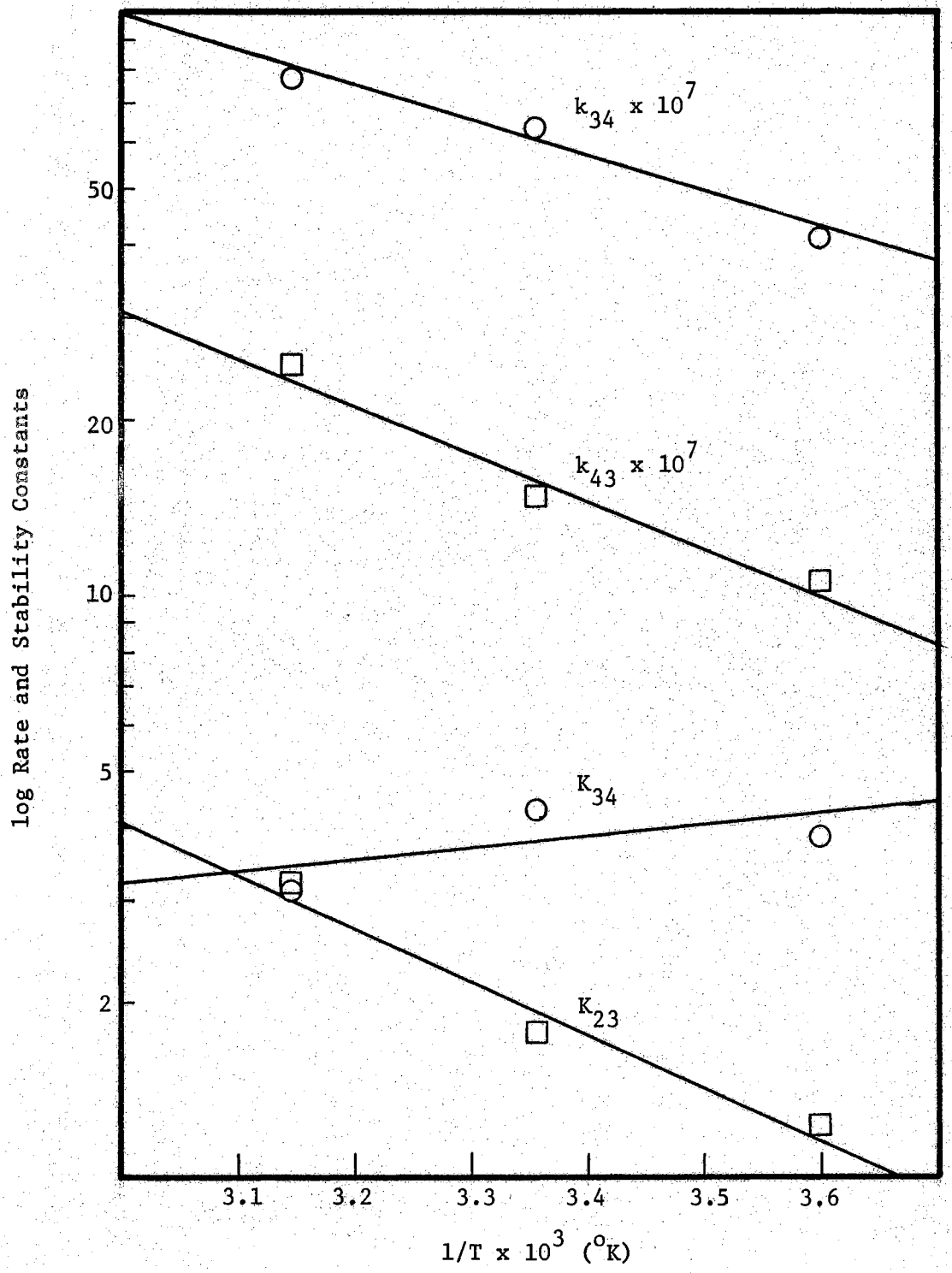

Figure 15. Plots of Rate Constants and Stability Constants for $Gd_2(SO_4)_3$ Versus 1/T (°K).

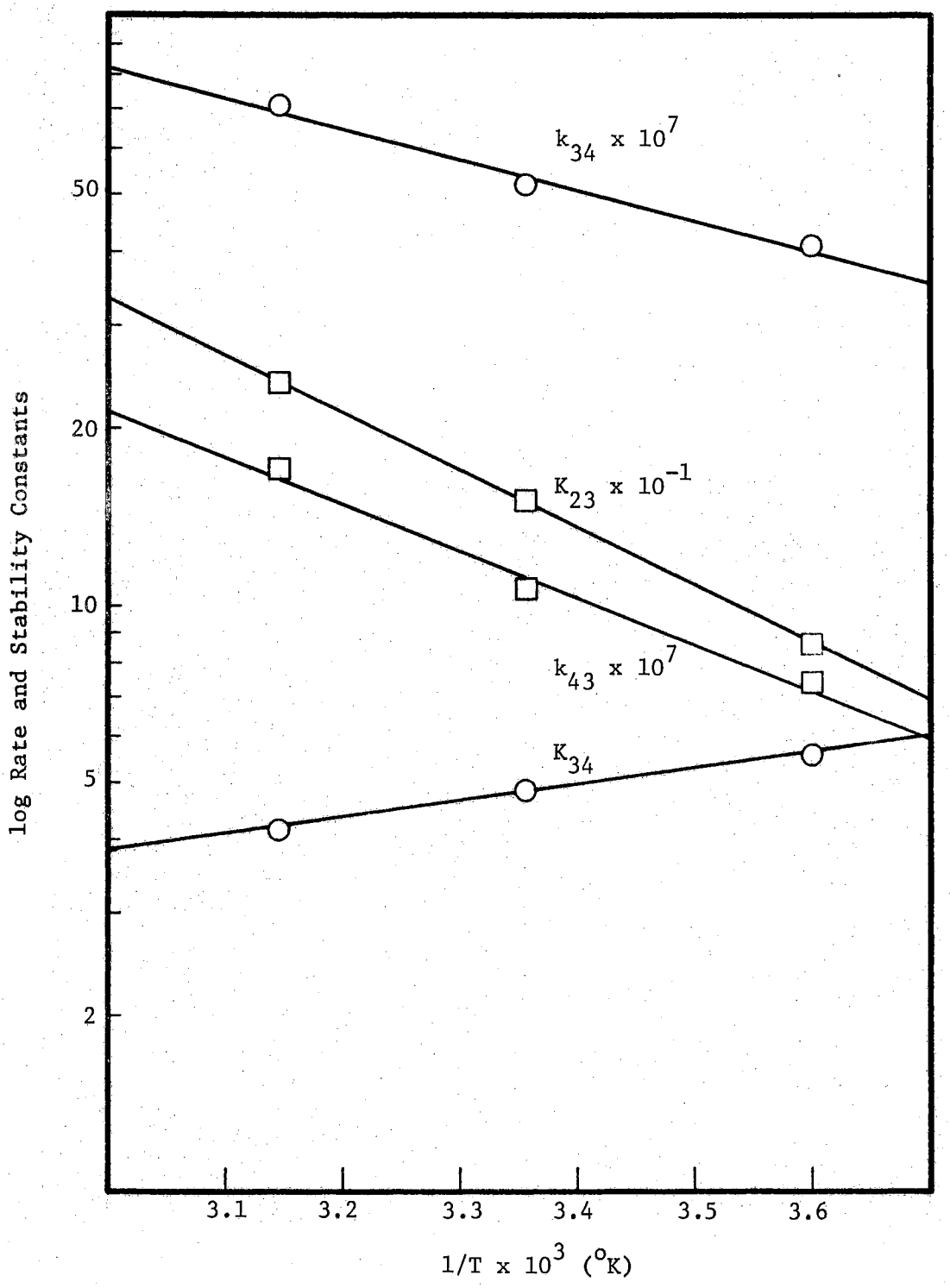

Figure 16. Plots of Rate Constants and Stability Constants for $Tb_2(SO_4)_3$ Versus 1/T (°K).

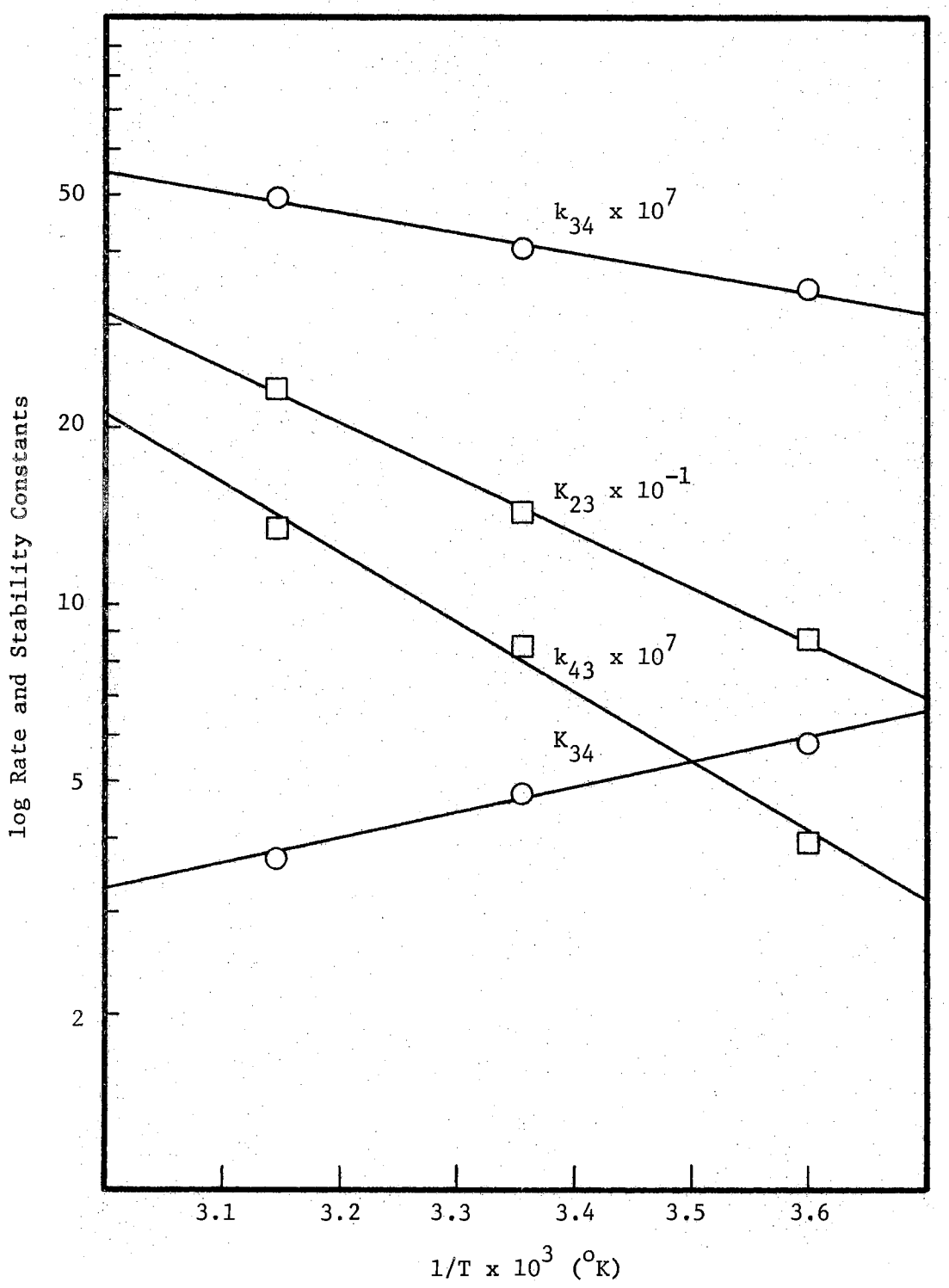

Figure 17. Plots of Rate Constants and Stability Constants for $Dy_2(SO_4)_3$ Versus 1/T (^oK).

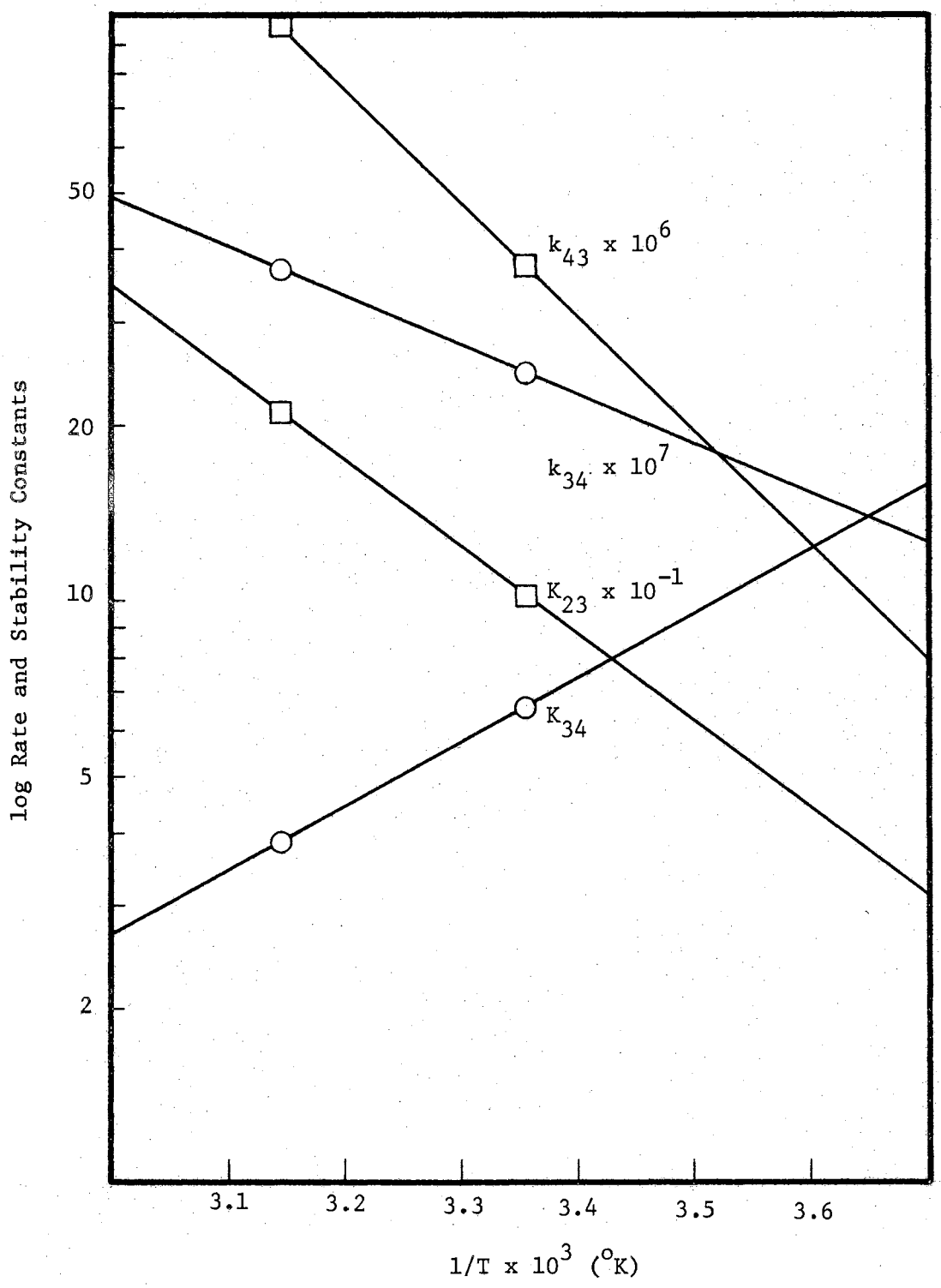

Figure 18. Plots of Rate Constants and Stability Constants for $Ho_2(SO_4)_3$ Versus 1/T (°K).

TABLE XVIII

VALUES OF STEP-WISE THERMODYNAMIC PARAMETERS AT 25° AS DETERMINED KINETICALLY

Ion	Function[a]	Inner Complex	Outer Complex	Ion Pair	Total (Kinetic)	Total (Calorimetric)
Ce^{3+}	ΔH	3.13	0.31	0.97	4.41	3.78
	$-\Delta G$	0.81	0.29	3.59	4.69	4.89
	ΔS	13.21	2.01	15.29	30.5	29.1
Pr^{3+}	ΔH	3.03	0.96	0.97	4.96	3.92
	$-\Delta G$	0.65	0.46	3.60	4.71	4.94
	ΔS	12.35	4.76	15.33	32.4	29.7
Nd^{3+}	ΔH	-0.15	3.69	0.97	4.51	4.15
	$-\Delta G$	0.78	0.39	3.60	4.77	4.96
	ΔS	2.11	13.68	15.33	31.1	30.6
Sm^{3+}	ΔH	-0.69	4.31	0.97	4.59	4.34
	$-\Delta G$	0.82	0.38	3.60	4.80	4.99
	ΔS	0.44	15.73	15.33	31.5	31.3
Eu^{3+}	ΔH	-0.62	4.04	0.97	4.39	4.13
	$-\Delta G$	0.74	0.36	3.60	4.70	4.99
	ΔS	0.40	14.76	15.33	30.5	30.6
Gd^{3+}	ΔH	-0.95	4.22	0.97	4.24	4.10
	$-\Delta G$	0.86	0.34	3.60	4.80	4.99
	ΔS	0.30	15.29	15.33	30.3	30.5

TABLE XVIII (Continued)

Ion	Function[a]	Inner Complex	Outer Complex	Ion Pair	Total (Kinetic)	Total (Calorimetric)
Tb^{3+}	ΔH	-1.27	4.47	0.97	4.17	4.02
	$-\Delta G$	0.94	0.24	3.60	4.78	4.96
	ΔS	-1.11	15.80	15.33	30.0	30.1
Dy^{3+}	ΔH	-3.81	6.17	0.97	3.33	3.58
	$-\Delta G$	0.92	0.21	3.61	4.74	4.92
	ΔS	-9.69	21.40	15.36	27.1	28.5
Ho^{3+}	ΔH	-5.04	6.82	0.97	2.75	3.54
	$-\Delta G$	1.11	0.01	3.61	4.73	4.89
	ΔS	-13.18	22.91	15.36	25.1	28.3

[a] ΔH and ΔG in kcal/mole and ΔS in cal/mole/deg.

model would presumably allow the direct calculation of K_{13} from the Bjerrum expression[58] if an appropriate value for $\mathring{a}$ was chosen and would require at most only two relaxation times to satisfy the mechanism. The theoretical treatment of this model is entirely analogous to the three-step model but involves expressions for the various quantities which are less complicated. For such a model, the following equations would replace the corresponding ones in the three-step model:

$$1/\tau_I = 2\pi f_{cI} = k_{31} + k_{13}^{o}\,\theta(C) \tag{56}$$

$$1/\tau_{II} = 2\pi f_{cII} = k_{43} + \left[\frac{\theta(C)}{K_{13}^{-1} + \theta(C)}\right] k_{34}$$

$$= k_{43} + \Phi(C)\, k_{34} \tag{57}$$

$$K_T = K_{13}\,(1 + K_{34}) \tag{58}$$

This calculation was carried through on the data for samarium and the resulting values applied to the other cations of the series which were studied, namely, Ce(III) - Ho(III). The necessary modifications were made to the programs used in the first model. The procedure, at each temperature, was to first select an $\mathring{a}$ value of reasonable magnitude to calculate a value for K_{13}. The same $\mathring{a}$ value was used to calculate μ and therefore β and $\theta(C)$ in the iterative calculation and from equation (57) values for $\Phi(C)$. The resulting $\Phi(C)$ and $\theta(C)$ values were then inserted into the least-squares program to calculate k_{34}, k_{43}, K_{34} and to regenerate a new value for K_{13}. The process was cycled, choosing different values of $\mathring{a}$, until the difference between K_{13} from

the least-squares program and the Bjerrum value of K_{13} differed by less than 0.05. The values of $\overset{o}{a}$ at 5°, 25°, and 45° (6.21 Å, 5.52 Å, and 5.08 Å, respectively) obtained for samarium were then used, with the correct cation radius, in the calculation of the rate constants and association constants for the other systems studied. The values of k_{43} were unchanged from the previous model while the values of k_{34} were slightly smaller.

The purpose of the two-step model was to reduce, by K_{23}, the number of adjustable parameters needed in the kinetic solution. The rather arbitrary value of K_{23} might very readily dominate the magnitude of the ΔH^{o}_{T} from kinetics but more seriously might impose the wrong sign on ΔH_{34}. The rate constants, equilibrium constants, activation parameters, and the individual thermodynamic parameters for each step are given in Tables XIX, XX, and XXI. Since k_{43} was unchanged the activation parameters for the reverse reaction were also unchanged and are not repeated.

Volume Changes From Sound Absorption

As stated earlier, both temperature and pressure changes accompany the sound wave but in aqueous solutions temperature fluctuations are very nearly absent because of the small thermal expansion of water. Thus, the energy dissipated is mainly a function of the change in volume, ΔV. Theoretically, therefore, sound absorption measurements should yield the information necessary to calculate ΔV.

For any quantitative check of the theory of sound absorption based

TABLE XIX

VALUES OF RATE CONSTANTS AND ASSOCIATION CONSTANTS AS FUNCTIONS OF TEMPERATURE (TWO-STEP MODEL)

Ion	Temp (^{o}C)	$k_{34} \times 10^{-8}$ (sec^{-1})	K_{34}	$K_{13} \times 10^{-2}$ (ℓ/mole)	Bjerrum $K_{13} \times 10^{-2}$ (ℓ/mole)
Ce^{3+}	5	-----	----	-----	-----
	25	1.95	2.86	9.97	10.68
	45	4.97	4.32	10.79	16.32
Pr^{3+}	5	0.94	1.64	9.83	7.25
	25	2.45	2.38	12.32	10.78
	45	5.58	4.21	12.12	16.53
Nd^{3+}	5	1.28	2.25	8.06	7.28
	25	3.05	2.87	11.24	10.83
	45	5.90	3.36	15.45	16.63
Sm^{3+}	5	2.66	2.62	7.42	7.37
	25	4.68	3.13	11.02	11.02
	45	7.42	3.26	16.99	17.05
Eu^{3+}	5	2.46	2.48	7.90	7.39
	25	4.88	2.62	12.56	11.07
	45	8.40	3.39	16.07	17.15
Gd^{3+}	5	2.58	2.42	8.11	7.41
	25	4.86	3.28	10.62	11.12
	45	7.06	2.83	18.37	17.26

TABLE XIX (Continued)

Ion	Temp(°C)	$k_{34} \times 10^{-8}(sec^{-1})$	K_{34}	$K_{13} \times 10^{-2}(\ell/mole)$	Bjerrum $K_{13} \times 10^{-2}(\ell/mole)$
Tb^{3+}	5	2.19	2.97	6.68	7.46
	25	3.79	3.53	9.54	11.21
	45	6.11	3.59	14.39	17.47
Dy^{3+}	5	1.41	3.60	5.77	7.48
	25	2.86	3.38	9.32	11.26
	45	4.32	3.20	14.20	17.58
Ho^{3+}	5	----	----	-----	-----
	25	1.57	4.18	7.43	11.36
	45	2.96	3.05	13.82	17.79

TABLE XX

VALUES OF THE ACTIVATION PARAMETERS FOR THE FORWARD REACTION

$Ln^{3+}H_2O\ SO_4^{2-} \rightleftharpoons Ln^{3+}SO_4^{2-} + H_2O$ AT 25° (TWO-STEP MODEL)

Ion	$K^{\ddagger} \times 10^5$	E_a(kcal/mole)	$\Delta H^{\ddagger}$(kcal/mole)	$\Delta G^{\ddagger}$(kcal/mole)	$\Delta S^{\ddagger}$(kcal/mole)
Ce^{3+}	3.13	8.83	8.24	6.15	7.01
Pr^{3+}	3.94	7.82	7.23	6.01	4.09
Nd^{3+}	4.91	6.71	6.12	5.88	0.80
Sm^{3+}	7.54	4.52	3.93	5.62	-5.67
Eu^{3+}	7.86	5.37	4.78	5.60	-2.75
Gd^{3+}	7.82	4.43	3.84	5.60	-5.90
Tb^{3+}	6.10	4.51	3.92	5.75	-6.14
Dy^{3+}	4.61	4.91	4.32	5.92	-5.37
Ho^{3+}	2.53	5.97	5.38	6.27	-2.99

TABLE XXI

VALUES OF STEP-WISE THERMODYNAMIC PARAMETERS AT 25° AS DETERMINED KINETICALLY (TWO-STEP MODEL)

Ion	Function[a]	Inner Complex	Outer Complex	Total (Kinetic)	Total (Calorimetric)
Ce^{3+}	ΔH	3.88	0.75	4.63	3.78
	$-\Delta G$	0.62	4.09	4.71	4.89
	ΔS	15.09	16.23	31.3	29.1
Pr^{3+}	ΔH	4.16	0.92	5.08	3.92
	$-\Delta G$	0.51	4.22	4.73	4.94
	ΔS	15.66	17.24	32.9	29.7
Nd^{3+}	ΔH	1.77	2.86	4.63	4.15
	$-\Delta G$	0.62	4.16	4.78	4.96
	ΔS	8.02	26.26	34.3	30.6
Sm^{3+}	ΔH	0.96	3.64	4.60	4.34
	$-\Delta G$	0.68	4.15	4.83	4.99
	ΔS	5.50	26.13	31.6	31.3
Eu^{3+}	ΔH	1.38	3.12	4.50	4.13
	$-\Delta G$	0.57	4.23	4.80	4.99
	ΔS	6.54	24.65	31.2	30.6
Gd^{3+}	ΔH	0.69	3.60	4.29	4.10
	$-\Delta G$	0.70	4.13	4.83	4.99
	ΔS	4.66	25.93	30.6	30.5

TABLE XXI (Continued)

Ion	Function[a]	Inner Complex	Outer Complex	Total (Kinetic)	Total (Calorimetric)
Tb^{3+}	ΔH	0.83	3.37	4.20	4.02
	$-\Delta G$	0.75	4.06	4.81	4.96
	ΔS	5.30	24.92	30.2	30.1
Dy^{3+}	ΔH	-0.51	3.96	3.45	3.58
	$-\Delta G$	0.72	4.05	4.77	4.92
	ΔS	0.70	26.87	27.6	28.5
Ho^{3+}	ΔH	-3.00	5.84	2.84	3.54
	$-\Delta G$	0.85	3.92	4.77	4.89
	ΔS	-7.21	32.74	25.5	28.3

[a] ΔH and ΔG in kcal/mole and ΔS in cal/mole/deg.

upon pressure dependent dissociation reactions, it is helpful to know the volume change upon dissociation into ions for the complete reaction, $\Delta\bar{V}^{o}$. If sound is absorbed as a consequence of perturbing the dissociation equilibria, it should be possible to arrive at the same $\Delta\bar{V}^{o}$ from sound absorption measurements as from the pressure dependence of the dissociation constant. $\Delta\bar{V}^{o}$ is determined by the pressure dependence of the overall dissociation constant

$$\left(\frac{\partial \ln K_m}{\partial p}\right)_{T,m} = \frac{-\Delta\bar{V}^{o}}{RT} \tag{59}$$

Because the mechanism consists of successive equilibria, the volume change in any one step is necessarily coupled to the preceding steps. The volume changes for the individual steps are therefore not obtained directly from the experimentally observed maximum sound absorption but rather from the weighted sum of the individual volume changes, ΔV_{ij}, which are the differences between the partial molal volumes of products and reactants for each step. Although molar or formal units of concentration were used in this study they are nearly equal to molal units for dilute solutions. The necessary relationships as derived by Tamm[62] are

$$\Delta V_{I} = \Delta V_{12} \tag{60}$$

$$\Delta V_{II} = \Delta V_{23} + \frac{k_{21}}{k_{12}' + k_{21}} \Delta V_{I} \tag{61}$$

$$\Delta V_{III} = \Delta V_{34} + \frac{k_{23}'}{k_{23}' + k_{32}} \Delta V_{II} \tag{62}$$

For such a three-step mechanism Tamm[62] has also shown that

$$(\Delta V_{III})^2 = \frac{\beta_o RT}{8.686\ \pi} \frac{2\ (\alpha_{chem}\lambda)_{max}}{C_o} \frac{1}{G_{III}^{+}} \tag{63}$$

where β_o is the adiabatic compressibility of the solvent as the frequency goes to zero and

$$G_{III}^{+} = \frac{1 + K_{12}\ \theta(C)\ [1 + K_{23}]}{1 + K_{34}^{-1}\ [1 + K_{23}^{-1}]} G_D^{+} \tag{64}$$

G_D^{+} is related to the expression G_D

$$G_D^{+} = [\frac{1}{G_D} + \frac{\partial\ \ell n\ \pi^f}{\partial\sigma}]^{-1}$$

where σ is the degree of dissociation and

$$G_D = (\frac{C_A}{C_o} + \frac{C_B}{C_o} + \frac{C_{AB}}{C_o}) \tag{65}$$

If C_o is the initial concentration of solute for the reaction

$$Ln_2(SO_4)_3 \rightleftharpoons 2\ LnSO_4^{+} + SO_4^{2-} \tag{66}$$

then for the dissociation of the complex

$$LnSO_4^{+} \rightleftharpoons Ln^{3+} + SO_4^{2-} \tag{67}$$

the concentrations of the species are

$$2C_o\ (1 - \sigma) \rightleftharpoons 2C_o\sigma + C_o\ (2\sigma + 1) \tag{68}$$

Substitution of $2C_o\sigma$, $C_o(2\sigma + 1)$, and $2C_o(1 - \sigma)$ for C_A, C_B, and C_{AB} respectively, yields

$$G_D = \frac{2\sigma\ (2\sigma^2 - \sigma - 1)}{(2\sigma^2 - 4\sigma - 1)} \tag{69}$$

and therefore

$$G_D^{+} = \left[\frac{(2\sigma^2 - 4\sigma - 1)}{2\sigma\ (2\sigma^2 - \sigma - 1)} + \frac{1}{\sigma}\ \frac{\partial\ \ell n\ \pi^f}{\partial\ \ell n\ \sigma}\right]^{-1} \tag{70}$$

Combining equations (64) and (70) and substituting into equation (63) gives

$$(\Delta V_{III})^2 = \frac{\beta_o RT}{8.686\ \pi} \cdot \frac{2\ (\alpha_{chem}{}^{\lambda})_{max}}{C_o}\ \cdot$$

$$\frac{1 + K_{34}{}^{-1}\ [1 + K_{23}{}^{-1}]}{1 + K_{12}\ \theta(C)\ [1 + K_{23}]}\ \ \frac{2\sigma^2 - 4\sigma - 1}{2\sigma\ (2\sigma^2 - \sigma - 1)} + \frac{1}{\sigma}\frac{\partial\ \ell n\ \pi^f}{\partial\ \ell n\ \sigma} \tag{71}$$

To a close approximation $\beta_o = (\rho c^2)^{-1}$ where ρ is the density and c is the sound velocity and thus $\beta_o = 4.46 \times 10^{-11}$ ml/erg at 25°. All other parameters are directly measureable or can be calculated using the computer program in Appendix B. The unknown quantities in equation (71) necessary to calculate ΔV_{III} are given in Table XXII along with the values of ΔV_{III} and ΔV_{34}.

TABLE XXII

VALUES OF ΔV_{III} AND ΔV_{34} FOR $Ln_2(SO_4)_3$ AT 25°

Salt	Conc., F x 10^3	σ	$-\frac{\partial \ln \pi^f}{\partial \ln \sigma}$	$-\Delta V_{III}$	$-\Delta V_{34}$
La^{3+}	8.80	0.0987	0.1119	19.1	20.7
Ce^{3+}	9.80	0.1002	0.1107	19.6	21.6
Pr^{3+}	9.80	0.0936	0.1062	20.4	22.7
Nd^{3+}	9.61	0.0912	0.1051	22.1	26.5
Sm^{3+}	9.76	0.0873	0.1021	22.3	26.7
Eu^{3+}	9.80	0.0871	0.1020	23.7	28.1
Gd^{3+}	9.50	0.0886	0.1040	19.5	23.9
Tb^{3+}	9.98	0.0909	0.1048	20.3	24.8
Dy^{3+}	9.70	0.0971	0.1104	18.9	23.4
Ho^{3+}	10.76	0.0963	0.1069	20.2	25.0

CHAPTER V

DISCUSSION

Throughout the presentation of this investigation, it has been presumed that the kinetic model is fully understood, the only justification being in reference to other somewhat related systems. If this model is correct then the summation of the values for the various parameters involved in each individual step should correspond to the overall macroscopic values measured by calorimetry[11,13,21] or other conventional methods. This in itself would be a concrete test and would lead to the adoption of the proposed mechanism for this system. In this discussion comparisons will be made which will illustrate the validity of the three-step model. Conversely a number of questions cannot be answered at this time but must await comparable studies on other systems.

Basically the kinetic method demonstrates which species is predominant from a simple consideration of the step-wise specific rate constants and as such can be used to test the utility of the rules based entirely on macroscopic properties. It fails, however, to yield any information on the detailed structure of any of the complex species and one has to resort to other methods. Of these methods, spectroscopy, where applicable, is most informative, but by considering the trends in thermodynamic parameters within a series of closely related cations it may be possible to form some conclusions about relative structural differences.

Calorimetry

The variation of thermodynamic properties of complexes of the trivalent lanthanide ions is not simple. Yatsimirskii[16] has summarized the possible variations from a compendium of experimental results. Several explanations have been suggested but the most accepted is that a change in coordination number of the cation occurs somewhere in the middle of the series[3]. The experimental bases for this interpretation are enumerated in the kinetic section of the discussion. The relative independence of the free energy of complexation of the monosulfate complexes on atomic number might indicate that these complexes are an exception. However, the enthalpy and resultant entropy dependences would confirm that the monosulfate complexes are in no way unique. The results compare favorably with those measured in a 2.0 M perchlorate medium[21] and with other values corrected to zero ionic strength[11]: only a few values lie outside the assigned error limits. More important is the lack of similarity when the dependence of enthalpy of complexation on atomic number is compared with a number of complexes in which the entering group is an organic ligand[3]. The monosulfate complexes have a maximum enthalpy change around samarium. The organic ligand complexes, on the other hand, irrespective of the sign of the enthalpy term, e.g. positive for monoacetates[63] and negative for monoglycolates[19,63], pass through a minimum around the members in the middle of the series. Plotted on a common graph the dependence for the monosulfates is inverse to that for the organic ligands. It must be presumed that the change in coordination number prevails in the monosulfate series but the question of what is the predominant struc-

ture in solution has to be answered. The conclusion must be consistent with the observed trends in the thermodynamic parameters with atomic number or inverse cation radius (since a plot of atomic number versus inverse cation radius is nearly linear the two are used interchangeably).

It is now generally believed that a solution of ions which complex will consist of contact ion pairs (inner complexes) in equilibrium with solvent separated ion pairs (designated outer complexes if separated by only one solvent molecule or simply ion pairs if separated by more than one solvent molecule). This is a consequence of the multi-step mechanism for complex formation[41]. Free energy relationships alone permit no definite conclusions to be made about the predominant species. However, a comparative analysis of the signs of the overall enthalpy and entropy changes during complexation have been used for this purpose, especially for complexes of the rare earth cations. Typical of the criteria are those due to Moeller[1] which were outlined in Chapter I. As previously mentioned there are many exceptions to these rules when compared with the experimental results obtained kinetically. As an example, the alkaline earth monosulfates are predicted to be inner-sphere complexes from thermodynamics yet kinetic results are indicative of only a 10% contribution from inner-sphere species calculated from the ratio k_f/k_b.[3]

There is inferred in these "rules" a direct correlation between the sign of the overall change in enthalpy, ΔH_T^o and the change in enthalpy for the step in which the predominant species is formed, ΔH_{ij}. From the kinetic studies of the lanthanide sulfates these have been

confirmed to be inner-sphere complexes[34,35,36], in agreement with spectroscopic results[22]. The percent inner complex, which varies randomly throughout the series, is of the order of 80% and is similar to that reported for trivalent chromium sulfate[64]. In this case the "rules" are justified but the endothermic ΔH_T^o is a consequence not of a positive ΔH_{34} but rather as a result of a large positive enthalpy change for the formation of the outer-sphere complexes.

Having established the structure to be predominantly inner-sphere, it remains to explain the anomalous trend in the enthalpy of complexation relative to the other systems, some of which have been referred to previously. In the regular series of alkaline earth monosulfates and in the monosulfate complexes of the first row divalent transition metal ions, exclusive of ligand field effects, i.e. Ca^{2+}, Mn^{2+}, and Zn^{2+}, the enthalpy of complexation becomes less favorable with decreasing cationic size[3]. Magnesium, for example, is considered to order several solvent layers in excess of calcium, and on substitution of a ligand for a water molecule in the inner coordination sphere requires a greater reorganization of the solvent with a concomitant increase in endothermicity. Furthermore, the increase is linear with the reciprocal cationic radius, provided, as Duncan[4] has pointed out, there is no change in coordination number. If there was no coordination number change within the rare earths, it is believed that an analogous linear dependence would prevail throughout the series. (It is relevant that the lanthanide contraction is comparable, in magnitude to the decrease in radius from calcium to zinc.) But because of the decrease in cation size, it is inferred that the heavy lanthanides would have a lower coordination number than the light ones. If only

one change in coordination number is assumed, the heat of complexation would be expected to increase monotonically with atomic number within each subdivision so that the smaller lanthanides would, like magnesium, form complexes with a less favorable enthalpy change. Although this is observed for the early and late members of the series the trend is reversed from europium to thulium.

Contrary to the suggestion of Choppin and DeCarvalho[21], the degree of inner complexation, being random throughout, would not account for the variation. It is proposed that, in addition to the deviation from linearity resulting from a coordination number change, there is a further deviation with its origin in the ligand contribution to the overall enthalpy change. This is contrary to the assumption that in the consideration of complexes of a series of similar cations with a common ligand that the ligand contribution is constant. More will be said about this in the discussion of the step-wise thermodynamic parameters obtained from kinetics.

A plausible model which accounts for such a change is the formation of a "hemi-chelate", similar to that proposed by Grenthe in the formation of lanthanide complexes with glycolate[63]. It assumes that the early members form predominantly a unidentate complex, but after samarium, hydrogen bonding between a sulfate oxygen and a vicinial coordinated water molecule occurs to a larger extent such as is shown in Figure 19. The resultant stable six-membered ring is formed when the geometry, dictated by the cation size, permits. This exothermic change is supplemented by a reduced endothermic contribution as a consequence of a lesser reorganization of the solvent.

Consistent with the enthalpy change, the entropy also decreases

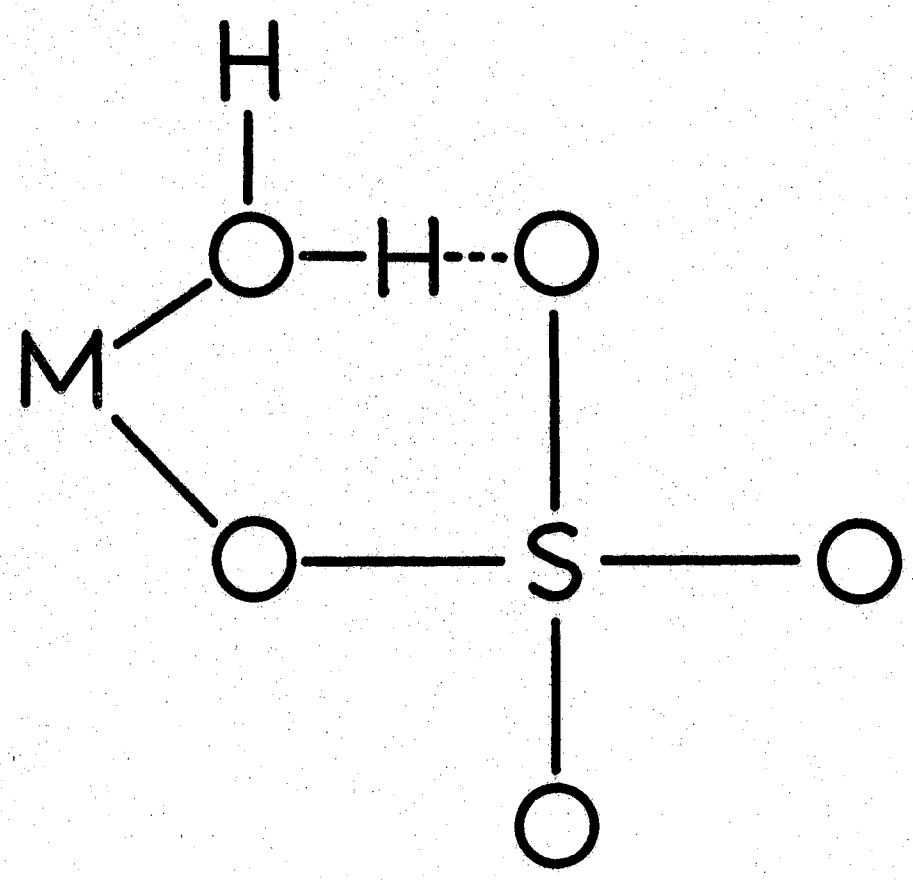

Figure 19. Schematic Diagram of "Hemi-Chelate" Structure

from europium to thulium; once again an inverse trend with decreasing radius compared to Ca^{2+}, Mn^{2+}, and Zn^{2+}.[3] The loss of free rotation by the water molecule and the sulfate ligand, together with the reduced solvent reorganization when the "hemi-chelate" is formed, satisfactorily explains the decrease in entropy observed after samarium. It is interesting to point out that between Y^{3+} and La^{3+}, the former would be expected to form a complex with a less favorable enthalpy and more favorable entropy change, based only on cation size. From Figure 20, which gives the plots of ΔG^{o}_{T}, ΔH^{o}_{T}, and ΔS^{o}_{T} versus atomic number, it will be seen that yttrium occupies a position between Yb^{3+} and Lu^{3+} as would be expected from the cation radius. It may also be accounted for by the "hemi-chelate" model if there is a coordination number change between Y^{3+} and La^{3+}.

Linear Correlation of ΔH and ΔS of Complexation

When ΔH is plotted against ΔS for the series a linear dependence is observed (Figure 21). The equation for the line is

$$\Delta H = -4.11 + 0.270\ \Delta S \qquad (72)$$

within the experimental error limits on ΔH. Some authors[65] have cited this relationship as indicative of a common structure for all complexes in the series, or conversely, the linear correlation will not be observed unless the species present are identical. However, the colinearity is a consequence of a restriction placed on the system by a nearly constant ΔG and as such is no more informative than is the overall free energy change alone with regard to structure.

From the Gibbs Free Energy (G.F.E.) equation, a linear correlation

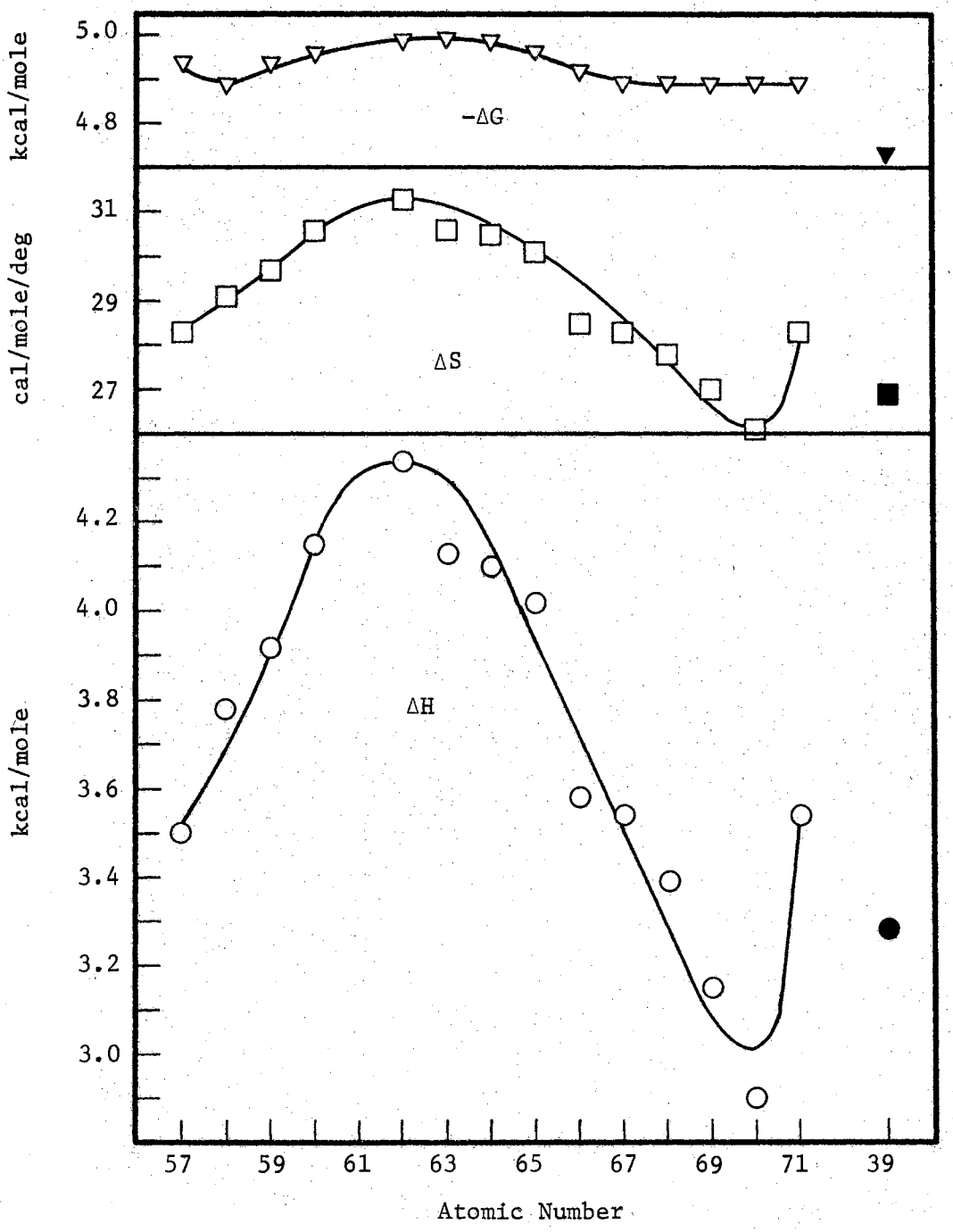

Figure 20. Plots of $-\Delta G$, ΔS, and ΔH of Complexation of the Lanthanide Monosulfates at 25° Versus Atomic Number.

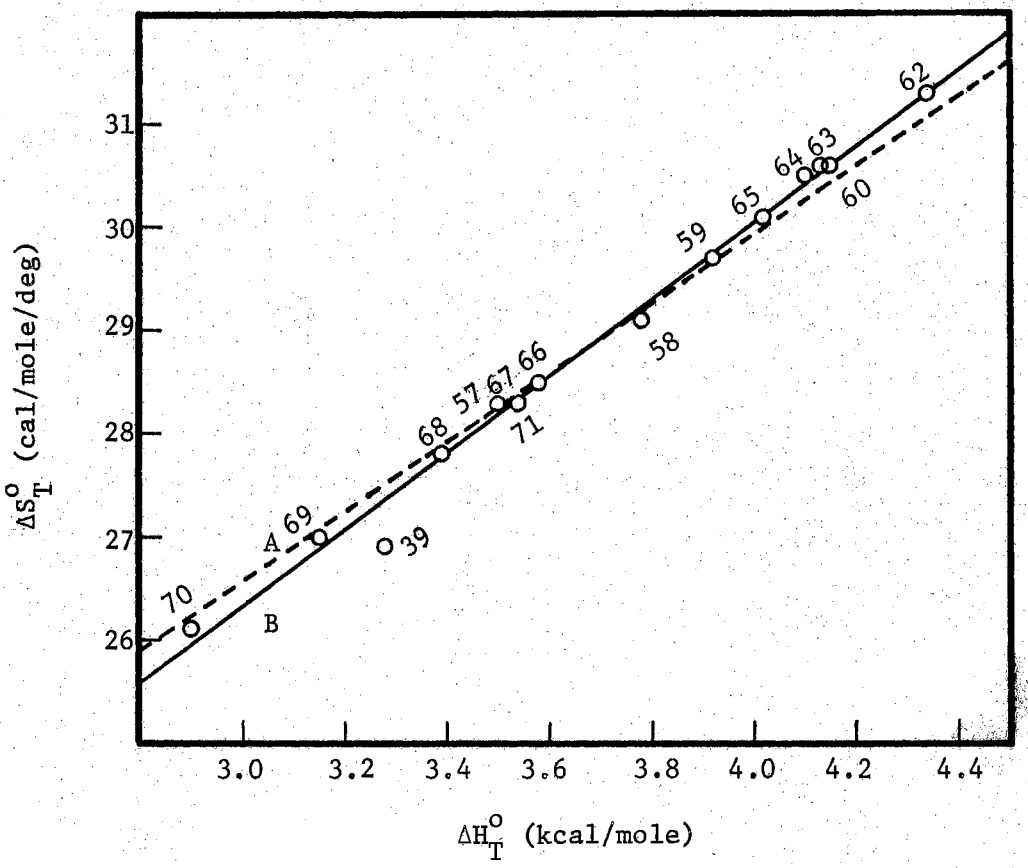

Figure 21. Plot of ΔS_T^o Versus ΔH_T^o at 25° for the 1:1 Lanthanide Sulfate Complexes. A(---) is the G.F.E. Theoretical Line and B(-) is the Least-Squares Line.

of ΔH and ΔS for a series of $\underline{n}$ related reactions (for example the lanthanide ions with a common ligand) is an obvious result if the ΔG values for the reactions are zero or constant and the slope of the line is, by definition, the temperature T ($^{o}K/1000$) i.e. $\Delta H_{\underline{n}} = \Delta G_{\underline{n}} + 0.298\ \Delta S_{\underline{n}}$, for a temperature of 25^{o}. In the real situation, however, there very often is variation in $\Delta G_{\underline{n}}$ within the series. For the series of $\underline{n}$ related reactions, therefore, in which this variation exists, one can construct, for each member, a line of slope T ($^{o}K/1000$) through the individual $\Delta H_{\underline{n}}$ and $\Delta S_{\underline{n}}$ values obtained by experiment and the corresponding intercept at $\Delta S_{\underline{n}} = 0$ where $\Delta G_{\underline{n}} = \Delta H_{\underline{n}}$. When the $\Delta G_{\underline{n}}$ values are zero or constant, the intercepts would be coincident and the various $\Delta H_{\underline{n}} - \Delta S_{\underline{n}}$ values would fall on a single line.

This is precisely the situation observed also by Mesmer and Baes[66] for the formation of the LnF^{2+} complexes in that the variation in $\Delta G_{\underline{n}}$ for the series is small. The fact that there is a wide spread in the $\Delta H_{\underline{n}}$ values across the series is of secondary importance. From Table XXIII, in which a comparison is made between the equations for the G.F.E. or $\Delta H_{\underline{n}}$ line and the least squares, ΔH_{LS} line, it is immediately apparent that the relationship is not limited to a few cases. The degree of agreement between the slope and intercept of each least squares line and those of the $\Delta H_{\underline{n}}$ lines is an indication of the relative variance in the individual $\Delta G_{\underline{n}}$ values.

In every system in Table XXIII, with the exception of the lanthanide EDTA complexes, the average deviation in the calculated $\Delta H_{\underline{n}}$ is

TABLE XXIII

THEORETICAL AND LEAST-SQUARES LINES FOR PLOTS OF ΔH VERSUS ΔS

System of 1:1 Complexes	Equation of Line	Ionic Strength, Mole/Liter	$\Delta(\Delta G)$, kcal. Mole	$\Delta(\Delta H)$, kcal. Mole	$\Delta(\Delta S)$, cal/ Mole.deg.	Maximum Absolute Deviation in ΔH_{calc}	Average Deviation in ΔH_{calc}
Ln·Fluoride[66]	$\Delta H_{LS} = -2.83 + 0.257\ \Delta S$	1.0	1.29	5.56	22.9	0.43	0.22
	$\Delta H_{n} = -4.50 + 0.298\ \Delta S_{n}$					0.87	0.36
	$\Delta H_{M\cdot B} = -2.38 + 0.246\ \Delta S$					0.50	0.19
Ln·EDTA[3]	$\Delta H_{LS} = -12.84 + 0.149\ \Delta S$	0.1	5.39	3.03	19.5	1.46	0.58
	$\Delta H_{n} = -23.47 + 0.298\ \Delta S_{n}$					2.75	1.45
Ln·Diglycolate[3]	$\Delta H_{LS} = -7.18 + 0.292\ \Delta S$	0.1	0.98	2.78	8.7	0.60	0.18
	$\Delta H_{n} = -7.33 + 0.298\ \Delta S_{n}$					0.61	0.18

TABLE XXIII (Continued)

System of 1:1 Complexes	Equation of Line	Ionic Strength, Mole/Liter	$\Delta(\Delta G)$, kcal./Mole	$\Delta(\Delta H)$, kcal./Mole	$\Delta(\Delta S)$, cal/Mole.deg.	Maximum Absolute Deviation in ΔH_{calc}	Average Deviation in ΔH_{calc}
Alkaline Earth Formate[67]	$\Delta H_{LS} = -1.87 + 0.289\ \Delta S$	→0	0.07	2.87	10.3	0.07	0.06
	$\Delta H_n = -1.91 + 0.298\ \Delta S_n$					0.11	0.07
Alkaline Earth Acetate[67]	$\Delta H_{LS} = -1.63 + 0.296\ \Delta S$	→0	0.12	3.23	11.2	0.07	0.06
	$\Delta H_n = -1.63 + 0.298\ \Delta S_n$					0.07	0.06
Ln·Sulfate[13]	$\Delta H_{LS} = -4.11 + 0.270\ \Delta S$	→0	0.26	1.19	4.4	0.13	0.02
	$\Delta H_n = -4.92 + 0.298\ \Delta S_n$					0.18	0.05
Ln·Sulfate[21]	$\Delta H_{LS} = -4.41 + 0.438\ \Delta S$	2.0	0.39	0.69	2.0	0.25	0.10
	$\Delta H_n = -1.69 + 0.298\ \Delta S_n$					0.22	0.07

TABLE XXIII (Continued)

System of 1:1 Complexes	Equation of Line	Ionic Strength, Mole/Liter	$\Delta(\Delta G)$, kcal. Mole	$\Delta(\Delta H)$, kcal. Mole	$\Delta(\Delta S)$, cal/ Mole.deg.	Maximum Absolute Deviation in ΔH_{calc}	Average Deviation in ΔH_{calc}
Ln·Acetate[63]	$\Delta H_{LS} = -3.68 + 0.378\ \Delta S$	2.0	0.63	2.05	5.3	0.34	0.13
	$\Delta H_n = -2.38 + 0.298\ \Delta S_n$					0.40	0.17
Ln·Propionate[18]	$\Delta H_{LS} = -3.45 + 0.360\ \Delta S$	2.0	0.66	2.42	6.2	0.41	0.10
	$\Delta H_n = -2.34 + 0.298\ \Delta S_n$					0.36	0.16
Mg^{2+}, Ca^{2+}, Mn^{2+}, Co^{2+}, Zn^{2+}. Sulfate[3]	$\Delta H_{LS} = -2.88 + 0.280\ \Delta S$	→0	0.18	2.90	10.0	0.12	0.07
	$\Delta H_n = -3.18 + 0.298\ \Delta S_n$					0.18	0.06

probably still within the error limits on the experimentally determined heats and a good comparison is observed. For the EDTA complexes[3], $\Delta(\Delta G)$ = 5.4 kcal./mole., and the scatter in the ΔH-ΔS data is such that they can not be fitted to a single straight line of any slope within the experimental error limits in ΔH for all members.

The alkaline earth acetates[67] and formates[67] are the two examples which best illustrate the validity of the added constraint of a virtually constant ΔG. In both systems $\Delta(\Delta G)$ is approximately 0.1 kcal./mole. and no extrapolation to $\Delta S = 0$ is necessary, since values of ΔH are both positive and negative. The least squares and ΔH_n lines give a nearly perfect fit to the experimental data and the intercepts are equal to the average ΔG values.

Since the linear correlation is contingent upon certain restrictions on ΔG and since ΔG tells us nothing about the structures of the complexes in solution, then conversely the linear dependence of ΔH-ΔS should be independent of the structural properties of the complexes. Therefore inner-sphere complexes, e.g. $LnSO_4^+$ and LnF^{2+}, as well as ion-pairs[65], comply with the relationship. Furthermore, the case of magnesium and calcium acetates is most striking in that although ΔG is constant, the signs of ΔH are opposite, a certain indication of dissimilar structures. The reason for the correlation is thus more fundamental than one of structure.

Kinetics

It was pointed out by Purdie and Vincent[34] in their investigation of the lanthanide monosulfate complexes that some additional insight into the complexation process might be obtained if the thermodynamic

parameters for the cation desolvation step could be obtained from a temperature dependence study of the rates of complexation and the step-wise volume changes could be compared with the volume change for the overall reaction determined in an independent study of the pressure dependence of the dissociation constant. From the results obtained at 25^{o} it was apparent that not all of the members could be studied over a sufficiently wide temperature range. The characteristic relaxation frequency varies directly with temperature and those members whose maximum relaxation frequency values at 25^{o} were close to 5 MHz, the lower limit of the apparatus, could not be studied at lower temperatures. Praseodymium and dysprosium are the real limits in the series for a study over the entire 40^{o} range but the results for cerium and holmium at only two temperatures are included. Although the results for these two systems are subject to some scepticism they have been treated as being equally reliable to those cases where three temperatures were studied. The temperature coefficient of f_{cIII} is sufficiently small that additional measurements within the temperature range studied were considered unlikely to add anything to the overall accuracy of the calculated values.

It should be re-emphasized that in the kinetic analysis the overall association constants at 5^{o} and 45^{o} were calculated from a linear van't Hoff isochore extrapolation and the rate constants are subject to this same approximation. The same criticism can be leveled against the method used to determine the activation parameters and step-wise thermodynamic values in that a linear Arrhenius plot was assumed.

Considerable attention has been given to the detailed mechanism of the individual steps involved in ion association by Eigen[25,30] and his

co-workers. In particular, they have shown that a constant value for k_{34} is obtained for complexation of Mg^{2+} with a series of anions such as SO_4^{2-}, CrO_4^{2-}, and $S_2O_3^{2-}$, i.e. that the complexation rate is independent of the entering group. This observation has been used in the assignment of relaxations to a particular step. Furthermore, the values of k_{34} measured by ultrasonic absorption correspond closely with the rates of exchange of labelled water molecules into the inner coordination spheres of a number of paramagnetic ions, as determined by Connick[27] from nmr studies. There is much evidence to support the theory that the removal of a water molecule from the inner coordination sphere of the cation by an S_N1 elimination is the rate-determining process of step III which, on the microscopic scale, would become for this system

$$Ln(H_2O)_n^{3+} \underset{\text{fast}}{\overset{\text{rate determining}}{\rightleftharpoons}} Ln(H_2O)_{n-1}^{3+}$$

$$+ H_2O \underset{\text{slow}}{\overset{\text{fast } (SO_4^{2-})}{\rightleftharpoons}} Ln(H_2O)_{n-1}SO_4^{+} \qquad (73)$$

with a reduction in the coordination number in going to the transition state. In other words the role of water exchange is of paramount importance in complex formation. Support of the proposed mechanism for the systems studied here also receives direct evidence from nmr studies of the rate of water exchange for Gd^{3+} in perchlorate medium[40]. Marianelli[40] reports the rate of water exchange to be 9×10^8 sec^{-1} or 8×10^8 sec^{-1} assuming nine and eight coordination, respectively. Both values are in excellent agreement with the value of $k_{34} = 6.4 \times 10^8$

sec^{-1} for Gd^{3+} determined in this study. In addition the activation energy determined for water exchange[40] of 3.2 ± 0.3 kcal/mole and entropy of activation of -7 ± 4 eu. agree very well with the corresponding values obtained from this study of 2.8 kcal/mole and -11 eu. Temperature dependence studies of the second order rate of complexation of anthranilate[37,38] and oxalate[39] have also been made by T-jump and P-jump, respectively. The bimolecular rate constants for both systems are of the order of 5×10^7 M^{-1} sec^{-1} for Gd^{3+}. For gadolinium anthranilate[38] the activation energy is 8.5 kcal/mole and the entropy of activation is +9 eu. while the corresponding values of the oxalate system[39] are 6.5 kcal/mole and -5.2 eu. Thus although the rates for the lanthanide sulfates are approximately one order of magnitude greater than for the other systems studied, the rates are in excellent agreement with the rate of water exchange indicating that the rate determining step in the mechanism is that of cation desolvation.

In the solid state all the lanthanides may exist as either nona- or octahydrates[5]. It is a possibility, therefore, that in solution there are two relatively stable coordination numbers for the trivalent lanthanide ions and that the equilibrium ratio of one species to the other changes progressively across the series. On the basis of changes in the partial molal volume at infinite dilution[68], conductivities at infinite dilution[10,69,70,71], apparent molal heat capacities[72], heats of dilution[73], and B coefficients from viscosity data in aqueous solution[74], it has been suggested that a decrease in coordination number occurs between neodymium and terbium. The decrease in coordination number is consistent with the fact that the ion size decreases across the series and on a hard sphere model a larger ion would accommodate more coordi-

nated solvent molecules. At the same time the total hydration number would increase across the series as the polarizing power increases with the decreasing cationic size. From conductance data[75] hydration numbers of 12.8 ± 0.1 (La-Nd) and 13.9 ± 0.1 (Dy-Yb) were obtained and from molar volumes[76] values of 9.0 ± 0.5 (La-Nd) to 11.0 (Dy-Er).

Arguments based on variations in the stability constants for many lanthanide complexes suggest a coordination number change at gadolinium. An X-ray study of EDTA complexes shows coordination numbers of 9 and 8 for the europium and gadolinium complexes[77]. Powell and Rowlands[78] have reported that complexation of lanthanides results in a change in coordination number at gadolinium or europium. Structures for the solvated lanthanide ion have been suggested from spectral measurements of aqueous solutions containing europium salts[79]. From X-ray studies of concentrated erbium chloride solutions Brady[80] suggested a highly ordered region of solvent about the lanthanide ion. Thus there is evidence which is consistent with both a change in the coordination number of the solvated lanthanide in the series and a highly ordered solvent structure about the ion.

If it is assumed that a rare earth ion in solution may exist in an equilibrium between two possible coordination numbers, where this equilibrium may be sharply displaced toward a lower coordination number below a critical ionic radius, the data may be qualitatively explained. According to this postulate, the equilibrium between the possible coordination numbers favors the higher coordination number for the lanthanides between La and Nd. After Nd a displacement of this equilibrium toward the lower coordination number begins to take place that results in the lower coordination number becoming increasingly more

favorable from Pm to around Tb. The ions from around Dy to Lu have essentially the same coordination number.

In view of these considerations, assuming 9 and 8 as possible coordination numbers, the rate determining step for La^{3+} would be

$$La(H_2O)_9^{3+} \rightarrow La(H_2O)_8^{3+} + H_2O \quad (74)$$

and for Lu^{3+}

$$Lu(H_2O)_8^{3+} \rightarrow Lu(H_2O)_7^{3+} + H_2O \quad (75)$$

For Gd^{3+}, a coordination number of 8.5 would mean a statistical distribution of 50% $Gd(H_2O)_9^{3+}$ and 50% $Gd(H_2O)_8^{3+}$ and the two possible rate determining paths

$$Gd(H_2O)_9^{3+} \rightarrow Gd(H_2O)_8^{3+} + H_2O \quad (76)$$

$$Gd(H_2O)_8^{3+} \rightarrow Gd(H_2O)_7^{3+} + H_2O \quad (77)$$

It is proposed that reaction (77) will be faster than (76) and also faster than either (74) or (75), since the postulate of approximately equal stability for $Gd(H_2O)_9^{3+}$ and $Gd(H_2O)_8^{3+}$ results in the relative lowering of the activation energy for the elimination step. In general, an enhanced rate of water elimination would be the result of two adjacent coordination numbers having similar energy levels.

From the plot of log k_{34} versus atomic number (Figure 22) a maximum around the middle of the series is seen for the lanthanide sulfate complexes. Evidence to explain this observed trend can be seen in Figure 23 which shows a minimum in the activation energy as a function of atomic number around the middle of the series supporting the previous

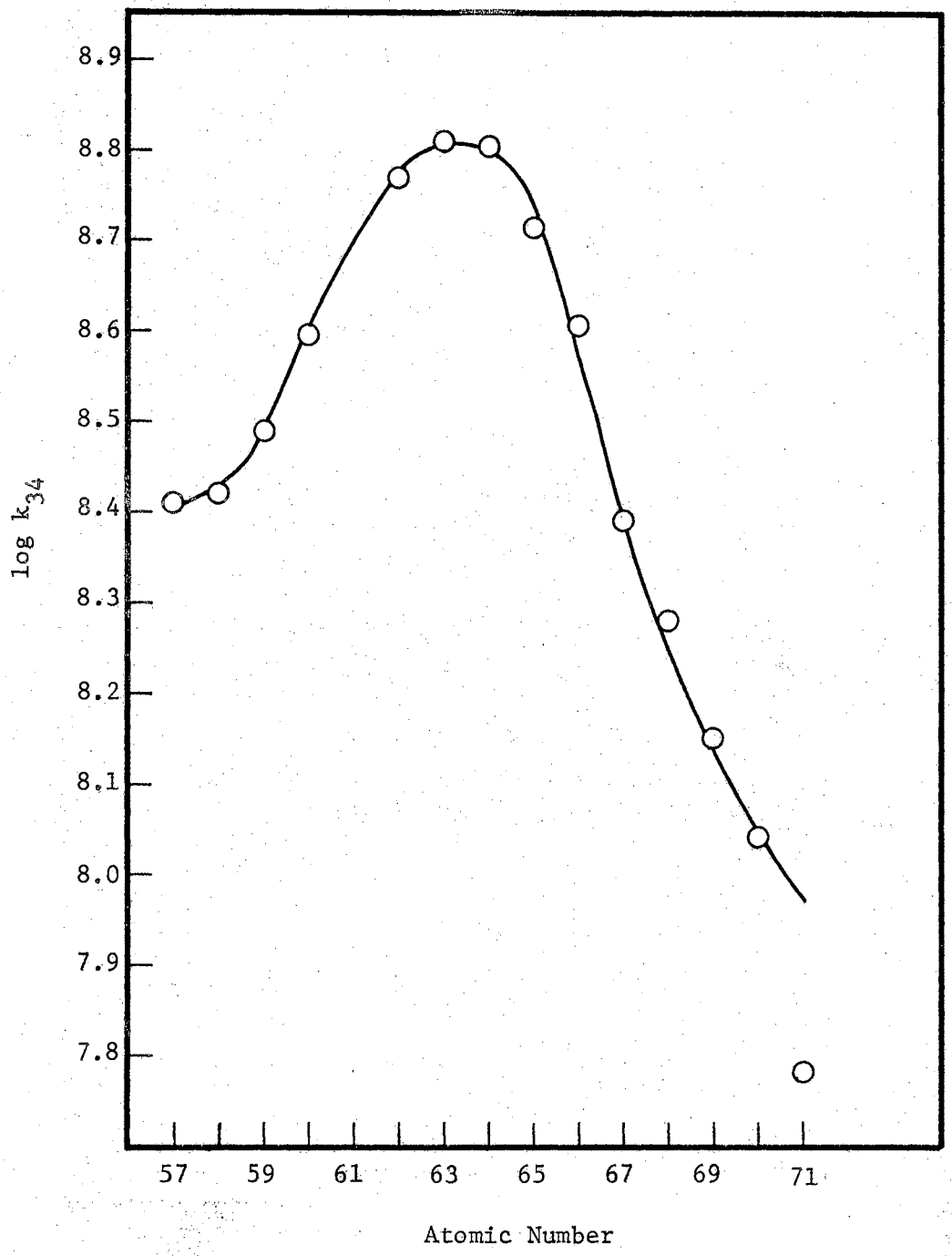

Figure 22. Plot of log k_{34} at 25° Versus Atomic Number

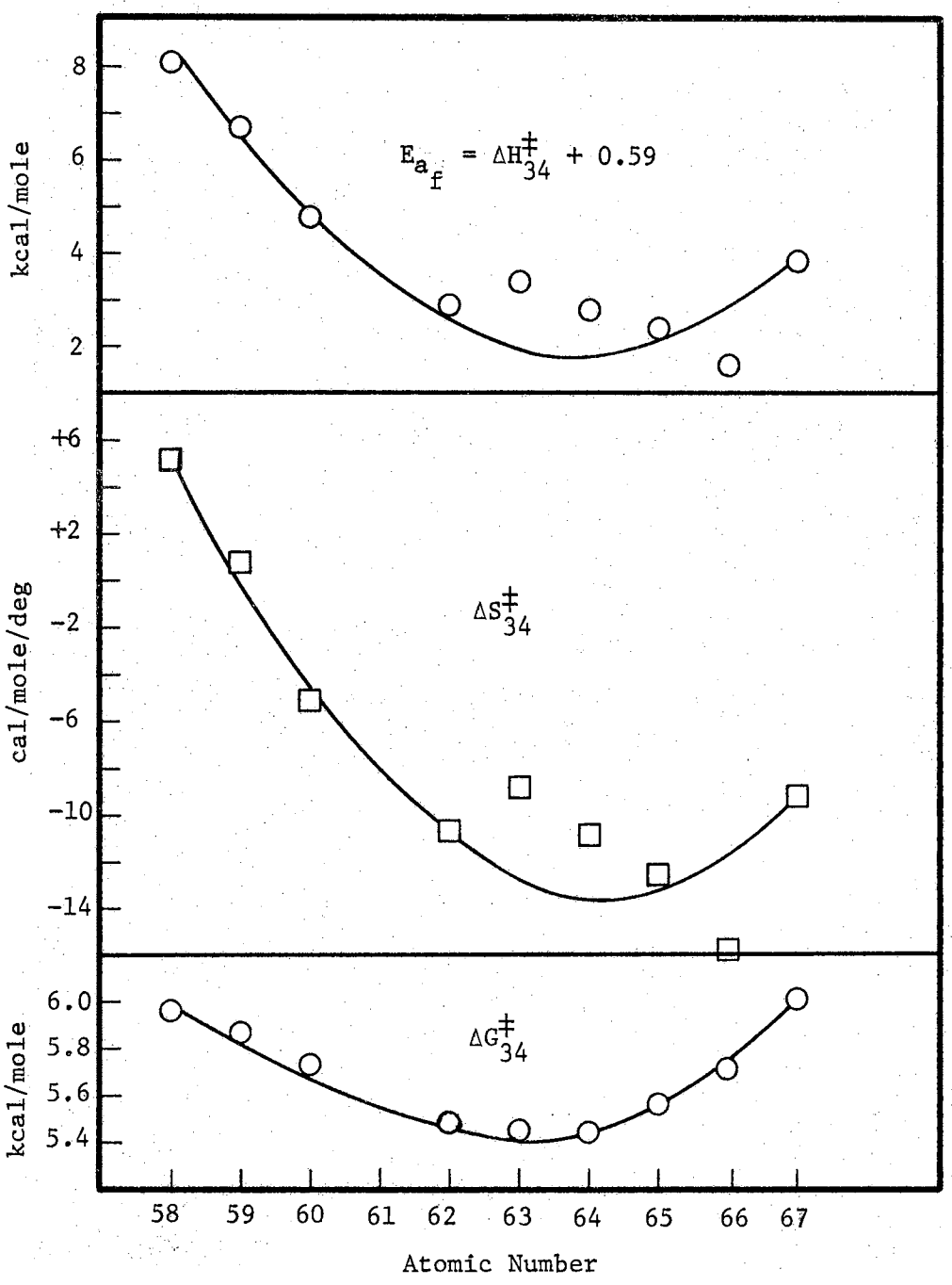

Figure 23. Plots of E_{a_f}, $\Delta S^{\ddagger}_{34}$, and $\Delta G^{\ddagger}$ at 25° Versus Atomic Number for the Lanthanide Monosulfate Complexes.

ideas. The values for the volume change for step III, ΔV_{34}, from Table XXII, also show a maximum volume change near the middle of the series, perhaps indicative of the change in coordination number. Although it is incorrect as a general proposition that the reaction rates should tend to parallel the equilibrium constants, it has been suggested that for a series of reactions involving only a single mechanism, there is some likelihood that the rate constants will vary monotonically with equilibrium constants[81]. The slope of such a plot is considered to be an estimate of the degree to which the transition state resembles either the products or reactants. It is proposed that as the value of the slope increases the transition state tends to more closely resemble the products. For the lanthanide monosulfates a plot of log k versus log K at 25° is linear over the members cerium through holmium, Figure 24, with a slope of 5.6. Such a large value would again indicate that elimination of water is the rate determining step in the mechanism and that, once this has been accomplished, formation of the complex is very fast. The departure from linearity for the last few members may be a result of the increased error in calculating rate constants and the fact that two of the stability constants were obtained by interpolation. It is interesting that the correlation is linear over the part of the series where the change in ΔG is greatest and where the change in coordination number is presumed to occur. The rate constants have been identified with the unimolecular desolvation of the lanthanide ions which is the rate-controlling step in the multi-step complex formation mechanism[41]. Diffusion-controlled encounter of the ions is much faster with a relaxation time too short to be observed by sound absorption in the available frequency range. A dissociative or S_N1 mechanism may

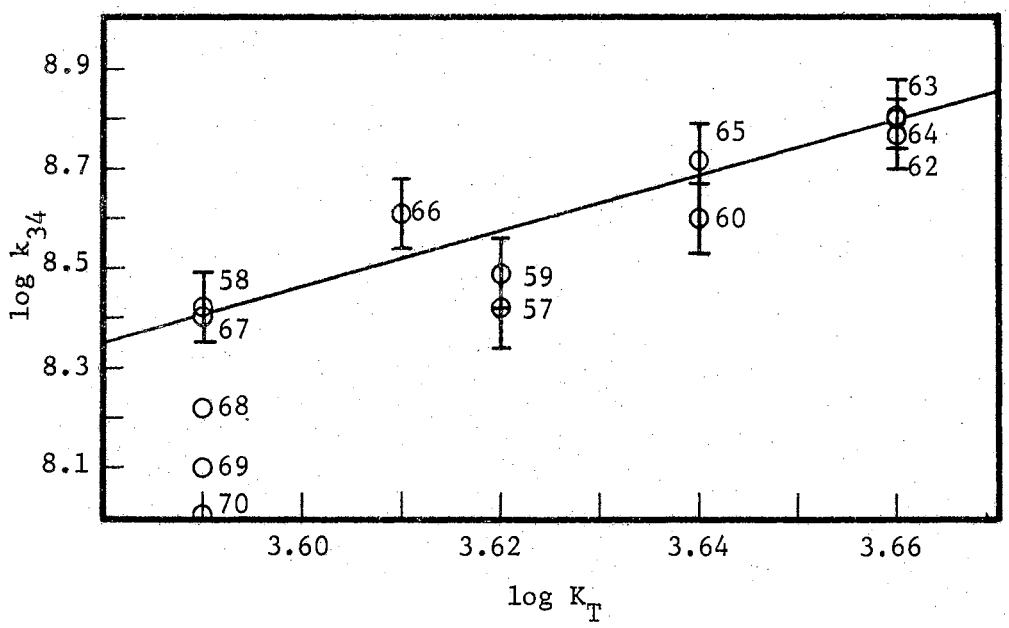

Figure 24. Plot of log k_{34} Versus log K_T for the Lanthanide Monosulfate Complexes at 25°.

therefore, be in operation, illustrating, as stated earlier, that with these cations the role of water exchange is paramount.

Figures 25 and 26 show the plots of ΔH_{ij} and ΔS_{ij} versus atomic number for the second and third steps. Probably the most important observations to be made are that the breaks in the curves occur where it has been proposed that there is a coordination number change and that the trends in these values do not follow the trends in ΔH_T^o and ΔS_T^o as determined calorimetrically[13]. The dependences of ΔH_{23} and ΔS_{23}, for anion desolvation, also indicate that the ligand contribution across the series is not constant as has often been assumed.

Although data have also been presented which are based on a two-step mechanism, direct evidence for the three-step model has been reported. Any possible explanations of the observed trends would be merely speculative at the present time. The number and complexity of the contributing variables such as a change in coordination number, change in the effective hydration number, changes in metal-ligand and metal-water bond strengths, effects of polarization of the water molecules near the cation, and the variability in ligand contribution make any explanation improbable. The relaxation processes in $MgSO_4$ over the frequency range 10^5 to 10^9 Hz[43] have been observed and have been ascribed to the three steps in the proposed mechanism. Combining steps I and II does not change the observed trends in ΔH_{ij} and ΔS_{ij} versus atomic number but only serves to make the values more positive. In either case the summation of the step-wise thermodynamic parameters are found to be in excellent agreement with the values obtained calorimetrically[13]. Since direct experimental evidence has been reported for a

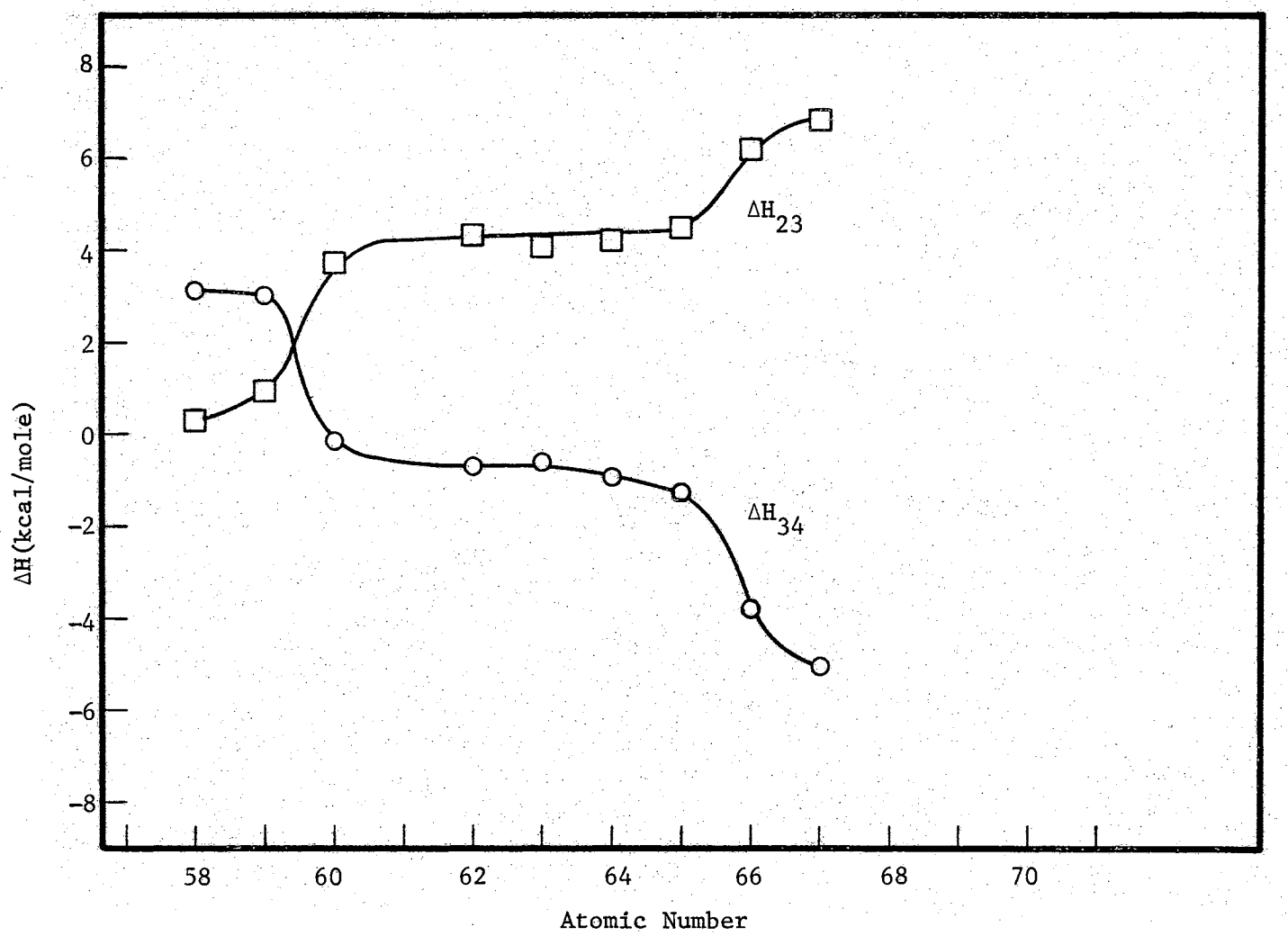

Figure 25. Plots of ΔH_{23} and ΔH_{34} Versus Atomic Number for the Lanthanide Monosulfate Complexes at 25°.

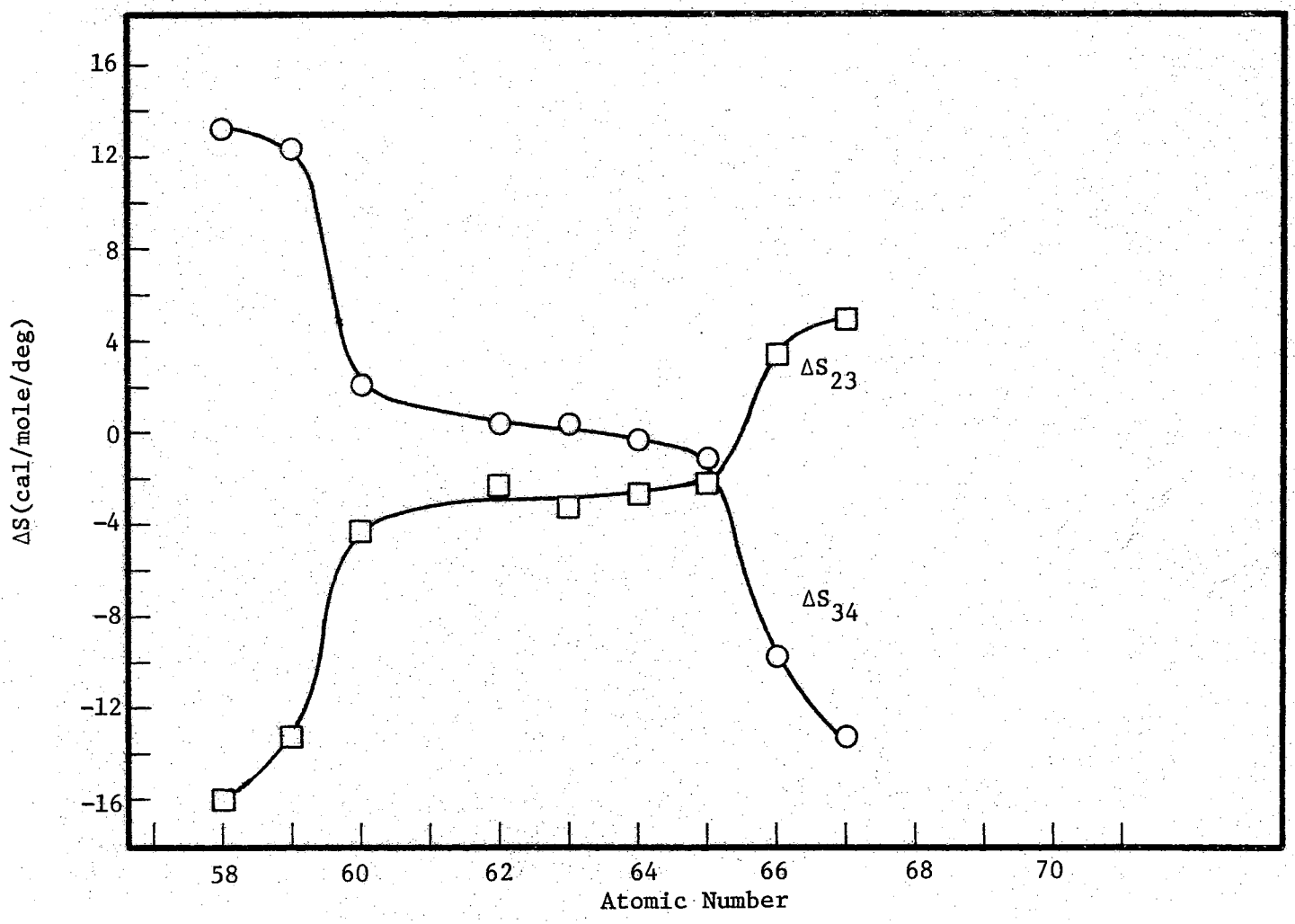

Figure 26. Plots of ΔS_{23} and ΔS_{34} Versus Atomic Number for the Lanthanide Monosulfate Complexes at 25°.

process involving three relaxations, at least for $MgSO_4$, the three-step mechanism is probably to be preferred over the two-step model.

In his investigation of the $MgSO_4$ system Tamm[43,62] has reported two sets of values for ΔV_{ij} for the three steps. In an early investigation[62] he reported the values: ΔV_{12} = 0 ml/mole, ΔV_{23} = -10, -14, and -18 ml/mole, depending on the method of calculation, and ΔV_{34} = -3 ml/mole. From the more recent work in the GHz range[43], in which the three relaxation processes were distinguishable, values of ΔV_{12} = -18.0 ml/mole, ΔV_{23} = + 13.2 ml/mole, and ΔV_{34} = -3.5 ml/mole were calculated. For the latter values the total volume change, $\Sigma\Delta V_{ij}$ = -8.3 ml/mole agrees quite well with that of -6.4 ml/mole determined from the pressure dependence of the dissociation constant[82]. Assuming the values of ΔV_{12} and ΔV_{23} to be independent of the cation, as the mechanism would suggest, ΔV_{34} for the lanthanide sulfates may be calculated from the equations derived at the end of Chapter IV. Using the second set of values from $MgSO_4$ where ΔV_{12} = -18.0 ml/mole and ΔV_{23} = + 13.2 ml/mole, ΔV_{34} = -20.7 ml/mole. The summation of the individual values of ΔV_{ij} gives $\Delta\bar{V}^o$ = -25.6 ml/mole for 8.80 x 10^{-3} M $La_2(SO_4)_3$[35]. In view of the necessary assumptions in this calculation the comparison with the average value obtained from a pressure dependence study of the dissociation constant of $\Delta\bar{V}^o$ = -25.7 ml/mole for 8.20 x 10^{-3} M $La_2(SO_4)_3$[61] is remarkably good. However, it should be noted that even with the first set of values for $MgSO_4$ a $\Delta\bar{V}^o$ = -27.7 ml/mole is obtained, which is still in excellent agreement with the value obtained by Fisher and

Davis[61]. The values of ΔV_{34} for the other rare earth ions have been given in Table XXII. The larger volume change for the third step is probably reasonable since the sound absorption in the $Ln_2(SO_4)_3$ salts is much larger than for any divalent metal ion.

In summary, every experimental test made so far confirms the multi-step mechanism in which the rate controlling step is desolvation of the cation. Personal prejudice will enter when deciding between a two- or three-step mechanism but this is not too important if indeed meaningful. The most unsatisfactory result is to be unable to contribute any new information which could be used in the assignment of coordination numbers.

In order to explain the dependences of the thermodynamic parameters for the individual steps it will be necessary to remove the contributions of several variables such as the change in coordination number, change in effective hydration number, relative strengths of the metal-water and metal-ligand bonds, polarization of the water molecules by the cation, and the variability of the ligand contribution. Other experimental studies which might aid in this respect are the replacement of H_2O by D_2O in a temperature dependence study of the rates of complexation of the lanthanides with sulfate and temperature dependence studies of the complexation of sulfate with Ca^{2+}, Mn^{2+}, and Zn^{2+} and with Mg^{2+}, Sr^{2+}, and Ba^{2+}. Entropy titrations at other temperatures might also be helpful in determining values of K_T and ΔH directly rather than by graphical methods. Extension of the frequency range of the ultrasound gear would allow measurement of the temperature dependence of the rates of complexation for those salts whose maximum

relaxation frequencies at 25^{o} are near the present frequency limits.

A SELECTED BIBLIOGRAPHY

1. Moeller, T., Proc. 6th Rare Earth Research Conf., May 3-5, 1967, Gatlinburg, Tenn., p. 318.

2. Frank, H. S. and W. Wen, Disc. Faraday Soc., 24, 133 (1957).

3. Nancollas, G. H., "Interactions in Electrolyte Solutions", Elsevier Publishing Co., London, 1966.

4. Duncan, J. F., Aust. J. Chem., 12, 356 (1959).

5. Moeller, T., et. al., Chem. Rev., 65, 1 (1965).

6. Moeller, T., et. al., Prog. Sci. Tech. Rare Earths, 3, 61 (1968).

7. Gurney, R. W., "Ionic Processes in Solution", McGraw-Hill, New York, 1953, Chapter 22.

8. Grenthe, I., Acta Chem. Scand., 18, 293 (1964).

9. Jenkins, J. L. and C. B. Monk, J. Amer. Chem. Soc., 72, 2695 (1950).

10. Spedding, F. H. and S. Jaffe, J. Amer. Chem. Soc., 76, 882 (1954).

11. Izatt, R. M., et. al., J. Chem. Soc., A, 47 (1969).

12. Martell, A. E. and L. G. Sillén, "Stability Constants of Metal Ion Complexes", Spec. Publ. 17, The Chemical Society, London, 1965.

13. Fay, D. P. and N. Purdie, J. Phys. Chem., 73, 0000 (1969).

14. Grenthe, I., Acta Chem. Scand., 17, 2487 (1963).

15. Staveley, L. A. K., D. R. Markham, and M. R. Jones, Nature, 211, 1172 (1966).

16. Yatsimirskii, K. B., "Alfred Werner Commemoration Volume", Verlag Helvetica Chimica Acta, 9th International Conference on Coordination Chemistry, St. Moritz, Switzerland, 1966, p. 166.

17. Choppin, G. R. and J. Ketels, J. Inorg. Nucl. Chem., 27, 1335 (1965).

18. Choppin, G. R. and W. F. Strazik, Inorg. Chem., 4, 1250 (1965).

19. Choppin, G. R. and H. G. Friedman, Inorg. Chem., 5, 1599 (1966).

20. Choppin, G. R. and J. B. Walker, Advan. Chem. Ser., 71, 127 (1967).

21. DeCarvalho, R. G. and G. R. Choppin, J. Inorg. Nucl. Chem., 29, 737 (1967).

22. Posey, F. A. and H. Taube, J. Amer. Chem. Soc., 78, 15 (1956).

23. Lamb, A. B. and J. W. Marden, J. Amer. Chem. Soc., 33, 1873 (1911).

24. H. Taube, Chem. Rev., 50, 69 (1952).

25. Eigen, M. and R. G. Wilkins, Advan. Chem. Ser., 49, 55 (1965).

26. Eigen, M. and L. DeMaeyer, "Technique of Organic Chemistry", Vol. VIII, Part II, A. Weissberger, Ed., Interscience, New York, 1963, Chapter 18.

27. Connick, R. E., "Advances in Chemistry of the Coordination Compounds", MacMillan, New York, 1961.

28. Wilkins, R. G., Quart. Rev. (London), 16, 316 (1962).

29. Kreevoy, M. M. and C. A. Mead, J. Amer. Chem. Soc., 84, 4596 (1962).

30. Eigen, M., Pure Appl. Chem., 6, 97 (1963).

31. DeMaeyer, L. and K. Kustin, Ann. Rev. Phys. Chem., 14, 5 (1963).

32. Eigen, M., Disc. Faraday Soc., 24, 25 (1957).

33. Geier, G., Ber. Bunsenges. Phys. Chem., 67, 753 (1963).

34. Purdie, N. and C. A. Vincent, Trans. Faraday Soc., 63, 2745 (1967).

35. Fay, D. P., D. Litchinsky, and N. Purdie, J. Phys. Chem., 73, 544 (1969).

36. Grecsek, J. J., "Ultrasonic Absorption in Aqueous Rare Earth Sulfate Solutions", (unpub. M.S. Thesis, University of Maryland, 1966).

37. Silber, H. B. and J. H. Swinehart, J. Phys. Chem., 71, 4344 (1967).

38. Silber, H. B., R. D. Farina, and J. H. Swinehart, Inorg. Chem., 8, 819 (1969).

39. Graffeo, A. J. and J. L. Bear, J. Inorg. Nucl. Chem., 30, 1577 (1968).

40. Marianelli, R., "Nuclear Magnetic Resonance Study of Water Ex-

change from the First Coordination Sphere of Gd(III) Ion", (unpub. Ph.D. dissertation, University of California, Berkeley, 1966).

41. Diebler, H. and M. Eigen, Z. Phys. Chem., N.F., 20, 299 (1959).

42. Smithson, J. and T. Litovitz, J. Acoust. Soc. Am., 28, 462 (1956).

43. Tamm, K., 6th International Congress on Acoustics, August 21-28, 1968, Tokyo, Japan, p. GP-25.

44. Dunn, T. M., "Modern Coordination Chemistry", J. Lewis and R. G. Wilkins, Ed., Interscience, New York, 1960, p. 286.

45. Caldin, E. F., "Fast Reactions in Solution", Blackwell, Oxford, 1964.

46. Stuehr, J. and E. Yeager, "Physical Acoustics", Vol. II, Part A, W. P. Mason, Ed., Academic Press, New York, 1965.

47. Harris, P. C. and T. E. Moore, Inorg. Chem., 7, 656 (1968).

48. Gutnikov, G. and H. Freiser, Anal. Chem., 40, 39 (1968).

49. Hale, J. D., R. M. Izatt, and J. J. Christensen, J. Phys. Chem., 67, 2605 (1963).

50. Izatt, R. M., et. al., J. Chem. Soc., A, 45 (1969).

51. Davies, C. W., "Ion Association", Butterworths, London, 1962.

52. Dunsmore, H. S., T. R. Kelly, and G. H. Nancollas, Trans. Faraday Soc. 59, 2606 (1963).

53. Freyer, E. B., J. Hubbard, and D. H. Andrews, J. Amer. Chem. Soc., 759 (1929).

54. Randall, C. R., Bur. Stand. J. Res., 8, 79 (1932).

55. Postmus, C. and E. L. King, J. Phys. Chem., 59, 1208 (1955).

56. Langford, C. H. and W. R. Muir, J. Phys. Chem., 71, 2602 (1967).

57. Kellerhals, G. E., unpublished results at 5^{o} and 45^{o} for work performed in this laboratory.

58. Robinson, R. A. and R. H. Stokes, "Electrolyte Solutions", 2nd ed., Butterworths, London, 1959.

59. Atkinson, G. and S. K. Kor, J. Phys. Chem., 69, 128 (1965).

60. Frost, A. A. and R. G. Pearson, "Kinetics and Mechanism", 2nd ed., John Wiley and Sons, New York, 1962, Chapter 5.

61. Fisher, F. H. and D. F. Davis, J. Phys. Chem., 71, 819 (1967).

62. Tamm, K., "Handbuch der Physik", Band XI, Akustic I, Springer-Verlag, Berlin, 1961, p. 129.

63. Grenthe, I., Acta Chem. Scand., 18, 283 (1964).

64. Fogel, N., J. M. J. Tai, and J. Yarborough, J. Amer. Chem. Soc., 84, 1145 (1962).

65. Duncan, J. F. and D. L. Kepert, "The Structure of Electrolytic Solutions", W. J. Hamer, Ed., John Wiley, New York, 1959, pp. 380.

66. Mesmer, R. E. and C. F. Baes, Jr., J. Phys. Chem., 72, 4721 (1968).

67. Nancollas, G. H., J. Chem. Soc., 744 (1956).

68. Spedding, F. H., M. J. Pikal, and B. O. Ayers, J. Phys. Chem., 70, 2440 (1966).

69. Spedding, F. H., P. E. Porter, and J. M. Wright, J. Amer. Chem. Soc., 74, 2055 (1952).

70. Spedding, F. H. and I. S. Yaffe, J. Amer. Chem. Soc., 74, 4751 (1952).

71. Spedding, F. H. and J. L. Dye, J. Amer. Chem. Soc., 76, 879 (1954).

72. Spedding, F. H. and K. C. Jones, J. Phys. Chem., 70, 2450 (1966).

73. Spedding, F. H., D. A. Csejka, and C. W. Dekock, J. Phys. Chem., 70, 2423 (1966).

74. Spedding, F. H. and M. J. Pikal, J. Phys. Chem., 70, 2430 (1966).

75. Choppin, G. R. and A. J. Graffeo, Inorg. Chem., 4, 1254 (1965).

76. Padova, J., J. Phys. Chem., 71, 2347 (1967).

77. Hoard, J. L., B. Lee, and M. D. Lind, J. Amer. Chem. Soc., 87, 1612 (1965).

78. Powell, J. E. and D. L. Rowlands, Inorg. Chem., 5, 819 (1966).

79. Miller, D. G., J. Amer. Chem. Soc., 80, 3576 (1958).

80. Brady, G. W., J. Chem. Phys., 33, 1079 (1960).

81. Leffler, J. E. and E. Grunwald, "Rates and Equilibria of Organic Reactions", Wiley, New York, 1963, p. 156.

82. Fisher, F. H., J. Phys. Chem., 66, 1607 (1962).

APPENDIX A

```
      C.........THIS PROGRAM CALCULATES THE DEGREE OF ASSOCIATION OF THE VARIOUS
      C.....LANTHANIDE MONOSULFATE COMPLEXES AS DETERMINED CALORIMETRICALLY.
      C.....THE CALCULATED VALUES OF THE CONCENTRATION OF THE COMPLEX ARE TO BE
      C.....DIVIDEDED INTO THE NUMBER OF CALORIES CHANGE OBSERVED IN THE REACTION
      C.....AND THIS QUOTIENT IS THEN DIVIDED BY THE VOLUME IN THE DEWAR FLASK.
      C.....THE RESULTING VALUE IS IN KILOCALORIES/MOLE AND MUST BE CORRECTED FOR THE
      C.....HEAT OF DILUTION OF THE SODIUM SULFATE TITRANT WHICH IS 0.65 KCAL./MOLE.
      C     ********************************************************************
      C
    1         DIMENSION GAM(3),Z(3),T(3),ARG(2)
    2         REAL NITRAT
    3         WRITE(6,104)
    4       104 FORMAT(1H1,48X,'PROGRAM TO CALCULATE THE DEGREE OF'//39X,'ASSOCIAT
             1ION BY REPEATED APPLICATION OF DAVIES EQUATION'//60X,'D. P. FAY')
      C.....Z IS THE CHARGE ON THE RESPECTIVE IONS.
    5         READ(5,99)(Z(I),I=1,3)
    6        99 FORMAT(3F3.0)
    7         N=0
      C.....ARG=NAME OF SALT, DISK=ASSOCIATION CONSTANT, C=TOTAL CONC. OF LANTHANIDE,
      C.....C2=TOTAL CONC. OF SULFATE.
    8         1 READ(5,100)ARG, DISK, C, C2, SODIUM, NITRAT
    9       100 FORMAT(2A3,5(F8.2,2X))
   10           IF(DISK*C.EQ.0.0) GO TO 90
   11           G=C
   12           G2=C2
   13           ALF=1.0
   14         5 N=N+1
   15           WRITE(6,107)N, ARG
   16       107 FORMAT(1HO,'CALCULATION NUMBER',I3,10X,'SALT OF ', 2A3)
   17           DO 2 J=1,3
   18         2 GAM(J)=1.0
   19           WRITE(6,105) DISK, C
   20       105 FORMAT(1HO,'ASSOCIATION CONSTANT',2X,E16.8,2X,'MOLES/LITER'//1X,'I
             1NITIAL CONCENTRATION',2X,E16.8,2X,'MOLES/LITER'//)
   21           WRITE(6,106)
   22       106 FORMAT(4HO  N,9X,'COMPLEX',15X,'PI(F)',10X,'IONIC STRENGTH',8X,'LA
             1NTHANIDE',10X,'SULFATE',12X,'CONC. COMPLEX')
   23           K=0
   24         3 K=K+1
      C.....THIS PART OF PROGRAM SOLVES THE QUADRATIC EQUATION.
      C.....ALF IS THE DEGREE OF DISSOCIATION
   25           PAL=ALF
   26           A=DISK*GAM(2)*GAM(3)
   27           B=((DISK*GAM(2)*GAM(3)*(C+C2))+GAM(1))*(-1.0)
   28           R=DISK*GAM(2)*GAM(3)*C*C2
   29           DS=B**2-4.0*A*R
   30           IF(DS)30,10,10
   31        30 WRITE(6,101)
   32       101 FORMAT(1HO,'THE VALUES APPARENTLY APPLY TO A COMPLEX QUADRATIC EQU
             1ATION - - HELP'////)
   33           GO TO 80
   34        10 ALF=(-B-SQRT(DS))/(2.0*A)
   35           IF(ALF.GE.C2) GO TO 12
   36           IF(ALF) 12,13,13
   37        12 ALF=(-B+SQRT(DS))/(2.0*A)
   38           IF(ALF) 30,13,13
      C.....T(1),T(2),AND T(3) ARE CONC. OF COMPLEX, SULFATE, AND CATION RESPECTIVELY.
   39        13 T(1)=ALF
   40           T(2)=G2-ALF
   41           T(3)=G-ALF
   42           DI=(SODIUM+NITRAT)*0.5
   43           DO 15 J=1,3
   44        15 DI=DI+Z(J)**2*T(J)*0.5
   45           BI=SQRT(DI)
   46           PI=GAM(2)*GAM(3)/GAM(1)
   47           WRITE(6,200) GAM(1), GAM(2), GAM(3), A, B, R, DS, BI
   48       200 FORMAT(1HO,8(E10.3,2X))
   49           WRITE(6,102) K, ALF, PI, DI, T(3), T(2), T(1)
   50       102 FORMAT(1HO,I3,6(4X,E16.8))
   51       111 IF(ABS(ALF-PAL).LE.0.0001*ALF) GO TO 79
      C.....THIS PART OF PROGRAM DETERMINES THE ACTIVITY COEFFICIENTS USING DAVIES EQN
   52           DO 20 I=1,3
   53        20 GAM(I)=EXP((0.5092*Z(I)**2*((BI/(1.0+2.915*BI))-0.3*DI))*
             1(-2.302585))
   54           GO TO 3
   55        79 WRITE(6,103) K, ALF, PI, DI, T(3), T(2), T(1)
   56       103 FORMAT(1HO,'FINAL ANSWER'//1X,I3,6(4X,E16.8)//)
   57        80 GO TO 1
   58        90 STOP
   59           END
```

APPENDIX B

```
C     PROGRAM TO CALCULATE THE DEGREE OF DISSOCIATION USING DAVIES EQUATION
C     REPETITIVELY AND OTHER QUANTITIES NEEDED FOR THE EVALUATION OF THE
C     KINETICS OF THE SYSTEM.
C
C     THIS PROGRAM REQUIRES TWO DATA CARDS.  ONE TO INITIATE THE CHARGES OF THE
C     SPECIES FOR ALL THE DATA TO BE EVALUATED, AND ONE DATA CARD TO READ THE
C     VALUES OF A DEBYE-HUCKLE,B DEBYE-HUCKLE,A(NOUGHT) - THE DISTANCE OF
C     CLOSEST APPROACH,K(12) AND K(23).  THE SUCCEEDING CARDS ALLOW A 8
C     CHARACTER LABEL AND THEN THE VALUES OF THE DISSOCIATION CONSTANT AND
C     CONCENTRATION OF THE SALT.
C     ************************************************************************
C
      REAL KI,KII
      DIMENSION GAM(3),Z(3),T(3),ARG(2)
   99 FORMAT(3F3.0)
  100 FORMAT(2A4,2X,E10.3,10X,E12.3)
  101 FORMAT(1HO,69HTHE VALUES APPARENTLY APPLY TO A COMPLEX QUADRATIC E
     1QUATION - - HELP////)
  102 FORMAT(1HO,I3,6(4X,F16.8))
  103 FORMAT(1HO,12HFINAL ANSWER//1X,I3,6(4X,E16.8))
  104 FORMAT(1H1,48X,34HPROGRAM TO CALCULATE THE DEGREE OF//39X,55HDISSO
     1CIATION BY REPEATED APPLICATION OF DAVIES EQUATION//60X,14HDOUGLAS
     2 P. FAY)
  105 FORMAT(1HO,21HDISSOCIATION CONSTANT,2X,E16.8,2X,11HMOLES/LITER//22
     1H INITIAL CONCENTRATION,2X,E16.8,2X,11HMOLES/LITER/)
  106 FORMAT(4HO  N,7X,13HDEG OF DISSOC,11X,5HPI(F),10X,14HIONIC STRENGT
     1H,6X,14HCONC OF ION(+3),6X,14HCONC OF SULFAT,6X,15HCONC OF COMPLEX)
  107 FORMAT(1HO,18HCALCULATION NUMBER,I3,10X,8HSALT OF ,2A4)
C
C     WRITTEN BY DANIEL LITCHINSKY--CORRECTED BY DOUGLAS FAY--10/30/68.
C     PROGRAM CONVERTED TO S/360  1 NOVEMBER 1968.
C
      WRITE(6,104)
C     READ CHARGES ON IONS
      READ(5,99)(Z(I),I=1,3)
C
C     READ VALUE OF (A) AND (B) IN DEBYE-HUCKLE THEORY AS ADH AND BDH.
C     READ A SUPERSCRIPT ZERO AS ANOT AND K(12) AND K(23) AS KI AND KII.
C
  200 READ(5,150)ADH,BDH,ANOT,KI,KII,TEMP
  150 FORMAT(3(F6.4,4X),E9.3,4X,2(F6.4,4X))
      N=0
      DISK=0.0
      C=0.0
C
C     READ DATA CARDS FOR LABEL, DISSOCIATION CONSTANT AND CONCENTRATION.
C
    1 READ (5,100)ARG,DISK,C
      IF(DISK.EQ.0.00E-00) GO TO 200
      IF(DISK*C.EQ.0.0)GO TO 90
      ALF=1.0
    5 N=N+1
      WRITE(6,107)N,ARG
      DO 2 J=1,3
    2 GAM(J)=1.0
      WRITE(6,105)DISK,C
      WRITE(6,151)ADH,BDH,ANOT,KI,KII,TEMP
  151 FORMAT(1HO,15HA DEBYE-HUCKLE=,F6.4,4X,15HB DEBYE-HUCKLE=,F6.4,4X,8
     1HANOUGHT=,F6.4,4X,6HK(12)=,E9.3,4X,6HK(23)=,F6.4,8X,5HTEMP=,F7.4)
      WRITE(6,106)
      K=0
    3 K=K+1
      PAL=ALF
C
C     CALCULATE ALPHA = ALF (DEG. OF DISSOC.) USING QUADRATIC EQUATION.
C
      A=2.0*(1.0+GAM(2)*GAM(3)
      B=GAM(2)*GAM(3)*C+GAM(1)*DISK
      R=(-GAM(1)*DISK)
      DS=B**2-4.0*A*R
      IF(DS)30,10,10
   30 WRITE(6,101)
      GO TO 90
   10 ALF=(-B-SQRT(DS))/(2.0*A)
      IF(ALF)12,13,13
   12 ALF=(-B+SQRT(DS))/(2.0*A)
      IF(ALF)30,13,13
C
C     T(1),T(2),T(3) ARE CONC. OF CATION, SULFATE AND COMPLEX RESPECTIVELY.
C
   13 T(1)=2.0*C*(1.0-ALF)
      T(2)=C*(2.0*ALF+1.0)
      T(3)=2.0*ALF*C
      DI=0.0
      DO 15 J=1,3
   15 DI=DI+Z(J)**2*T(J)*0.5
      BI=SQRT(DI)
      PI=GAM(2)*GAM(3)/GAM(1)
      WRITE(6,102)K,ALF,PI,DI,T(3),T(2),T(1)
      IF(ABS(ALF-PAL).LE.0.001) GO TO 79
      DO 20 I=1,3
   20 GAM(I)=EXP((ADH*Z(I)**2)*((BI/(1.0+BDH*ANOT*BI))-0.3*DI)
     1*(-2.302585))
      GO TO 3
   79 WRITE(6,103)K,ALF,PI,DI,T(3),T(2),T(1)
C
C     AA AND BB CALC. DIFF-PARTIAL IN PI(F) W.R.T. PARTIAL IN ALPHA.
C
      AA=(12.0*ADH/(2.0*BI*(1.0+BDH*ANOT*BI)**2)-(12.0*ADH*0.3))
     1*(-2.302585)
      BB=12.0*ALF*C
      DIFF=AA*BB
      THETA=PI*C*((4.0*ALF+1.0)*(2.0*ALF+1.0)*DIFF)
      FEECE=THETA/((K1*KII)*(1.0+KII)*THETA)
      WRITE(6,109)AA,DIFF,THETA,FEECE
  109 FORMAT(1HO,10X,5HAA = ,E16.8,5X,7HDIFF = ,E16.8,5X,8HTHETA = ,
     1E16.8,5X,8HFEECE = ,E16.8///)
   90 GO TO 1
   91 CALL EXIT
      END
```

APPENDIX C

```
C          PROGRAM TO CALCULATE RATE CONSTANTS AND STEP-WISE EQUILIBRIUM
C     CONSTANTS USING LEAST SQUARES TECHNIQUES.
C     ************************************************************************
C
      REAL K43,K34,K32,K23,K21,KT,K32EST
   99 KOUNT= 0
      READ(5,1)SALT, TEMP
    1 FORMAT(A2,2X,F4.1)
      READ(5,2)FEC1,FEC2,FEC3,THETA1,THETA2,THETA3,K21,KT
    2 FORMAT(3(F6.4,2X),3(E10.4,2X),E9.3,2X,E9.3)
      READ(5,3)A1,A2,A3,PIF1,PIF2,PIF3,K32EST
    3 FORMAT(6(F5.1,2X),F6.4)
      WRITE(6,4)
    4 FORMAT(1H1,32X,'PROGRAM TO CALCULATE RATE CONSTANTS USING LEAST SQ
     1UARES TECHNIQUES'////)
      WRITE(6,5)SALT,TEMP,KT,A1,K32EST,A2,K21,A3
    5 FORMAT(1HO,T32,'SALT =',A2,T66,'TEMP =',F4.1//T32,'KT =',E10.4,T66
     1,'A(1) =',E10.4//T32,'K32(EST.)=',E10.4,T66,'A(2) =',E10.4//T32,'K
     221 =',E10.4,T66,'A(3) =',E10.4)
      WRITE(6,6)THETA1,PIF1,THETA2,PIF2,THETA3,PIF3
    6 FORMAT(1HO,T32,'THETA(1)=',E10.4,T66,'2PIF(1)=',E10.4//T32,'THETA(
     12)=',E10.4,T66,'2PIF(2)=',E10.4//T32,'THETA(3)=',E10.4,T66,'2PIF(3
     2)=',E10.4/)
      WRITE(6,9)FEC1,FEC2,FEC3
      N=3
      SUMA=A1+A2+A3
      SUMASQ=A1**2+A2**2+A3**2
      SUMPIF=PIF1+PIF2+PIF3
      SUMPI2=PIF1**2+PIF2**2+PIF3**2
  100 SUMFEC=FEC1+FEC2+FEC3
      SUMAFE=A1*FEC1+A2*FEC2+A3*FEC3
      SUMPFE=PIF1*FEC1+PIF2*FEC2+PIF3*FEC3
C.....LFAST SQUARES ROUTINE FOR PLOT OF FEC VS. A
C     SUMFEC=N    *C1+SUMA  *C2
C     SUMAFE=SUMA*C1*SUMASQ*C2
      QUOTA=SUMA/N
      C2A=(SUMAFE-QUOTA*SUMFEC)/(SUMASQ-QUOTA*SUMA)
      IF(C2A.EQ.0.00E-00) GO TO 999
      C1A=(SUMFEC-SUMA*C2A)/N
C     FECA=C2A*A+C1A
C     WHEN A=0.0, FECA=C1A
C.....LEAST SQUARES ROUTINE FOR PLOT OF FEC VS. 2PIF
C     SUMFEC=N      *C1+SUMPIF*C2
C     SUMPFE=SUMPIF*C1+SUMPI2*C2
      QUOTP=SUMPIF/N
      C2P=(SUMPFE-QUOTP*SUMFEC)/(SUMPI2-QUOTP*SUMPIF)
      C1P=(SUMFEC-SUMPIF*C2P)/N
      WRITE(6,8)C2A,C2P,C1A,C1P
    8 FORMAT(1HO,T32,'C2A =',E11.4,T66,'C2P =',E11.4//T32,'C1A =',E11.4,
     1T66,'C1P =',E11.4///)
C     FECP=C2P*PIF+C1P
C     WHEN A=0, FECP=FECA=C1A, FECP=SK43
C     SK43=BACKWARD RATE CONSTANT, SK34= FORWARD RATE CONSTANT-- IN MHZ.
      SK43=(C1A-C1P)/C2P
      SK34=1.0/C2P
      K43=SK43/SK34
      K34=1.0/K43
      K32=(1.0+K43)/(K43*(K21*KT-1.0))
      K23=1.0/K32
      WRITE(6,7)SK34,SK43,K34,K43,K23,K32
    7 FORMAT(1HO,T32,'SK34 =',E11.4,T66,'SK43 =',E11.4//T32,'K34 =', E11
     1.4,T66,'K43 = ',E11.4//T32,'K23 = ',E11.4,T66,'K32 = ',E11.4)
      IF(ABS(K32-K32EST).LE.0.0001) GO TO 900
      K32EST=K32
      FEC1=THETA1/(K21*K32+(1.0+K32)*THETA1)
      FEC2=THETA2/(K21*K32+(1.0+K32)*THETA2)
      FEC3=THETA3/(K21*K32+(1.0+K32)*THETA3)
      WRITE(6,9) FEC1,FEC2,FEC3
    9 FORMAT(1HO,T24,'FEC1=',E11.4,10X,'FEC2=',E11.4,10X,'FEC3=',E11.4)
      KOUNT=KOUNT+1
      IF(KOUNT.GT.20) GO TO 900
      GO TO 100
  900 GO TO 99
  999 CALL EXIT
      END
```

VITA

Douglas Paul Fay

Candidate for the Degree of

Doctor of Philosophy

Thesis: THERMODYNAMIC AND KINETIC INVESTIGATIONS OF COMPLEXATION IN AQUEOUS SOLUTIONS OF THE LANTHANIDE SULFATES

Major Field: Chemistry

Biographical:

Personal Data: The author was born in Fayette, Iowa, August 14, 1943, the son of John D. and Opal F. Fay. On June 4, 1966, he married Deanna Mae Powell. A son, Brian Emory, was born to this marriage in Stillwater, Oklahoma, July 29, 1967.

Education: The author attended elementary and secondary school in Fayette, Iowa, graduating from Fayette Community High School in May, 1961. In May, 1965, he received a Bachelor of Science degree in Chemistry and Mathematics from Upper Iowa College, Fayette, Iowa. He entered the Graduate College of Oklahoma State University in February, 1966, and completed the requirements for the Doctor of Philosophy degree in August, 1969.

Professional Experience: The author has served in the following capacities: Student Aide, Argonne National Laboratory, summer 1965; Freshman Chemistry Instructor, Upper Iowa College, fall 1965; Graduate Teaching Assistant in Chemistry Department, spring 1966, fall 1967, and fall 1968; NASA Fellow, September, 1966 to August, 1969.

Professional Societies: The author is a member of the American Chemical Society and Phi Lambda Upsilon, National Honorary Chemical Society.